

## **2.12.7 Dimensional Inspection Report**

THIS PAGE INTENTIONALLY LEFT BLANK

**RANOR / GE Energy / AOS**  
**AOS-165 Cask Drop Test**  
**Dimensional Summary Report No. 109699-01 (4-23-07)**

**RANOR Purchase Order No.:** 109699

**Part Names:** AOS-165 Cask Assembly and Impact Limiters  
**Document References:** Drawing Nos.105E9692 Rev. 2; 105E9694 Rev. 3;  
Specification No. 22A9418 Rev. 3  
**Serial Numbers:** AOS-165 105E9693-1 (RANOR S/N 050280-01)  
AOS-165 105E9694-1-1-01 (RANOR S/N 060452-01)  
AOS-165 105E9694-1-1-02 (RANOR S/N 060452-02)  
AOS-165 105E9694-1-1-03 (RANOR S/N 060452-03)  
AOS-165 105E9694-1-1-04 (RANOR S/N 060452-04)  
AOS-165 105E9694-1-1-05 (RANOR S/N 060452-05)  
**Inspection Dates:** March 16-30, 2007  
**Attachments:** FARO Calibration Certificate No. 4655 (10-19-2006)

**Inspection Conditions:**

**Location:** GE Nuclear Energy Vallecitos Nuclear Center Sunol, CA 95486  
**Material:** Stainless Steel  
**Measurement Units:** Inches

*East Coast Metrology* was contracted by RANOR, Inc. for performance of On-Site Laser Tracker Inspection Services of the AOS-165 Cask Assembly and Impact Limiters fabricated by RANOR. The items were located at GE Nuclear Energy Vallecitos Nuclear Center 6705 Vallecitos Road Sunol, CA 95486.

*East Coast Metrology* utilized a FARO Laser Tracker Model X System, Serial No. X01000601930 for performing the dimensional inspections. The equipment has been calibrated by the manufacturer - FARO Technologies Kennett Square, PA 19348 on October 18, 2006, calibration due October 18, 2007 (FARO Calibration Certificate Number 4655) using standards traceable to the National Institute of Standards and Technology (NIST).

All dimensional inspection was performed under the direction and observation of GE Nuclear Energy Raul Pomares, Project Manager for the AOS-165 Cask Assembly and components.

The AOS-165 Cask Assembly and accompanying Impact Limiters were inspected by *East Coast Metrology* before and after each drop test to determine the extent of deformation due to each type of drop. Each component was scanned and compared to its corresponding CAD model using a Laser Tracker. See the following for a summary of the inspections and data.

**AOS-165 Cask Assembly:**

For each set of scan data for the Cask, the 0, 90, 180, and 270 degree profiles were scanned. An alignment using the axis of the cylindrical part of the cask as the controlling datum was used. This axis was then intersected with the “Lid End” of the Cask and a point was constructed. Another point was measured at the 90 degree lifting lug to establish the other axis. This alignment was repeated for each measurement of the Cask.

The table below, *Table 1*, shows the maximum and minimum deviations of the profiles of the Cask when compared to its CAD model for each drop test. The maximum (positive) deviations indicate the profile of the Cask was larger than that of the model. Similarly, the minimum (negative) deviations indicate that the profile of the Cask was smaller than that of the model.

***Table 1: Cask Assembly Pre- and Post- Drop Profile Deviations from CAD Model (inches)***

Cask Condition	Pre End Drop	Post End Drop	Post Side Drop	Post Slap Down
Maximum Deviation	0.0068	0.0046	0.0053	0.0047
Minimum Deviation	-0.0094	-0.0101	-0.0109	-0.0105

Over the course of all three drop tests, the maximum deviations varied by a total of 0.0022 inches, while the minimum deviations varied by a total of 0.0015 inches. This indicates that the effect of the drop tests had a negligible impact on the profile of the Cask.

Below is a sample of the Cask profile from the Pre- End Drop scan. There are 2 pictures, *Image A* is the 0-180 Cross-Section of the Cask, and *Image B* is the 90-270 Cross-Section. The red areas represent the positive (maximum deviations) and the yellow areas represent the negative (minimum deviations).

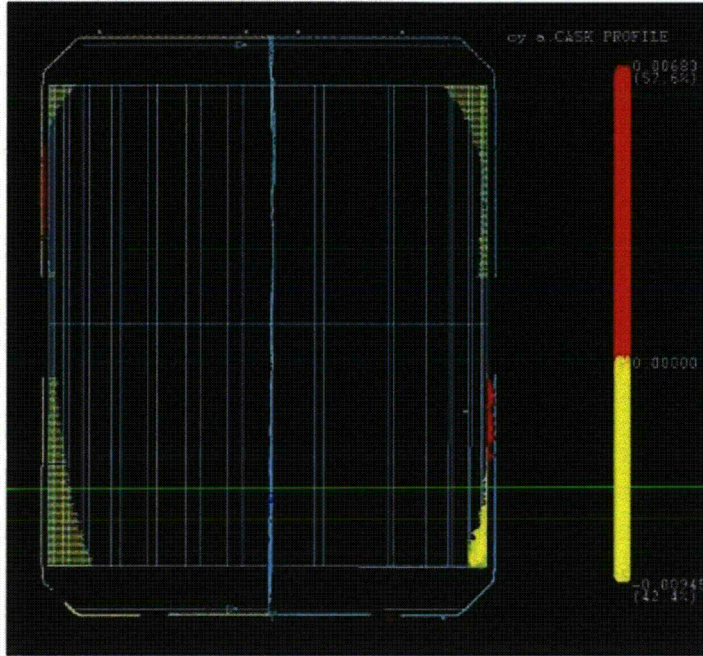


*Image A: Cask Assembly Pre-End Drop Scan Data, 0-180 Degree Cross-Section*

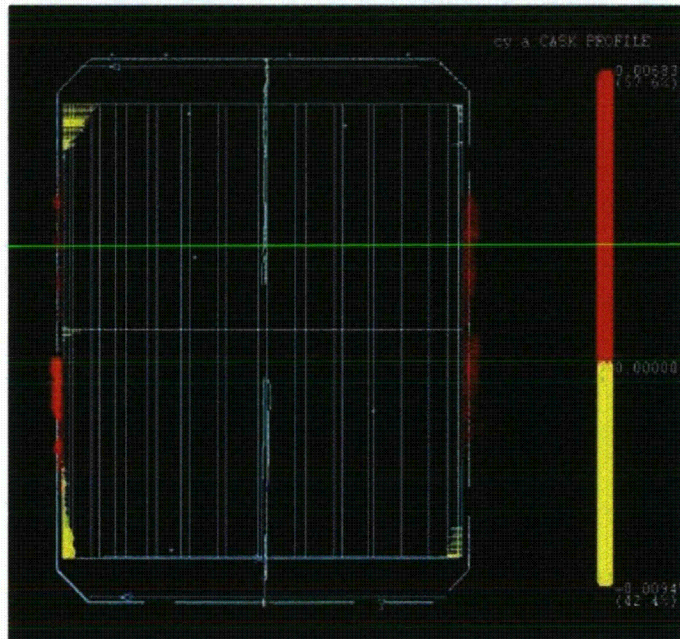


*Image B: Cask Assembly Pre-End Drop Scan Data, 90-270 Degree Cross-Section*

## AOS-165 Cask Impact Limiter Assemblies:

For the Impact Limiters, scan data was taken at the 0, 30, 60, 90, 120, 150, 180, 210, 240, 270, 300 and 330 degree profiles. In order to compare each impact limiter in its pre- and post-drop condition, an alignment using the bottom perimeter (opposite the domed-end), measured as a circle, was used as a reference. By measuring it as a circle, the center point and vector of the measured circle were established. The portions of this circle that were deformed due to each drop test were not used in this calculation. The vector of this axis was defined to be the primary datum in this alignment. A point was then measured at the 90 degree lifting lug to establish the second axis in the coordinate system. This process provided the only repeatable means to align each impact limiter and subsequently compare the results.

Once the pre- and post-drop scan data was collected for each Impact Limiter, the 90-270 degree profile cross-sections were overlaid in order to calculate the magnitude of deformation for each drop. In the images below, each Impact Limiter has been analyzed in this manner and the deformations reported. They are listed below in the same order that the drop tests occurred: End Drop (Impact Limiter 5), Side Drop (Impact Limiters 1 & 3) and Slap Down (Impact Limiters 2 & 4).

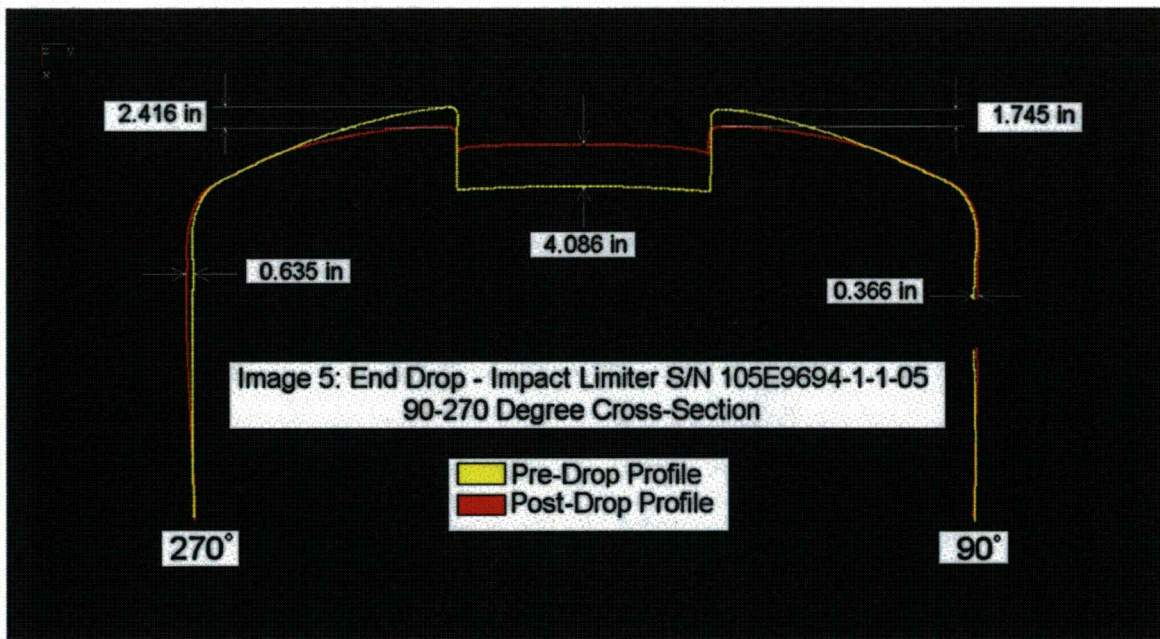


*Image 5: Impact Limiter Serial No. 105E9694-1-1-05 - End Drop Cross-Section Overlay*

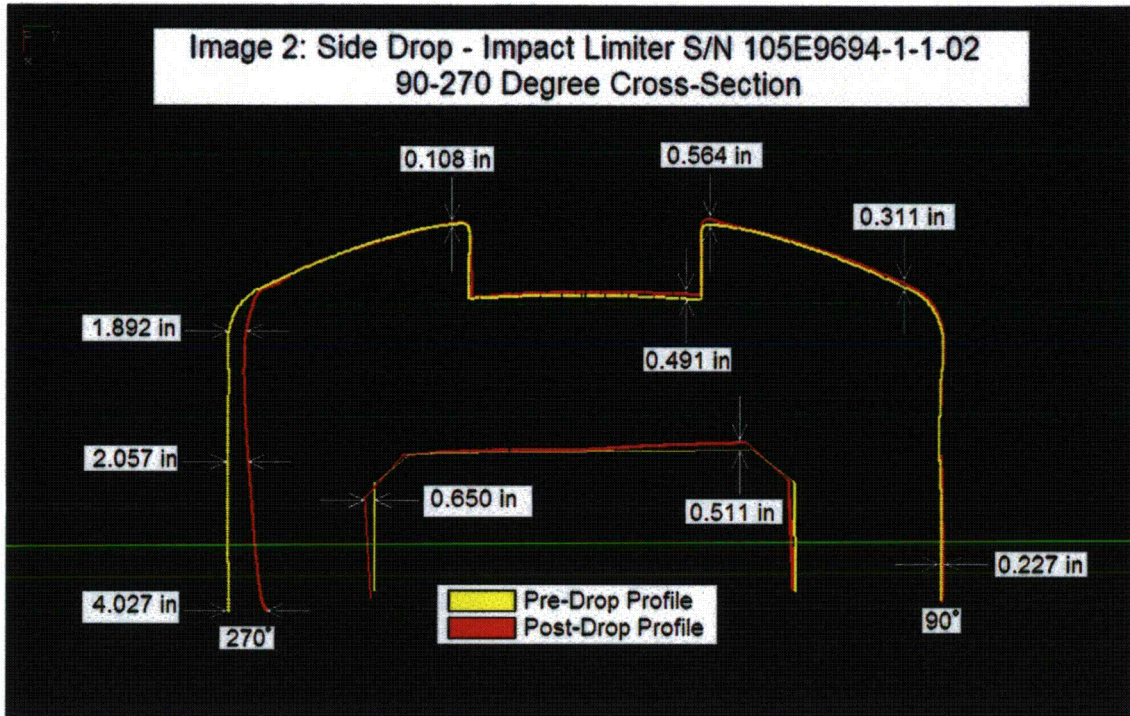


*Image 2: Impact Limiter Serial No. 105E9694-1-1-02 - Side Drop Cross-Section Overlay*

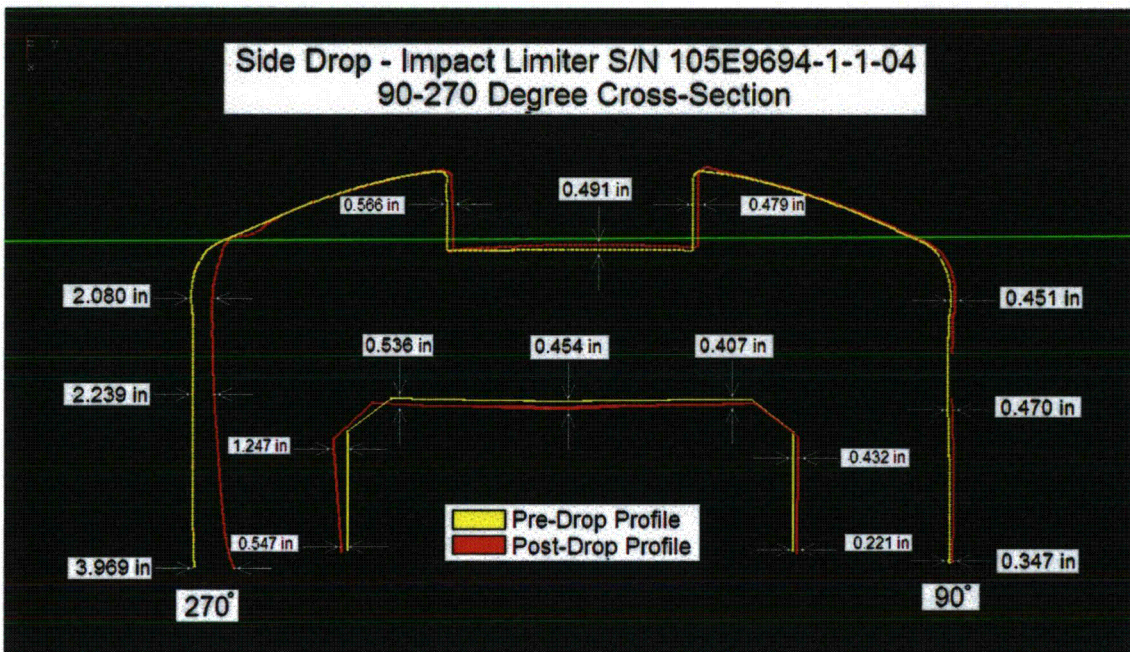


*Image 4: Impact Limiter Serial No. 105E9694-1-1-04 - Side Drop Cross-Section Overlay*

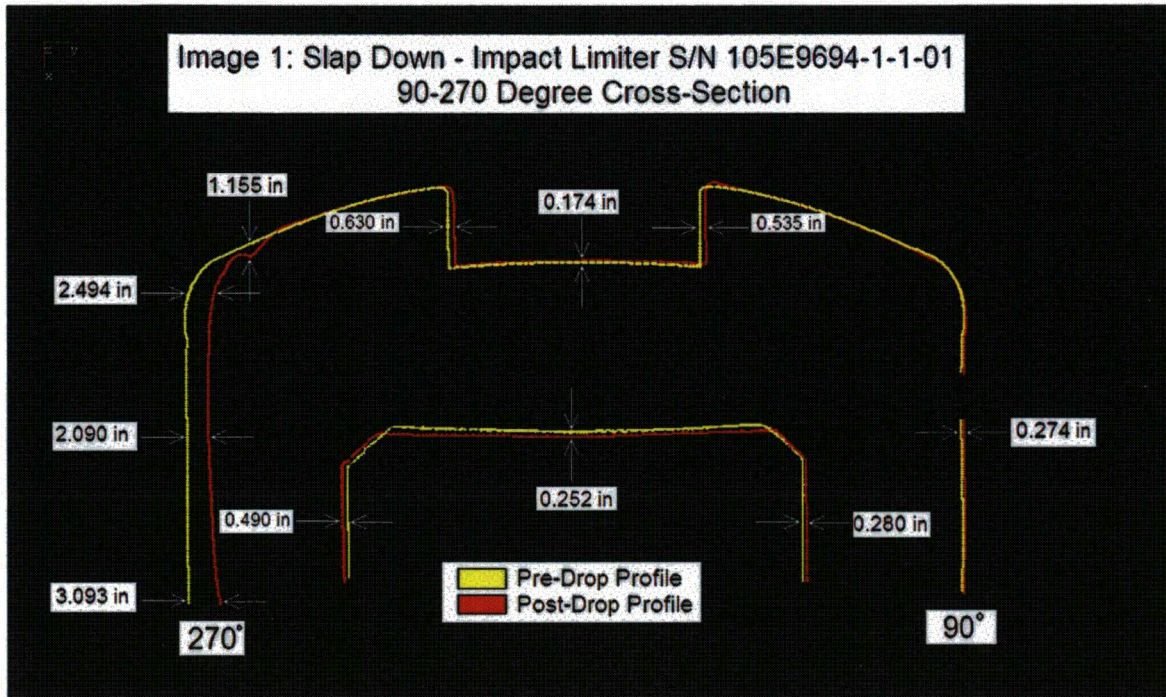


*Image 1: Impact Limiter Serial No. 105E9694-1-1-01 - Slap Down Cross-Section Overlay*

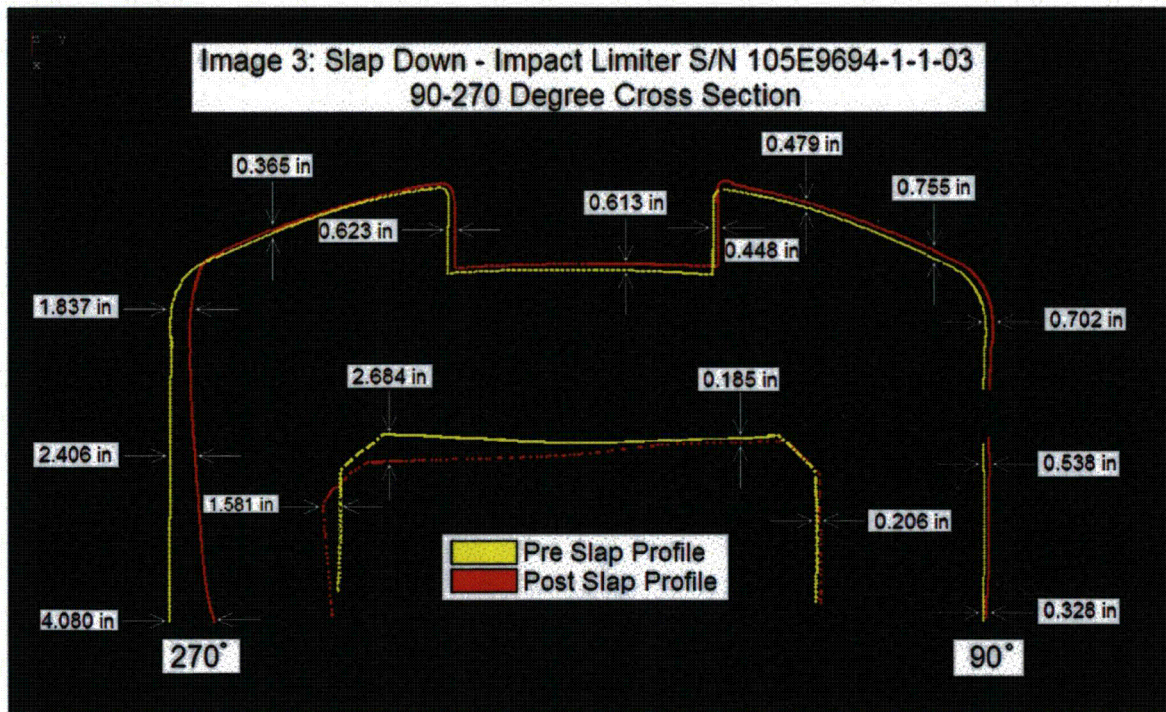


*Image 3: Impact Limiter Serial No. 105E9694-1-1-03 - Slap Down Cross-Section Overlay*



# EAST COAST METROLOGY

461 Boston Street ♦ Topsfield, Massachusetts 01983 ♦ Tel: 978-887-5781 ♦ Fax: 978-887-5782 ♦ [www.EastCoastMetrology.com](http://www.EastCoastMetrology.com)

## *Contact Information*

As part of this report, *East Coast Metrology* appreciates the request for any additional information, which will help our customers find solutions to their measurement problems.

We proudly consider ourselves as allied partners to our customers, and can assist in the positioning and alignment of features, along with our ability to perform high accuracy measurements.

The key to our success is to be able to provide our customers with complete solutions, and the information that is most valuable to their cause, in a clear and concise manner.

We welcome any questions you may have, and look forward to working together in the near future.

Please feel free to contact us for additional information or concerns that may arise.

David K. Kramer  
Project Engineer  
East Coast Metrology  
461 Boston Street (A4)  
Topsfield, Massachusetts 01983  
Tel: 503.997.7055  
Fax: 603.251.5678  
E-mail: [dkramer@eastcoastmetrology.com](mailto:dkramer@eastcoastmetrology.com)

## Attachments:

AOS-165 Cask Assembly Impact limiter, Serial No. 105E9694-1-1-01 Pre- and Post- Slap Down Scan Data (12 pgs)  
AOS-165 Cask Assembly Impact limiter, Serial No. 105E9694-1-1-02 Pre- and Post- Side Drop Scan Data (10 pgs)  
AOS-165 Cask Assembly Impact limiter, Serial No. 105E9694-1-1-03 Pre- and Post- Slap Down Scan Data (14 pgs)  
AOS-165 Cask Assembly Impact limiter, Serial No. 105E9694-1-1-04 Pre- and Post- Side Drop Scan Data (12 pgs)  
AOS-165 Cask Assembly Impact limiter, Serial No. 105E9694-1-1-05 Pre- and Post- Head Drop Scan Data (10 pgs)

RANOR/GE/AOS  
Report No. 109699-01

AOS-165 Cask Drop Test Dimensional Summary Report  
Page 7 of 7

RANOR P.O. No. 109699  
Date: 4/23/2007

THIS PAGE INTENTIONALLY LEFT BLANK

## 2.12.8 Analysis of Content-Cask Lid Impact

Content accelerations due to head-on 30-ft. package drops and content-cask lid gaps are determined by equating impact kinetic energy to strain energy within the impact limiter. The cask and impact limiter are modeled as a generalized single degree of freedom (SDOF) spring-mass system, using an approximation of the impact limiter force-displacement relation determined in the 30-ft. drop analyses. The content is also modeled as a generalized lumped mass, and content impact kinetic energy determined from a central impact formulation. The velocities applied in the central impact calculation are determined from equations of motion for the two generalized masses under gravitational force and initial velocity.

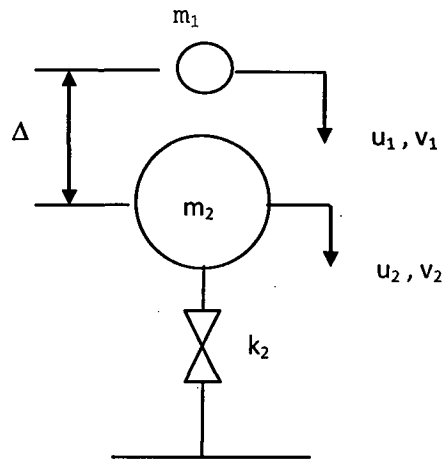


Figure 2-68. Generalized Model of Impact I

a	=	Content acceleration	T	=	Kinetic energy
e	=	Coefficient of restitution	U	=	Strain energy
g	=	Gravitational acceleration	$v_0$	=	Initial velocity
k	=	Impact limiter spring stiffness	$v_1$	=	Content velocity
m	=	Effective mass	$v_2$	=	Cask velocity
$m_1$	=	Content mass	$w_1$	=	Content weight
$m_2$	=	Package mass	$w_2$	=	Package weight
P	=	Impact force	$\delta$	=	Spring displacement
$u_1$	=	Content displacement	$\Delta$	=	Gap
$u_2$	=	Cask displacement	$\omega$	=	Frequency, $\sqrt{(k_2 / m_2)}$

Content equation of motion for initial velocity  $v_0$  and force  $g$ :

$$\begin{aligned}g &= d^2u_1 / dt^2 \\u_1 &= g * t^2 / 2 + v_0 * t \\v_1 &= du_1 / dt = g * t + v_0\end{aligned}$$

Cask equation of motion for initial velocity  $v_0$  and force  $g$ :

$$\begin{aligned}g &= d^2u_2 / dt^2 + (k_2 / m_2) * u_2 \\ \omega &= \sqrt{(k_2 / m_2)} \\u_2 &= (v_0 / \omega) * \sin \omega t + g * t^2 / 2 \\v_2 &= du_2 / dt = v_0 * \cos \omega t + g * t\end{aligned}$$

$$\text{for, } \sin \omega t = \omega t - (\omega t)^3 / 6,$$

$$\begin{aligned}u_2 &= (v_0 / \omega) * [\omega t - (\omega t)^3 / 6] + g * t^2 / 2 \\u_2 &= v_0 * t - v_0 * \omega^2 t^3 / 6 + g * t^2 / 2\end{aligned}$$

Equating cask and content displacements:

$$\begin{aligned}\Delta &= u_1 - u_2 \\ &= v_0 * \omega^2 * t^3 / 6 \\t &= (6 * \Delta) / (v_0 * \omega^2)^{1/3}\end{aligned}$$

Impact kinetic energy:

$$\begin{aligned}T &= 0.5 (1 - e^2) * (v_2 - v_2)^2 * [m_1 * m_2 / (m_1 + m_2)] \\m &= [m_1 * m_2 / (m_1 + m_2)] \\e &= 0.0 \\T &= 0.5 * m * (v_1 - v_2)^2 \\ &= 0.5 * m * v_0^2 * (1 - \cos \omega t)^2\end{aligned}$$

Equating strain and kinetic energy:

$$T = k \cdot \delta^2 / 2$$

$$\delta = \sqrt{(2 \cdot T / k)}$$

$$P = k \cdot \delta = \sqrt{(2 \cdot T \cdot k)}$$

$$a = P / w_1 = \sqrt{(2 \cdot T \cdot k)} / w_1$$

Applying equations to AOS casks:

Model	W1 (lb)	W2 (lb)	K (lb/in)	Gap (in)	Freq (hz)	Acc (g)
AOS-025	1.500E+01	1.680E+02	1.390E+05	1.000E-01	8.999E+01	8.662E+02
AOS-050	6.000E+01	1.181E+03	1.040E+05	1.000E-01	2.936E+01	1.868E+02
AOS-100	5.000E+02	9.510E+03	2.330E+05	5.000E-01	1.549E+01	1.798E+02

Fortran program for equation evaluation (ContentAcc.for):

```
c
c   a   - content acceleration in g
c   f   - package frequency
c   g   - gap
c   xk  - impact limiter stiffness
c   xm  - effective mass
c   xm1 - content mass
c   xm2 - package mass
c   t   - time to contact
c   T   - 2x kinetic energy
c   v0  - initial velocity
c   w1  - content weight
c   w2  - package weight
c
c       implicit real*8 (a-h,o-z)
c
c   open files & initialize output
c       open(1,file='contentacc.in')
c       open(2,file='contentacc.out')
c       write(2,'(5x,5hModel,5x,6hW1(lb),5x,6hW2(lb),3x,8hK(lb/in),
&               4x,7hGap(in),3x,8hFreq(hz),5x,6hAcc(g))')
c       write(2,'(5x,5h-----,5x,6h-----,5x,6h-----,3x,8h-----,
&               4x,7h-----,3x,8h-----,5x,6h-----)')
c
c       initialize constants
c       v0=527.5
c       exp=0.333333
c       pi2=6.28319
c
c       loop on models
c       do n=1,3
c       read(1,*) model,w1,w2,xk,g
c       xm1=w1/386.4
c       xm2=w2/386.4
c       xm=xm1*xm2/(xm1+xm2)
c       f=dsqrt(xk/xm2)
c       t=(6*g/(v0*f**2))**exp
c       T=xm*v0**2*(1-dcos(f*t))**2
c       a=dsqrt(T*xk)/w1
c       write(2,'(i10,6es11.3)') model,w1,w2,xk,g,f/pi2,a
c       enddo
c
c       end
```

Input data (ContentAcc.in):

```
100,500,9510,2.33e5,0.5
50,60,1181,1.04e5,0.1
25,15,168,1.39e5,0.1
```

## 2.12.9 Comparison of Libra Static and Dynamic Impact Analysis

Date February 9, 2010

Libra static and dynamic impact analyses are compared to assess applicability of the static method to AOS cask drop analyses. Results of static and dynamic analyses of a 30-ft. head-on drop are compared. A model 165 cask with 20 psf density foam is used in the analyses. Both impact forces and displacements given by the two solutions are shown to be in good agreement.

In the Libra dynamic analysis, the impact velocity corresponding to a 30-ft. drop is applied as an initial condition, and cask response is determined by a direct integration solution. An axisymmetric, 2D model of the foam and cask is used. The FEA model is shown in Figure 2-69, where the foam and cask are distinguished by different colors. The cask is modeled as a solid steel cylinder, with density adjusted to give a total cask and foam weight of 40k. A bi-linear foam constitutive model and von Mises yield criteria is used, with initial modulus of 19.0 ksi, secondary modulus of 5.4 ksi, and an equivalent yield stress of 2.0 ksi. The initial modulus and yield stress are based on foam stress at 10% strain, and the secondary modulus is based on the foam stress at 10% and 65% strains. Both foam to ground and foam to cask interfaces are modeled by gapped, compression-only, spring elements.

Cask time-history displacement determined in the dynamic analysis is shown in Figure 2-70. The maximum displacement is 5.76 in, and occurs at 0.016 sec. Forces in ground impact springs are shown in Figure 2-71 and Figure 2-72. Figure 2-71 shows forces in individual ground contact springs, while Figure 2-72 shows the resultant of all ground contact springs. In Figure 2-71, time lapses before springs compress reflect developing foam-ground contact. From Figure 2-72, the maximum, total impact force is 6020 k. The deformed model at maximum displacement is shown in both Figure 2-73 and Figure 2-74. Figure 2-73 shows only the foam deformation, while Figure 2-74 shows both the foam and cask deformation, with displacement contours super-imposed.

Libra static drop analyses involve determining impact force and foam strain energy due to deformation at ground contact locations. Maximum impact force corresponds to the value of strain energy equal to the potential energy of the 30-ft. drop. A 180°, 3D foam model, shown in Figure 2-75, is used in the analysis. Results of the static analysis are shown in Figure 2-76 and Figure 2-77. Figure 2-76 shows the deformed model at maximum displacement, while Figure 2-77 shows force and energy developed in the analysis. For a 180° model, the required strain energy is half the potential energy of a 40 k structure drop, or 7200 in-k. From Figure 2-77, the corresponding displacement is 5.7 in, and the impact force is 6400 k. Figure 2-77 is based on an accurate foam constitutive model. A static analysis is also performed using the approximate bi-linear foam constitutive model applied in the dynamic analysis. Plots of force and energy for the bi-linear constitutive model are presented in Figure 2-78, and the impact force is 6800 k.

The 5.7 in displacement and 6400 k force determined in the static analysis from Figure 2-77 compare well to the 5.76 in displacement and 6020 k force determined in the dynamic analysis. In addition, the deformation patterns given by the two solutions are also in good agreement. For the same constitutive model, the static method gives 6800 k while the dynamic method gives 6020 k, indicating the static method is conservative.

MATERIALS:

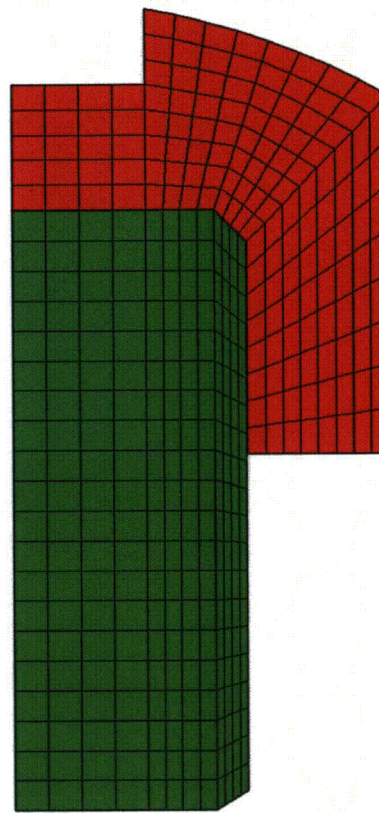
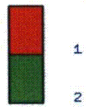
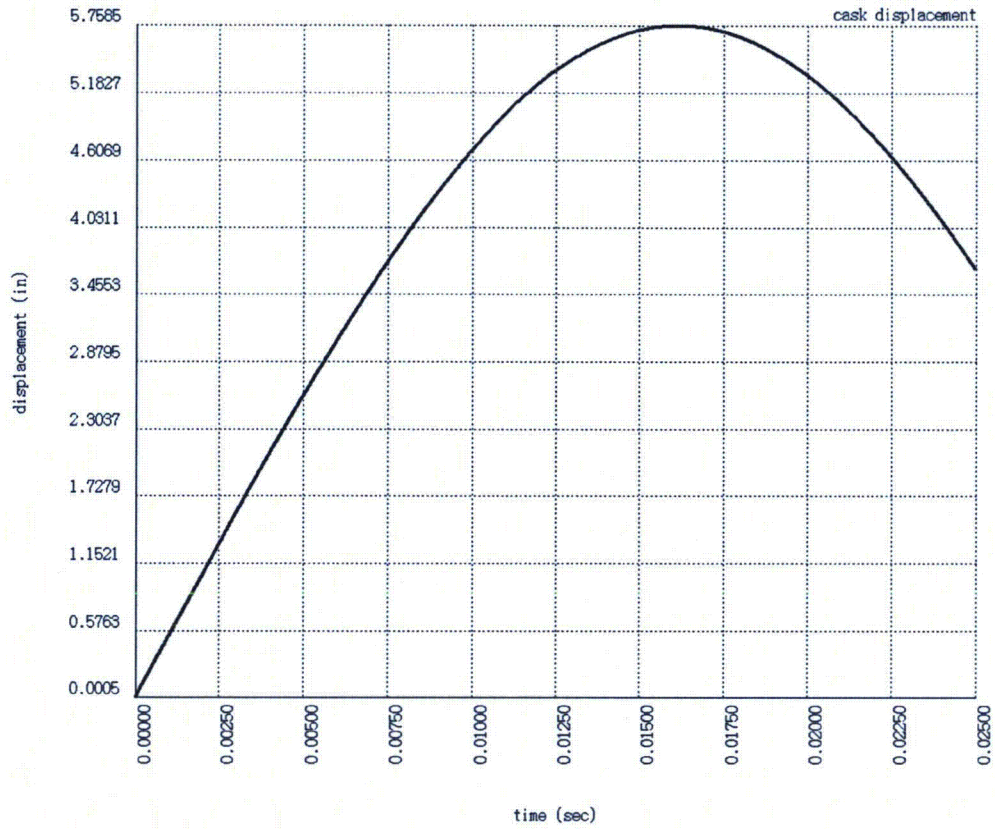


Figure 2-69. Dynamic Analysis FEA Model





**Figure 2-70. Cask Displacement Time-History**

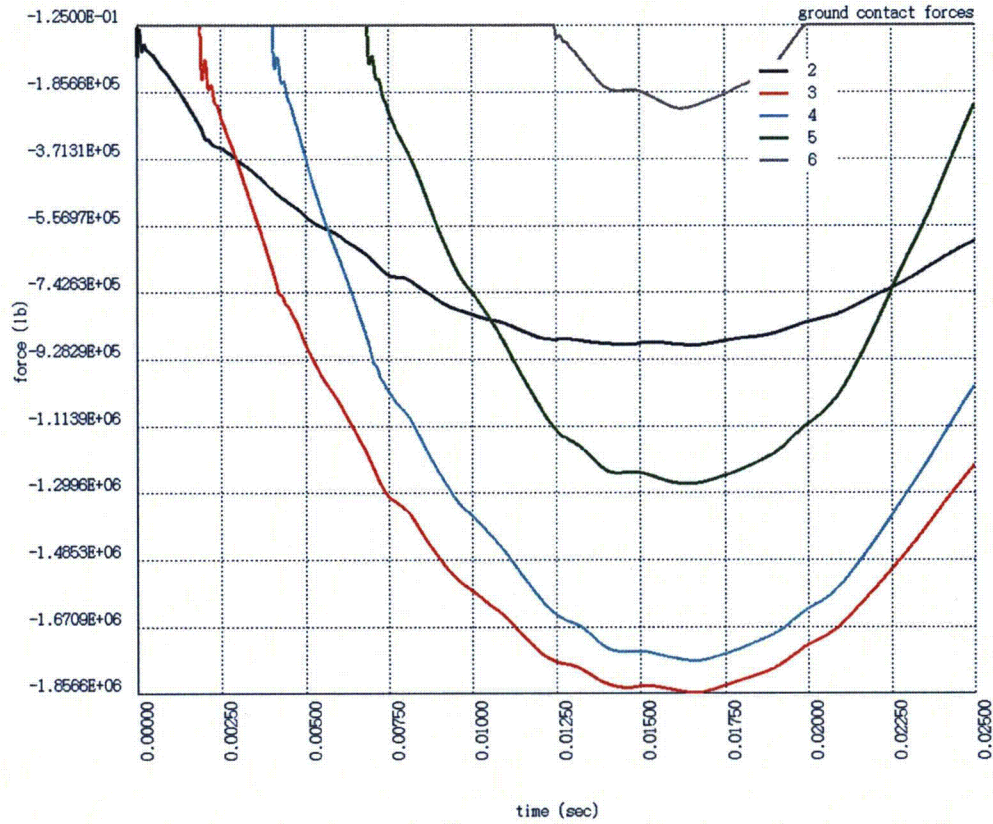


Figure 2-71. Ground Impact Forces in Dynamic Model

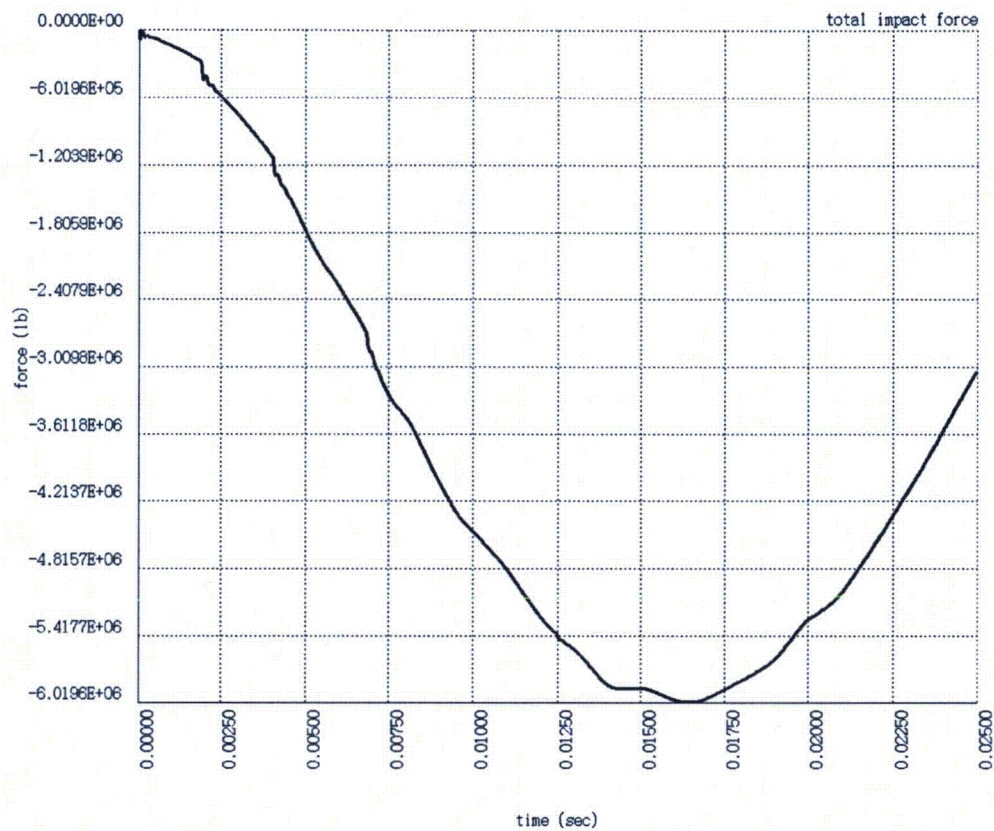


Figure 2-72. Total Ground Impact Force in Dynamic Model

```

VECTOR: 15
AMPL: 1.0
SCALE: 0.95
BOUNDARIES:
X1: 0.000
Y1: 37.500
Z1: 0.000
X2: -43.500
Y2: 37.700
Z2: 0.000

```

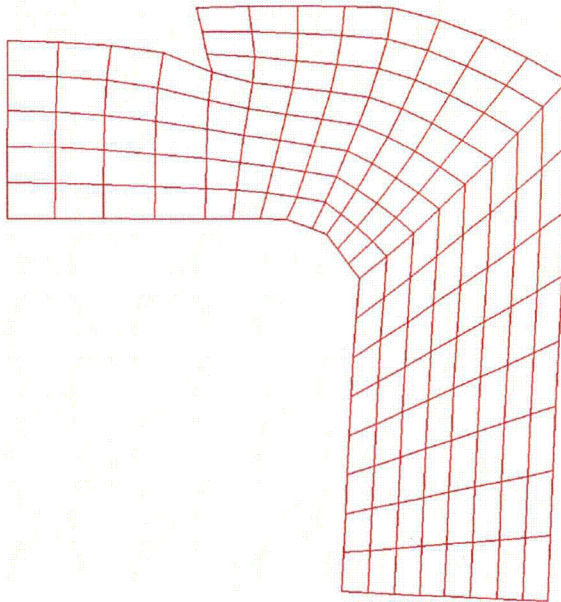


Figure 2-73. Deformed Dynamic Model at Maximum Displacement

```

VECTOR: 15
DOF: 2
MIN: 8.8874E-02
MAX: 5.7603E+00

```

8.8874E-02
2.9143E-01
4.9396E-01
6.9653E-01
8.9906E-01
1.1015E+00
1.3042E+00
1.5067E+00
1.7093E+00
1.9118E+00
2.1144E+00
2.3169E+00
2.5195E+00
2.7220E+00
2.9246E+00
3.1271E+00
3.3297E+00
3.5322E+00
3.7348E+00
3.9373E+00
4.1399E+00
4.3424E+00
4.5450E+00
4.7475E+00
4.9501E+00
5.1526E+00
5.3552E+00
5.5577E+00
5.7603E+00

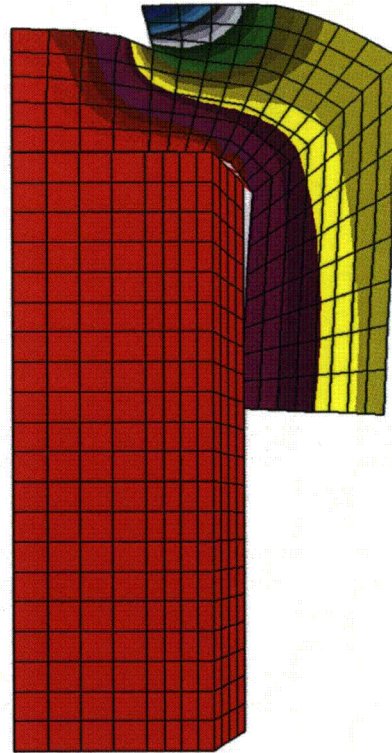


Figure 2-74. Displacement Contours in Deformed Dynamic Model

VEC: 0  
AMPL: 0.000E+00  
SQUARE: OFF  
SCALE: 0.95  
  
BOUNDARIES:  
X: -37.500  
37.500  
Y: -8.000  
36.700  
Z: 0.000  
37.295

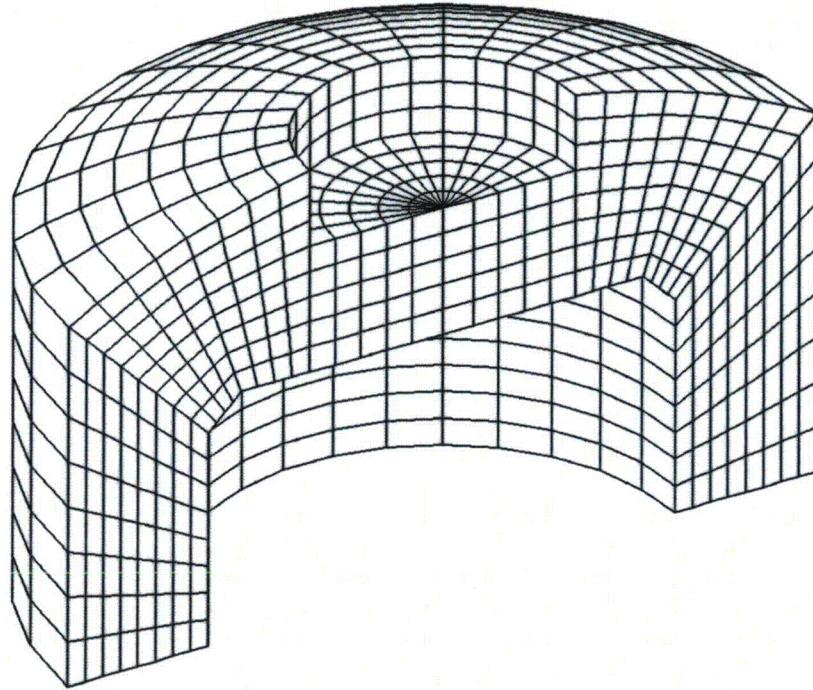


Figure 2-75. Foam Static Analysis FEA Model

VEC: 550  
AMPL: 1.0  
SQUARE: OFF  
SCALE: 0.95  
  
BOUNDARIES:  
X: -37.500  
37.500  
Y: -8.000  
36.700  
Z: 0.000  
37.295

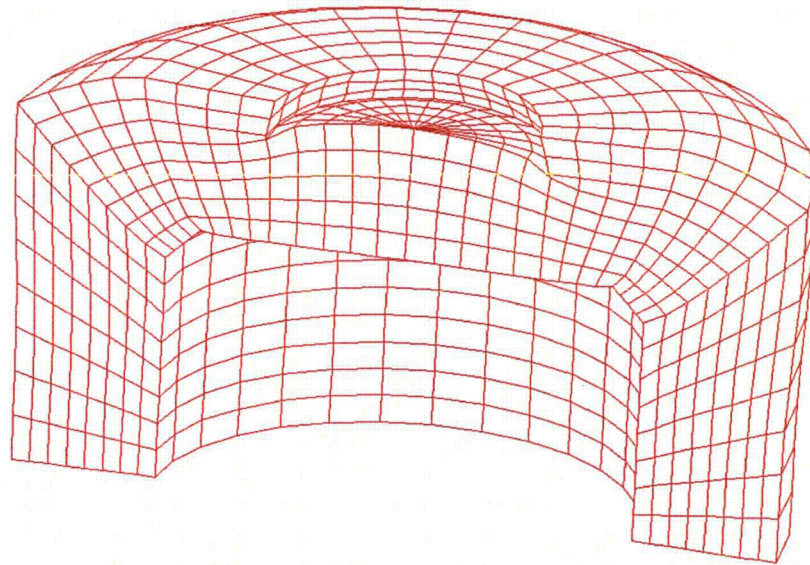


Figure 2-76. Deformed Foam Static Model at Maximum Displacement

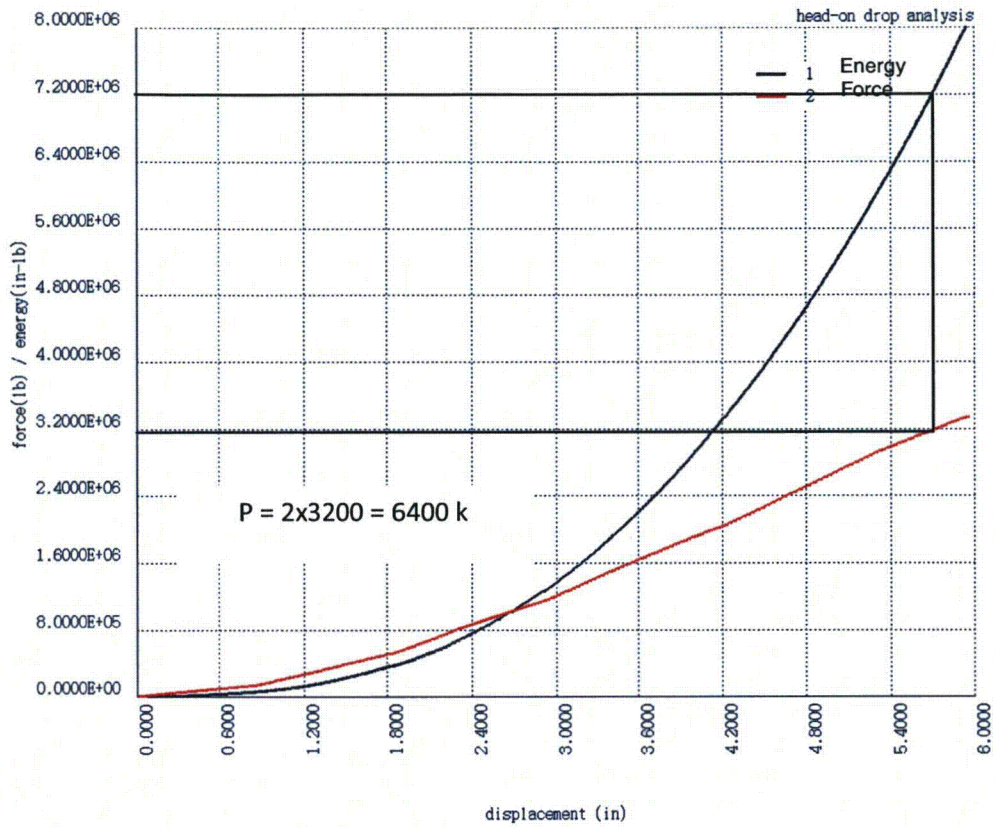


Figure 2-77. Energy and Force Plots for Static Analysis

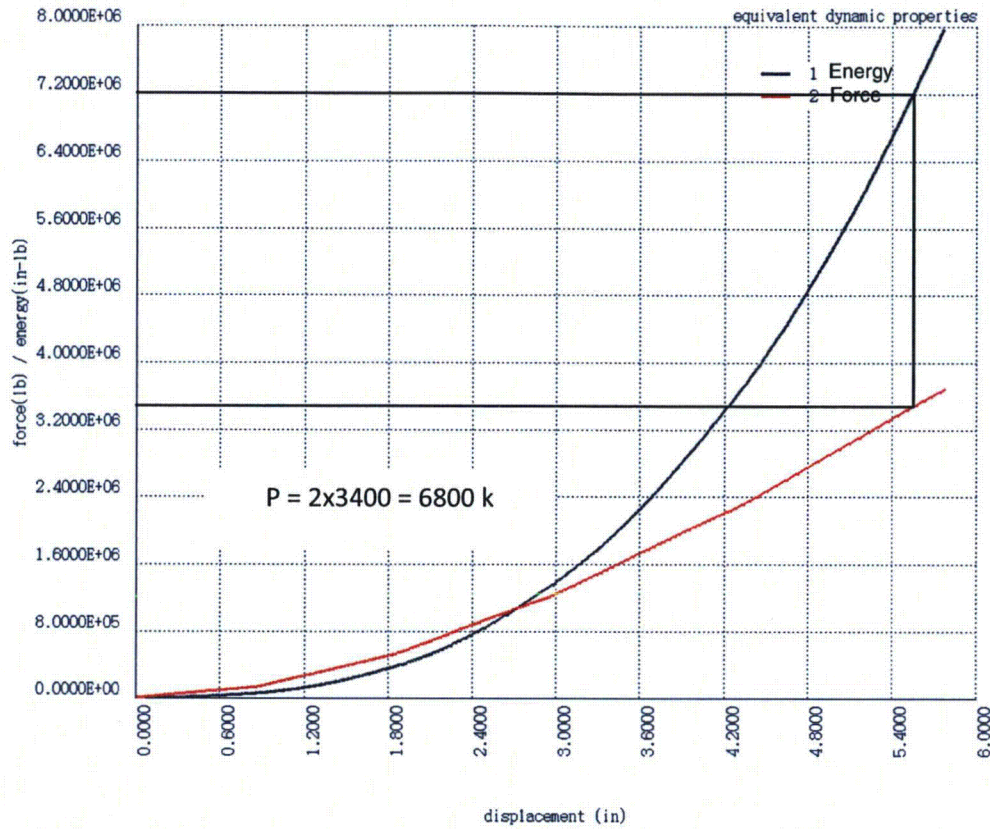


Figure 2-78. Energy and Force Plots for Static Analysis with Bi-Linear Stress-Strain

## 2.12.9.1 Appendix A – Libra Dynamic Impact Analysis Input File

ti dynamic impact analysis

\*

mc 9

\*

cnd 1, 23.3,-8,0  
, 2, 37.5,-8,0  
, 3, 37.5,27.9,0  
, 4, 23.3,13.3,0  
, 5, 20.1,16.5,0  
, 6, 25.6,33.4,0  
, 7, 13.3,36.7,0  
, 8, 13.3,29.125,0  
, 9, 0.0,16.5,0  
, 10, 0.0,29.125,0  
, 11, 19.4,35.3,0  
, 12, 31.7,30.9,0  
, 13, 13.3,16.5,0

\*

\* foam

\*

g10

9,9, 1,1, 8,1, 0,1  
1,2,3,4  
-1

\*

g10

9,5  
4,3,6,5  
6, 12  
-1

\*

g10

9,5  
5,6,7,13  
6, 11  
-1

\*

g10

5,6  
9,13,8,10  
-1

\*

\* pseudo cask

\*

g10

5,21, 1001,1001, 8,2, 0,0  
0,-43.6,0, 13.3,-43.6,0  
13.3,16.4,0, 0,16.4,0  
-1

\*



```

g10
  5,21, 1201,1201, 8,2, 0,0
  13.3,-43.6,0, 20.1,-43.6,0
  20.1,16.4,0, 13.3,16.4,0
  -1
*
g10
  5,21, 1401,1401, 8,2, 0,0
  20.1,-43.6,0, 23.2,-41.6,0
  23.2,13.2,0, 20.1,16.4,0
  -1
*
* cask contact springs
*
el 2001,1,3, 1101,172, 4,1,1
, 2005,1,3, 1105,163
, 2006,1,3, 1302,154
, 2007,1,3, 1303,145
, 2008,1,3, 1304,136
, 2009,1,3, 1502,109
, 2010,1,3, 1503,100
, 2011,1,3, 1504,91
, 2012,1,3, 1505,73
*
* boundary contact springs
*
nd 3162, 16.3375, 36.7, 0
, 3153, 19.4, 36.7, 0
, 3144, 22.4875, 36.7, 0
, 3126, 25.6, 36.7, 0
, 3117, 28.6875, 36.7, 0
, 3108, 31.7, 36.7, 0
, 3171, 13.3, 37.7, 0
*
el 3001, 1, 4, 162,3162
, 3002, 1, 5, 153,3153
, 3003, 1, 6, 144,3144
, 3004, 1, 7, 126,3126
, 3005, 1, 8, 117,3117
, 3006, 1, 9, 108,3108
, 3007, 1,10, 171,3171
*
* merge nodes
*
me 0.001
*
* boundary cond
*
bc 3108,8,9, 12,0.0
*
* element properties
*
pr 1,101
, 101, 1.9e4,0.3,1.0e-6,3.0e-5,2.0e3,5.4e3

```

```

PR 2,102
, 102, 28.0E6,0.3,1.0E-5,0.00099,1.0e6,1.0e9
pr 3, 1.0e7,1.0e7,1.0e9, 1,0.0000,0, 0,0
pr 4, 1.0e7,1.0e7,1.0e9, 1,0.6375,0, 0,0
pr 5, 1.0e7,1.0e7,1.0e9, 1,1.4000,0, 0,0
pr 6, 1.0e7,1.0e7,1.0e9, 1,2.2875,0, 0,0
pr 7, 1.0e7,1.0e7,1.0e9, 1,3.3000,0, 0,0
pr 8, 1.0e7,1.0e7,1.0e9, 1,4.4875,0, 0,0
pr 9, 1.0e7,1.0e7,1.0e9, 1,5.8000,0, 0,0
pr 10, 1.0e7,1.0e7,1.0e9, 1,0.0000,0, 0,0
*
* MAIN9 solution data
*
sc 25000,1,0,1, 1.0e-6,1000,0, 0.00001,0,1.4, 1.0
ic 1,1505,2,0,527.5
mo 1,1101,2
mo 4,3001,1
, 4,3002,1
, 4,3003,1
, 4,3004,1
, 4,3005,1
, 4,3006,1
, 4,3007,1
*
end

```

## 2.12.9.2 Appendix B – Libra Static Impact Analysis Input File

```
ti static impact analysis
*
mc 23
*option list_input
option lh_check
*
lc 1,1, 0,0,0, 0,1,0, 0,0,1 ; head-on drop
lc 2,2, 0,0,0, 1,0,0, 0,0,1
*
skip
cnd 1, 23.3,-8,0
, 2, 37.5,-8,0
, 3, 37.5,27.9,0
, 4, 23.3,13.3,0
, 5, 20.1,16.5,0
, 6, 25.6,33.4,0
, 7, 13.3,36.7,0
, 8, 13.3,29.125,0
, 9, 3.0,16.5,0
, 10, 3.0,29.125,0
, 11, 19.4,35.3,0
, 12, 31.7,30.9,0
, 13, 13.3,16.5,0
*
* generate first meridian
*
g10
9,9, 1,1, 8,1, 0,1
1,2,3,4
-1
*
g10
9,5
4,3,6,5
6, 12
-1
*
g10
9,5
5,6,7,13
6, 11
-1
*
g10
5,6
9,13,8,10
-1
*
* merge nodes
*
me 0.05
end
```

```

skip
*
* generate 3d region
*
g32
  15,180, 1000,0
*
* center section
*
nd 101001, 0,16.5,0, 6, 0,2.525,0
el 101001,20,1,101001, 172, 1172,101002, 177, 1177,5,1,5,5,1,5,5
el 101011,20,1,101001, 1172, 2172,101002, 1177, 2177,5,1,5,5,1,5,5
el 101021,20,1,101001, 2172, 3172,101002, 2177, 3177,5,1,5,5,1,5,5
el 101031,20,1,101001, 3172, 4172,101002, 3177, 4177,5,1,5,5,1,5,5
el 101041,20,1,101001, 4172, 5172,101002, 4177, 5177,5,1,5,5,1,5,5
el 101051,20,1,101001, 5172, 6172,101002, 5177, 6177,5,1,5,5,1,5,5
el 101061,20,1,101001, 6172, 7172,101002, 6177, 7177,5,1,5,5,1,5,5
el 101071,20,1,101001, 7172, 8172,101002, 7177, 8177,5,1,5,5,1,5,5
el 101081,20,1,101001, 8172, 9172,101002, 8177, 9177,5,1,5,5,1,5,5
el 101091,20,1,101001, 9172,10172,101002, 9177,10177,5,1,5,5,1,5,5
el 101101,20,1,101001,10172,11172,101002,10177,11177,5,1,5,5,1,5,5
el 101111,20,1,101001,11172,12172,101002,11177,12177,5,1,5,5,1,5,5
el 101121,20,1,101001,12172,13172,101002,12177,13177,5,1,5,5,1,5,5
el 101131,20,1,101001,13172,14172,101002,13177,14177,5,1,5,5,1,5,5
el 101141,20,1,101001,14172,15172,101002,14177,15177,5,1,5,5,1,5,5
*
cs 0
*
* inside foam bc
*
bc 101001,1,1, 2,0
bc 1,16,1000, 13,0
, 10,16,1000, 13,0
, 19,16,1000, 13,0
, 28,16,1000, 13,0
, 37,16,1000, 13,0
, 46,16,1000, 13,0
, 55,16,1000, 13,0
, 64,16,1000, 123,0
, 73,16,1000, 123,0
, 91,16,1000, 123,0
, 100,16,1000, 123,0
, 109,16,1000, 123,0
, 118,16,1000, 123,0
, 136,16,1000, 2,0
, 145,16,1000, 2,0
, 154,16,1000, 2,0
, 163,16,1000, 2,0
, 176,16,1000, 2,0
, 175,16,1000, 2,0
, 174,16,1000, 2,0
, 173,16,1000, 2,0
, 172,16,1000, 2,0
*

```

```

* symmetry bc
*
nd 100001, -50, -8,0
, 100002, 50, -8,0
, 100003, 0, 50,0
*locate_bc 100001,100002,100003, 0.1,3,0, 0
*
me 0.05
*
* properties
*
* 20 lb foam @ 70 deg F
pr 1, 101
, 101, 0.3, .1,1890, .2,1915, .3,1940, .4,2168, 102
, 102, .5,2604, .6,3561, .65,4858, .7,5397
*
* bi-linear foam stress-strain properties
*pr 1, 101
, 101, 0.3, .1,1900, .2,2440, .3,2980, .4,3520, 102
, 102, .5,4060, .6,4600, .65,4870, .7,5140
*
pr 201,202,0.125
, 28.0E6,0.3,1.0E-5,0.000776, 1.0E6,40.0E3
*
* MAIN23 solution data
*
SC 700,0,0.01, 0.002,1,50, 0,1,8.0e6
*
end

```

### 2.12.9.3 Additional Information (December 1, 2011)

#### 2.12.9.3.1 Contact Elements in Foam-Cask Model

The two input files used to develop the presentation in Appendix 2.12.9 are:

- foam-cask.t5
- head-on-drop.t5

The foam-drop.t5 input file is a dynamic analysis, while the head-on-drop.t5 input file is a static analysis similar to the analyses used in the SAR. In many LIBRA analyses, the input file type is designated as t5. This is a throw-back to when input data was on TAPE 5.

In the dynamic analysis, foam-cask.t5, both the foam-ground and foam-cask contacts are modeled by STIF1 elements. The LIBRA STIF1 elements can model gapped, contact interfaces, as described in the LIBRA help file for STIF1, listed below.

Figure 2-79 is an illustration of the foam-cask.t5 Libra model, and shows the application of STIF1 elements as gapped interfaces. In Figure 2-79 the blue region is the foam, and the green region is the cask. STIF1 gap elements 3001 through 3007 model the interface between the ground and foam, while elements 2001 through 2012 model the interface between the foam and cask. In the dynamic analysis, both foam and cask are assigned an initial velocity corresponding to a 30-ft. free fall, and impact forces are based upon gap closures.

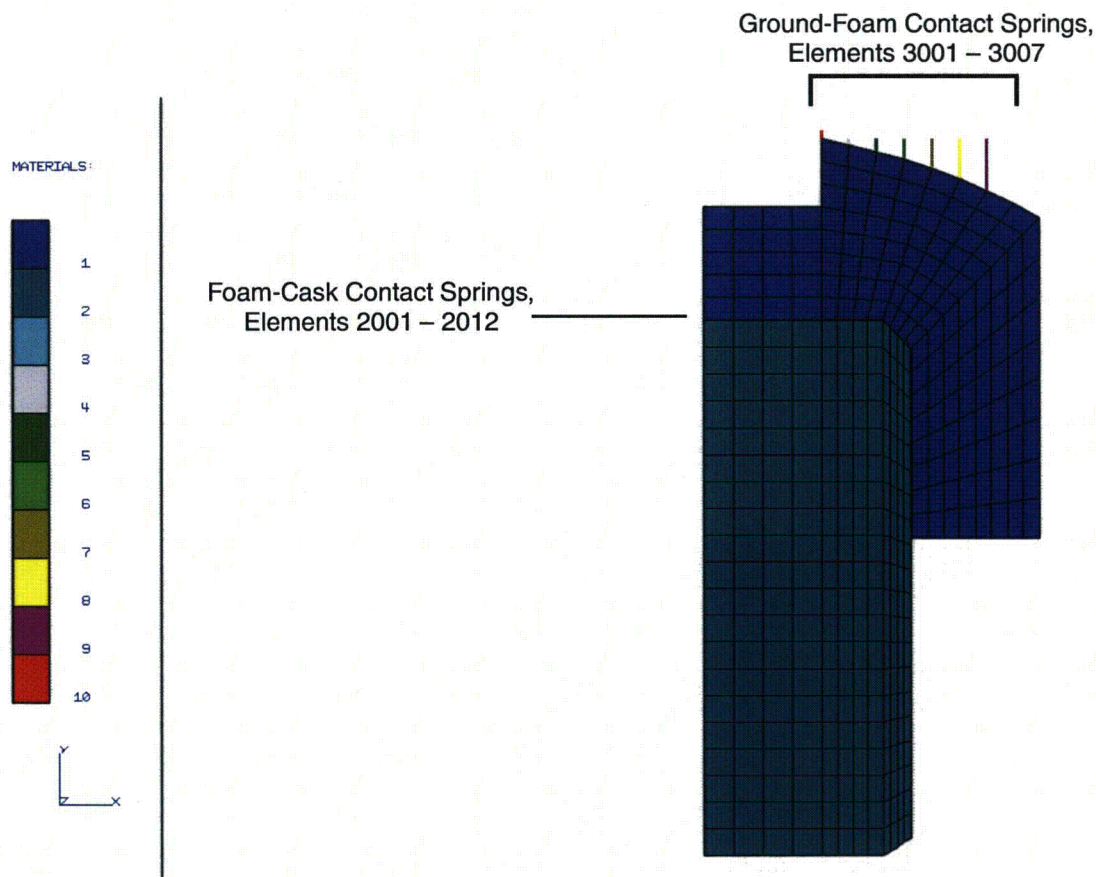


Figure 2-79. foam-cask.t5 LIBRA Model

### 2.12.9.3.2 Spring/Gap Element (STIF1)

STIF1 is a single degree of freedom spring element. The element is oriented by the two element nodes, or by a specified local coordinate system. The element can be applied in elastic, and elasto-plastic problems. This element can be used in both 2D and 3D problems.

STIF1 can be used to specify compression- or tension-only gaps in MAIN2 and MAIN9 analyses. If used as a gap element, the plasticity flag must be set on the Solution Control record. A single element cannot be modeled as both gapped and elasto-plastic.

If STIF1 is used as a gap element, LIBRA uses the penalty method to model the gap. As a result, it is important to enter a reasonably accurate value for the elastic stiffness; otherwise, the solution can be inaccurate. One method for determining nodal stiffness values is to apply unit loads in linear, static analyses.

#### 2.12.9.3.2.1 STIF1 Element Property Record

Table 2-338. STIF1 Element Property Record

Item	Description	Symbol
	Descriptor (PR)	
	Property set number	NM
1	Elastic stiffness	K
2	Inelastic stiffness	K1
3	Spring yield force	F <sub>y</sub>
4	Flag for gap/compression only effects <sup>a, b</sup>	IGAP
5	Initial gap value <sup>c</sup>	GAP
6	Local coordinate system for orienting spring <sup>d</sup>	NLCS
7	Dummy entry	(0)
8	Set initial gap to element length <sup>e</sup>	LGAP

a. Set IGAP = 1 for a compression-only gap; set IGAP=2 for a tension-only gap; otherwise, for ordinary spring, set IGAP = 0.

b. Gap elements are considered to be elastic; however, dummy values must be entered for K1 and F<sub>y</sub>, to maintain their data position.

c. GAP is entered as a positive value. For element nodal displacements U1 and U2, gaps are closed when the following is true:

$$\text{Compression (IGAP = 1)} \quad U2-U1 < -GAP$$

$$\text{Tension (IGAP = 2)} \quad U2-U1 > GAP$$

d. By default, the spring and gap are oriented by the two element nodes. To specify the spring and gap orientation, set NLCS to the number of a local coordinate (LC) system that defines the orientation. The spring is then oriented along the NLCS x-axis, and the gap is measured along the NLCS x-axis, with a positive gap in the +x direction.

e. If LGAP = 1, the initial gap size is set to the element length.

#### 2.12.9.3.2.2 STIF1 Stress Output

Post processing data components for both elastic and inelastic problems are spring load (P) and spring deflection (d).

### 2.12.10 Effect of Ribs on Stress at Foam-Cask Interface

The effect of ribs inside the foam at the cask-cask lid interface is analyzed by the FEA model shown in Figure 2-80 and Figure 2-81. This model represents a section of foam impact limiter, steel cask, and steel rib, simplified by removing curvature. The section analyzed is a 10 × 10 × 10 in. foam block, positioned on a 5-in. section of the steel cask, and a steel rib embedded inside the foam block. The entire FEA model contains approximately 320,000 DOF, and is shown in Figure 2-80. The embedded rib is shown in the FEA model section in Figure 2-81. The nodal spacing throughout the model is 0.25 in. In the analysis, a uniform, 1-in., Z-displacement is applied to the top of the foam block, and the block is fixed in the Z-direction, at the base of the cask.

Figure 2-82 and Figure 2-83 display a central section of the cask model. Cask Z-displacement is shown in Figure 2-82, and cask Z-directional stress is shown in Figure 2-83. A central model section is selected to remove model edge effects. These two figures show that both displacement and stress perturbations due to the rib are localized to within an inch of the rib location. In accordance with Saint-Venant's Principle, these perturbations do not have a significant effect on cask stress.

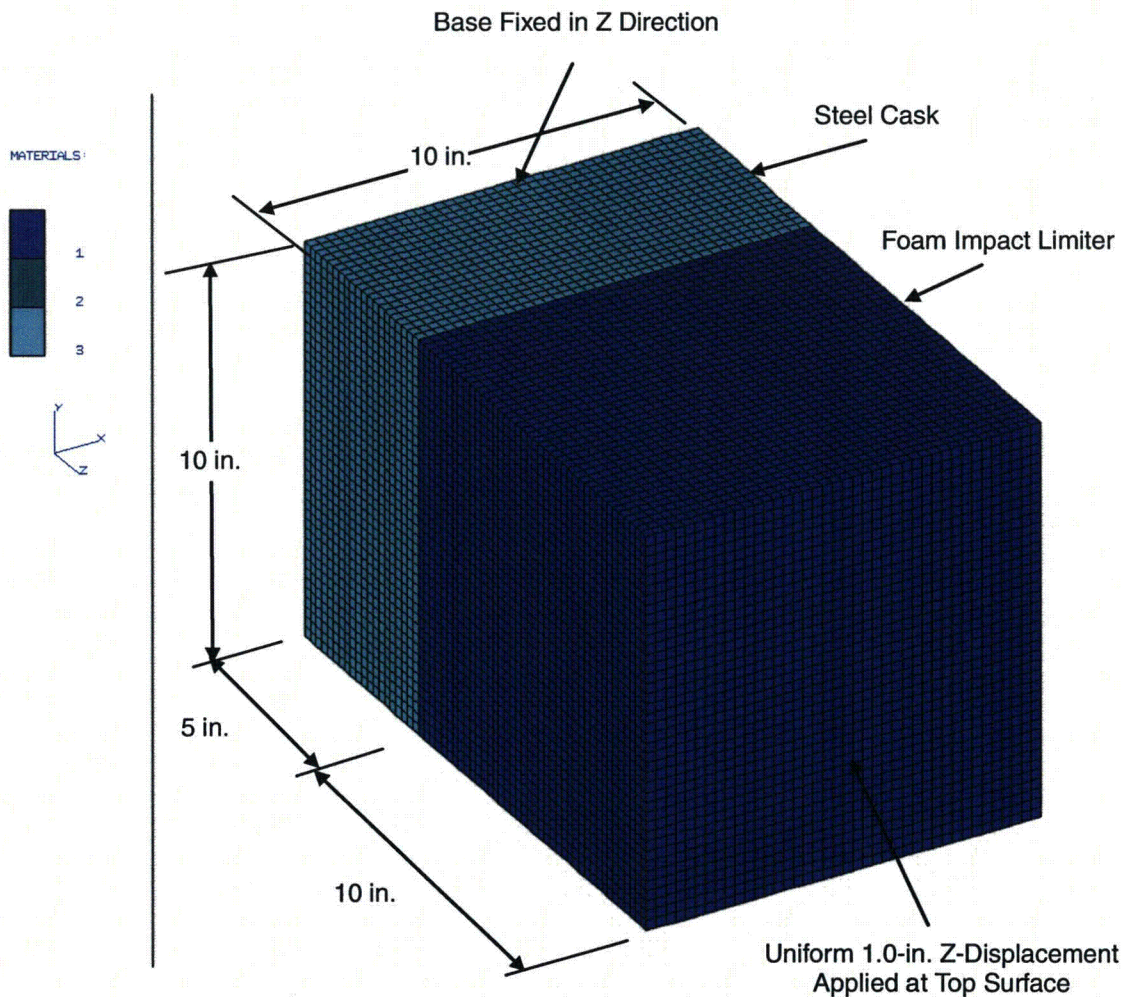


Figure 2-80. FEA Model Used in Rib Study



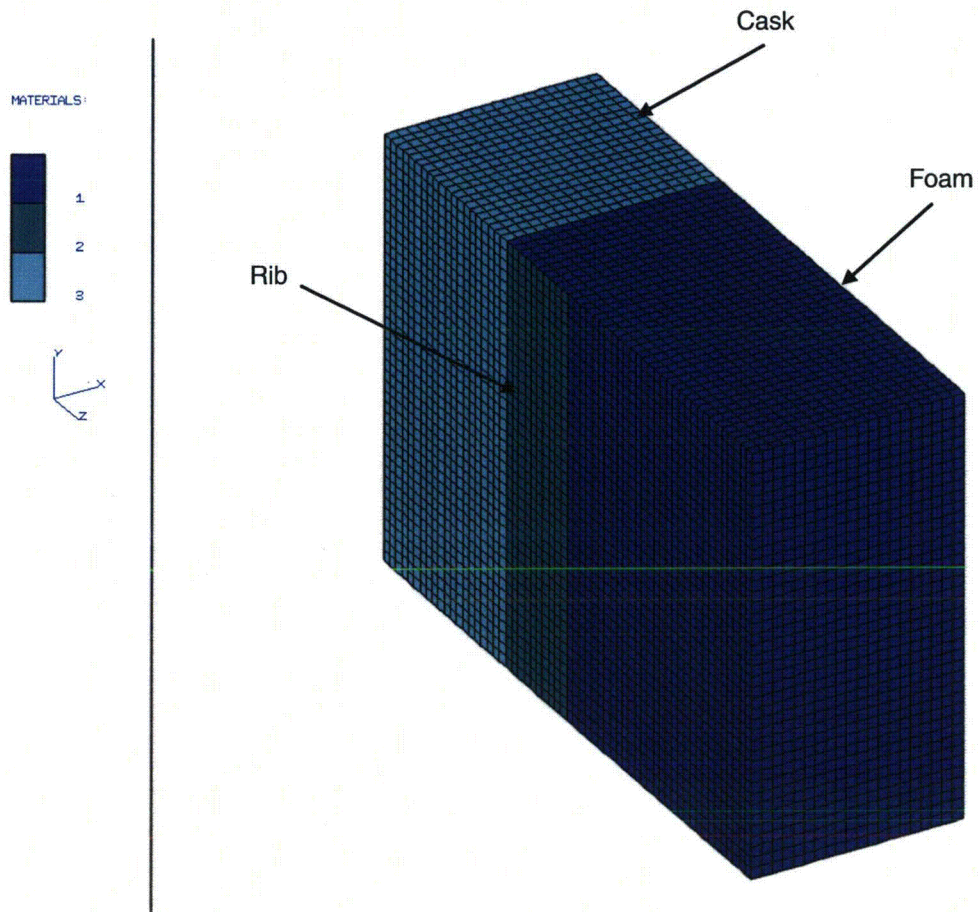


Figure 2-81. FEA Model Section Showing Rib

VECTOR: 1  
 DOF: 3  
 MIN: -6.5613E-03  
 MAX: 0.0000E+00

-6.5613E-03
-6.3269E-03
-6.0926E-03
-5.8583E-03
-5.6239E-03
-5.3896E-03
-5.1553E-03
-4.9210E-03
-4.6866E-03
-4.4523E-03
-4.2180E-03
-3.9836E-03
-3.7493E-03
-3.5150E-03
-3.2806E-03
-3.0463E-03
-2.8120E-03
-2.5776E-03
-2.3433E-03
-2.1090E-03
-1.8746E-03
-1.6403E-03
-1.4060E-03
-1.1717E-03
-9.3732E-04
-7.0299E-04
-4.6866E-04
-2.3433E-04
0.0000E+00

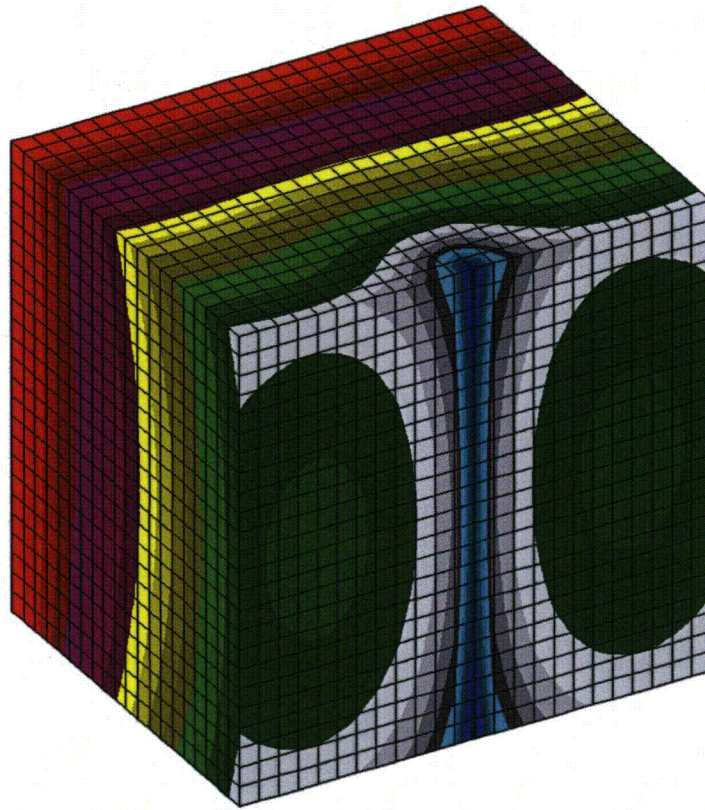


Figure 2-82. Z-Cask Section Z-Displacements

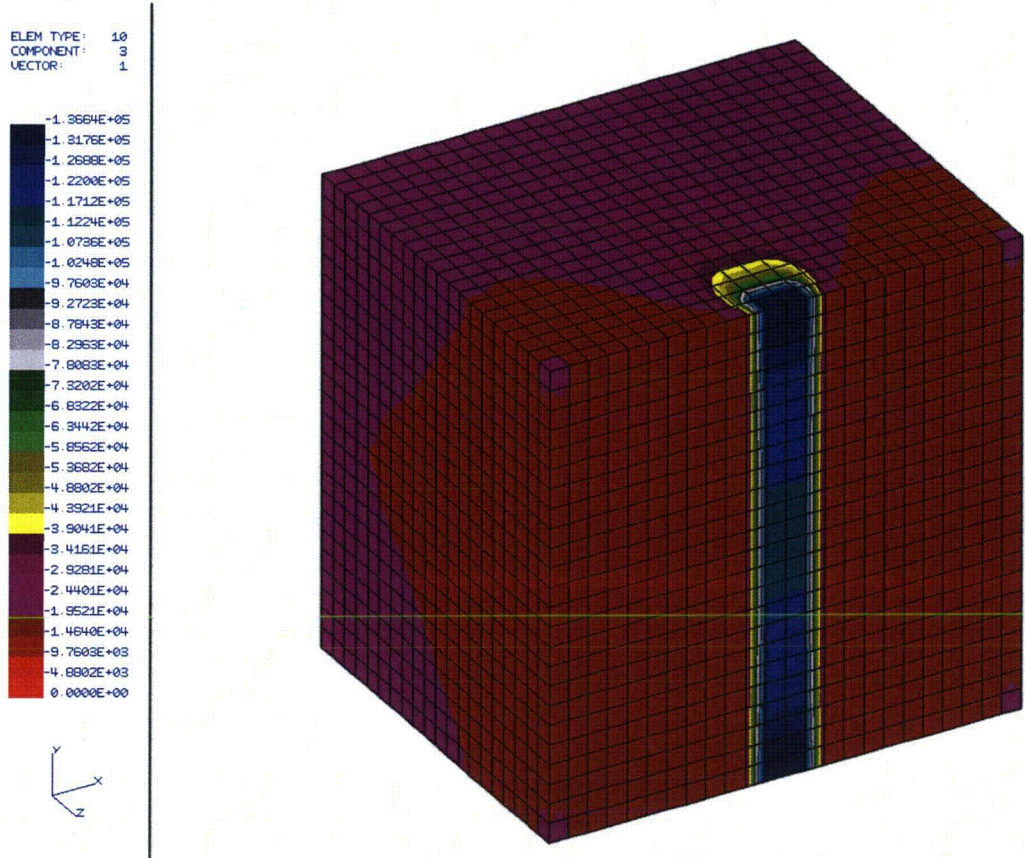


Figure 2-83. Cask Section Z-Stress

### 2.12.11 Analysis of 30-Ft. Drops with Shipping Cages

Shipping cages and pallets add to the cask impact forces for both Head-On and Cg/Corner 30-ft. Drops. In 30-ft. Side Drops, the shipping cage wire mesh panels impact the cask with negligible force. For Head-On and Cg/Corner Drops, the pallet impacts the cask through the upper impact limiter. As illustrated in Figure 2-84, the pallet impacts the upper impact limiter, while cask impacts the lower impact limiter.

The ground force reacts to both the pallet and cask inertia forces, as illustrated in Figure 2-84. In this analysis, the increase in the ground reaction force due to the pallet impact is evaluated. The upper and lower impact limiters exhibit different stiffness and frequency properties due to the difference in cask and pallet mass. As a result, the pallet inertia force and ground reaction force are not in phase. Dynamic analyses are required to account for the phase difference in the pallet and cask forces, so LIBRA-AGS analyses are performed for the 30-ft drops.

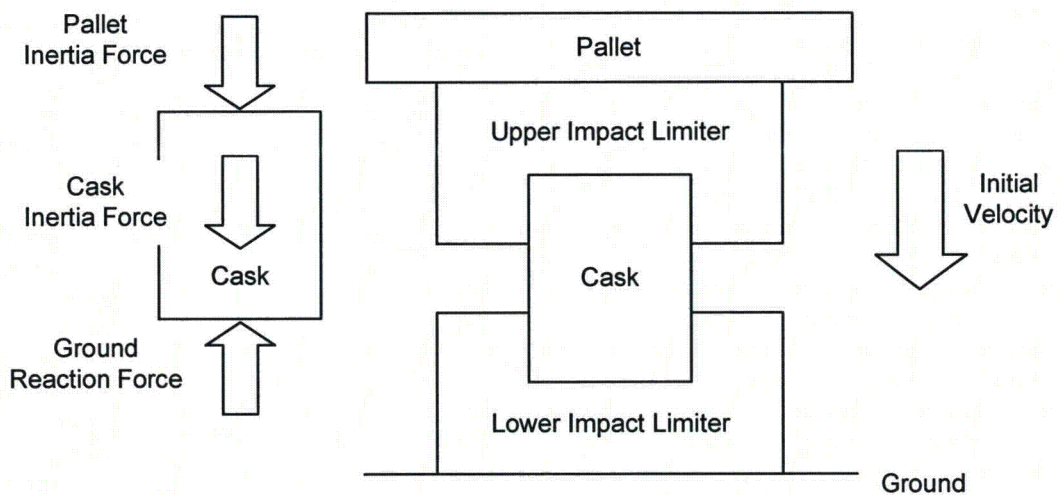


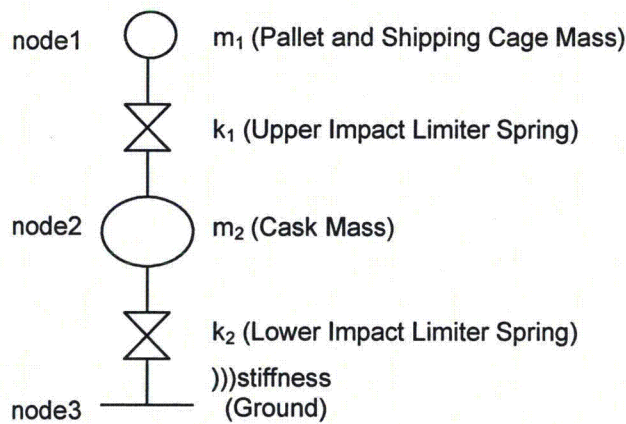
Figure 2-84. Configuration of Cask and Pallet Impact

**Note:** Figure 2-84 shows the scenario that the analysis evaluates. In this case, it is required that the assembled package be upside down.

### 2.12.11.1 Description of AGS Analyses

The LIBRA-AGS program is applied to the analyses of 30-ft. cask drops that include shipping cage impacts. The generalized dynamic model illustrated in Figure 2-85 is used for all drop analyses. The model contains two masses representing the pallet and cask, and two piecewise linear springs representing the upper and lower impact limiters. Spring stiffness values are taken from the impact limiter, load-displacement curves for 30-ft. drop analyses. A 30-ft. free-fall velocity is applied to both pallet and cask mass, as initial conditions. For each transport package model and each drop configuration, analyses are performed with, and without, the pallet mass. The effect of the pallet is measured by the difference in the ground impact force with, and without, the pallet mass.

AGS models for the Model AOS-025, AOS-050, and AOS-100 cask configurations differ only in nodal mass and element stiffness values, and AGS models for Head-On and Cg/Corner Drop analyses differ only in spring stiffness. A typical AGS input file is listed in Figure 2-85. The generalized stiffness and mass properties used in the analyses are presented in Table 2-339 and Table 2-340. Additionally, Table 2-339 lists the spring stiffness properties developed from the impact limiter load-displacement analyses. For Head-On Drop analyses, the generalized spring stiffness is modeled as bilinear. For Cg/Corner Drops, the generalized spring stiffness is modeled as trilinear.



```
ti  model 100 + pallet cg/corner drop
sc  10000,5.0e-6, 0.0,0.000, 3,0, 1
nd  1,3.88e-6
,   2,28.5
,   3,1.0
el  1,1, 1,2
,   2,1, 2,3
pr   1, 5.2e4,2.6e5, 8.6e4,6.0e5, 2.4e5,1.0e9
bc  3
iv  1,527.5
,   2,527.5
mo  1,1
,   2,1
,   1,4
,   2,4
end
```

Figure 2-85. AGS Model and Typical Input File

In Table 2-339, the first column lists the transport package model number and drop orientation. The generalized stiffness values are determined from the SAR figures listed in column 2.  $k_1$ ,  $k_2$ , and  $k_3$  are piecewise stiffness values.  $P_1$ ,  $P_2$ , and  $P_3$  are associated terminal force values. Figure 2-86 and Figure 2-87 are force-displacement plots that illustrate piecewise linear stiffness representations for the Model AOS-100. Piecewise linear stiffness representations for the Model AOS-025 and AOS-050 are similar. Table 2-340 lists the generalized pallet and cask mass values,  $m_1$  and  $m_2$ . Both the pallet and shipping cage mass are included in the  $m_1$  values.

**Table 2-339. Generalized Stiffness Properties – All Models**

Model and Drop Orientation	Reference Figure	$k_1$ (lb/in)	$P_1$ (lb)	$k_2$ (lb/in)	$P_2$ (lb)	$k_3$ (lb/in)	$P_3$ (lb)
AOS-025, Head-On	Figure 2-54	1.00E+05	6.00E+04	1.71E+05	1.00E+09	–	–
AOS-025 Cg/Corner	Figure 2-56	3.56E+04	4.00E+04	6.40E+04	8.00E+04	1.60E+05	1.00E+09
AOS-050 Head-On	Figure 2-57	8.88E+04	2.00E+05	1.37E+05	1.00E+09	–	–
AOS-050 Cg/Corner	Figure 2-59	2.91E+04	8.00E+04	5.00E+04	1.80E+05	8.22E+04	1.00E+09
AOS-100 Head-On	Figure 2-60	1.70E+05	5.00E+04	3.10E+05	1.00E+09	–	–
AOS-100 Cg/Corner	Figure 2-63	5.20E+04	2.60E+05	8.60E+04	6.00E+05	2.40E+05	1.00E+09

**Table 2-340. Generalized Pallet and Cask Mass Properties – All Models**

Model	$m_1$ (lb-sec <sup>2</sup> /in)	$m_2$ (lb-sec <sup>2</sup> /in)
AOS-025	0.142	0.505
AOS-050	0.621	3.26
AOS-100	3.88	28.5

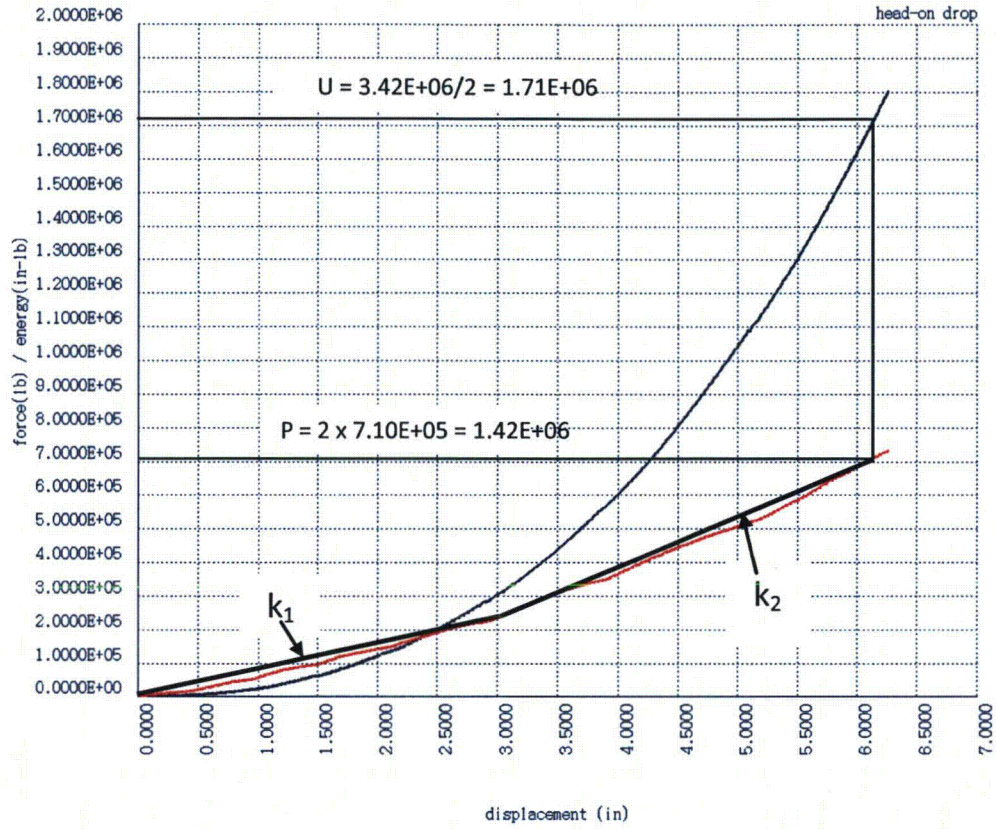


Figure 2-86. Bilinear Representation of Head-On Force-Displacement – Model AOS-100

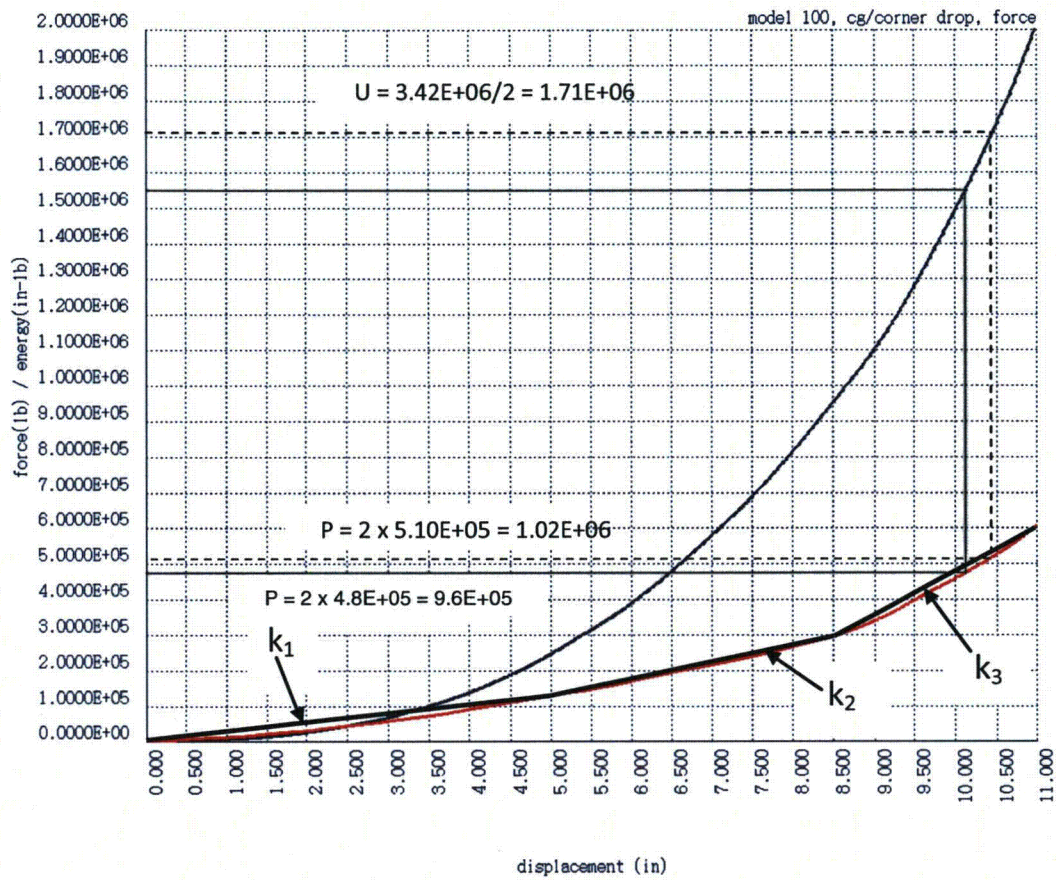


Figure 2-87. Trilinear Representation of Cg/Corner Force-Displacement – Model AOS-100



### 2.12.11.2 Results of AGS Analyses

Results of analyses for the Model AOS-100 are presented in Table 2-340, and Figure 2-88 and Figure 2-89. Figure 2-88 illustrates time-history plots of pallet mass displacement (1), and cask mass displacement (2). Figure 2-89 illustrates time-history plots of upper impact limiter spring force (3), and lower impact limiter spring force (4).

Table 2-341, Table 2-342, and Table 2-343 present results of analyses for Models AOS-025, AOS-050, and AOS-100, respectively. Each table lists maximum nodal displacements and maximum element forces. Definitions of column data for all three tables are listed after Table 2-341. Each model and drop configuration is analyzed with, and without, the pallet mass. Analyses including pallet mass are designated with "+ Pallet" (for example, "Head-On + Pallet"). Forces and displacements determined in the SAR static impact limiter analysis are included for comparison, in columns labeled  $F_s$  and  $\delta_s$ .

Table 2-344 presents the change in ground impact forces due to the pallets. The  $F_s$  column lists the impact forces determined in the impact limiter static drop analyses. The  $\Delta F$  column lists the increase in dynamic impact force due to the pallet. Values for  $\Delta F$  are differences in  $P_2$  force for impacts with, and without, the pallet. Using the information presented in Table 2-341, Table 2-342, and Table 2-343,  $\Delta F$  is the difference between rows 1 and 2 for Head-On Drops, and rows 3 and 4 for Cg/Corner Drops. The  $F_T$  column lists the sum of  $F_s$  and  $\Delta F$ . The Ratio column lists the  $F_T / F_s$  values, and measures the change in ground impact force due to pallet impact.

**Table 2-341. AGS Analysis – Model AOS-025**

Drop	$\delta_1$ (in.)	$\delta_2$ (in.)	$F_1$ (lbs.)	$F_2$ (lbs.)	$\delta_s$ (in.)	$F_s$ (lbs.)	Ratio
Head-On	–	1.09	–	1.46E+05	1.10	1.40E+05	–
Head-On + Pallet	1.35	1.09	0.30E+05	1.44E+05	–	–	1.06
Cg/Corner	–	1.86	–	9.84E+04	1.90	10.0E+04	–
Cg/Corner + Pallet	2.77	1.93	3.80E+04	10.9E+04	–	–	1.11

where:

- $\delta_1$  = Pallet deflection
- $\delta_2$  = Cask deflection
- $F_1$  = Upper impact limiter spring force
- $F_2$  = Lower impact limiter spring force
- $\delta_s$  = Foam static analysis displacement
- $F_s$  = Foam static analysis force
- Ratio = Ratio of  $P_2$  with pallet to  $P_2$  without pallet

**Table 2-342. AGS Analysis – Model AOS-050**

Drop	$\delta_1$ (in.)	$\delta_2$ (in.)	$F_1$ (lbs.)	$F_2$ (lbs.)	$\delta_s$ (in.)	$F_s$ (lbs.)	Ratio
Head-On	–	3.13	–	3.20E+05	3.25	3.40E+05	–
Head-On + Pallet	4.19	3.28	8.55E+04	3.40E+05	–	–	1.06
Cg/Corner	–	5.18	–	2.15E+05	5.30	2.40E+05	–
Cg/Corner + Pallet	7.12	5.36	5.91E+04	2.30E+05	–	–	1.07

**Table 2-343. AGS Analysis – Model AOS-100**

Drop	$\delta_1$ (in.)	$\delta_2$ (in.)	$F_1$ (lbs.)	$F_2$ (lbs.)	$\delta_s$ (in.)	$F_s$ (lbs.)	Ratio
Head-On	–	6.17	–	1.50E+06	6.10	1.42E+06	–
Head-On + Pallet	8.03	6.37	3.00E+05	1.56E+06	–	–	1.04
Cg/Corner	–	10.9	–	1.07E+06	10.5	1.02E+06	–
Cg/Corner + Pallet	14.4	11.1	2.09E+05	1.12E+06	–	–	1.05

**Table 2-344. Increased Ground Impact Forces – All Models**

Model	Drop Orientation	$F_s$ (lbs.)	$\Delta F$ (lbs.)	$F_T$ ( $F_s + \Delta F$ ) (lbs.)	Ratio ( $F_T / F_s$ )
AOS-025	Head-On	1.44E+05	0.80E+04	1.52E+05	1.06
	Cg/Corner	1.00E+05	1.06E+04	1.11E+05	1.11
AOS-050	Head-On	3.40E+05	2.00E+04	3.60E+05	1.06
	Cg/Corner	2.40E+05	1.50E+04	2.55E+05	1.06
AOS-100	Head-On	1.42E+06	6.00E+04	1.48E+06	1.04
	Cg/Corner	1.02E+06	5.00E+04	1.07E+06	1.05

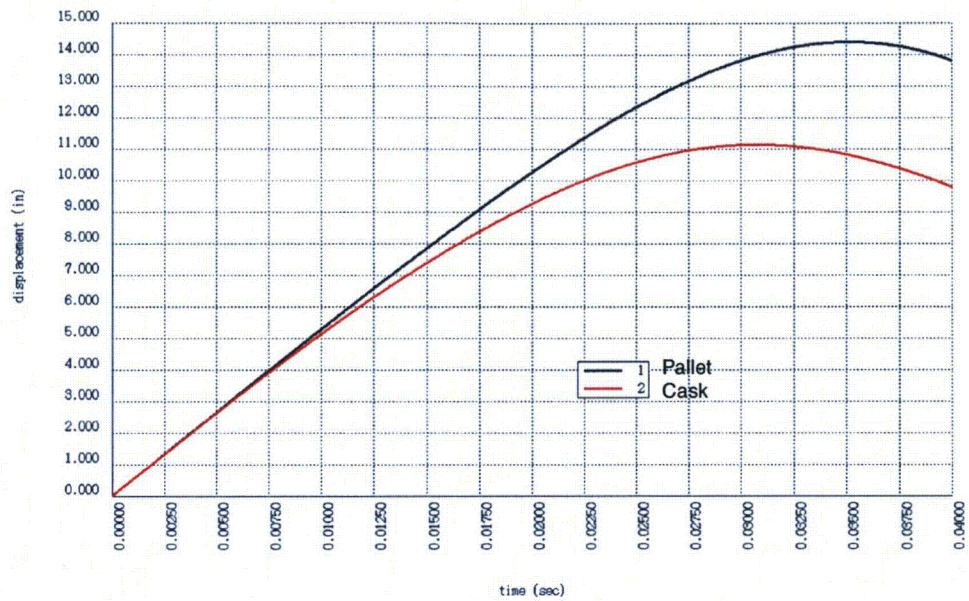


Figure 2-88. Model AOS-100 Cg/Corner Pallet and Cask Displacements

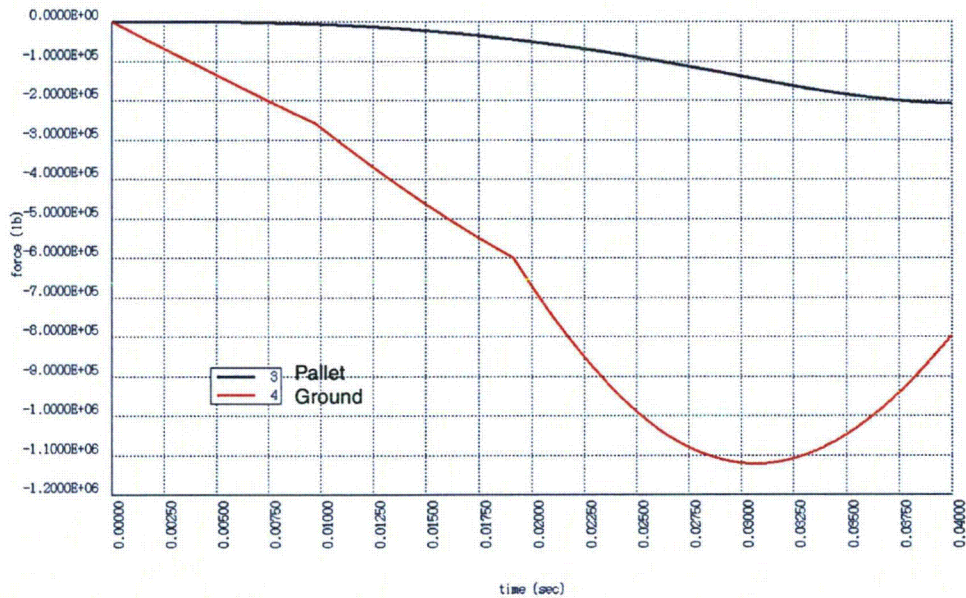


Figure 2-89. Model AOS-100 Cg/Corner Pallet and Ground Impact Forces

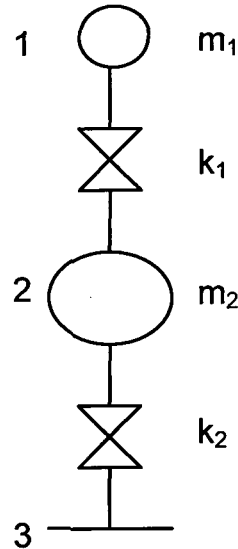
### 2.12.11.3 AGS Input Data for Cask and Pallet 30-Ft. Drop Analyses

```

ti    cask and pallet drop
*
sc    50000,5.0e-7, 0.0,0.000, 3,0, 0
*
*    model 100
*nd   1,3.88
*nd   2,28.5
*nd   3,1.0
*
*    model 050
nd    1,0.621
nd    2,3.26
nd    3,1.0
*
*    model 025
*nd   1,0.142e
*nd   2,0.505
*nd   3,1.0
*
el    1,1, 1,2
,     2,1, 2,3
*
*    100 head-on
*pr   1, 1.7e5,5.0e5, 3.1e5,1.0e9
*    100 cg/corner

*pr   1, 5.2e4,2.6e5, 8.6e4,6.0e5, 2.4e5,1.0e9
*
*    050 head-on
*pr   1, 8.88e4,2.00e5, 1.37e5,1.00e9
*    050 cg/corner
pr    1, 2.91e4,8.00e4, 5.00e4,1.80e5, 8.22e4,1.00e9
*
*    025 head-on
*pr   1, 1.00e5,6.00e4, 1.70e5,1.00e9
*    025 cg/corner
*pr   1, 3.56e4,4.00e4, 6.40e4,8.00e4, 1.60e5,1.0e9
*
bc    3
*
iv    1,527.5
,     2,527.5
*
mo    1,1
,     2,1
,     1,4
,     2,4
*
end

```



## 2.12.12 Analysis of Tie-Down Devices

### 2.12.12.1 Introduction

The Model AOS-050 and AOS-100 cask transport tie-down system is illustrated in Figure 2-90. The system consists of cables (four (4) in the Model AOS-050; eight (8) in the Model AOS-100), a shipping cradle under the lower LAST-A-FOAM FR-3700 series foam, and a tie-down ring over the upper LAST-A-FOAM FR-3700 series foam. The postulated inertia loading is 10g forward, 5g lateral, and 2g vertical. Lateral and vertical inertia forces are illustrated in Figure 2-90, as F and W, respectively. In Figure 2-90, the dimension H is the distance from the cask's center of gravity to lateral support.

The Model AOS-025 uses four tie-down straps.

Analyses are performed for 10g forward and 2g vertical inertia loads. Stress due to the 5g lateral load is interpolated from the 10g forward load analysis, because the tie-down configuration is axisymmetric. Stresses due to the three (3) inertia loads are combined where required, and compared to allowable stresses.

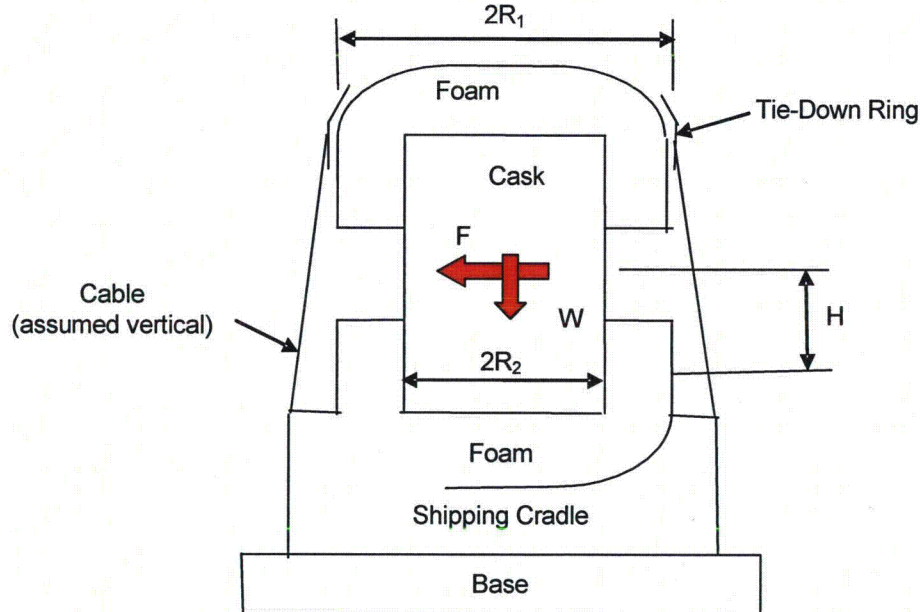


Figure 2-90. Tie-Down Schematic

### 2.12.12.2 Base Foam Vertical Bearing Force

The inertia force,  $F$ , illustrated in Figure 2-90 is assumed to produce the foam bearing traction illustrated in Figure 2-91, at the shipping cradle. The foam bearing traction is assumed sinusoidal in the circumferential direction, and linear in the horizontal direction, as illustrated in Figure 2-91. The bearing traction is provided by:

$$p = (\rho_0 / 2R_1) * (1 - \cos\theta) * r$$

where:

$$\rho_0 = \text{Maximum bearing traction}$$

The total bearing force is then:

$$\begin{aligned} P &= \rho_0 / 2R_1 \int_0^{2\pi} \int_{R_2}^{R_1} (1 - \cos\theta) * r^2 * dr * d\theta \\ &= \pi\rho_0 (R_1^3 - R_2^3) / 3R_1 \end{aligned}$$

The moment due to the bearing force is:

$$\begin{aligned} M &= \rho_0 / 2R_1 \int_0^{2\pi} \int_{R_2}^{R_1} (1 - \cos\theta)^2 * r^3 * dr * d\theta \\ &= 3\pi\rho_0 (R_1^4 - R_2^4) / 8R_1 \end{aligned}$$

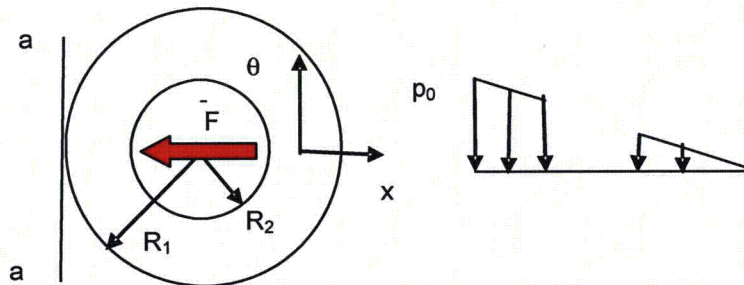


Figure 2-91. Bearing Traction Along Line  $\theta = 0 - 180$

The overturning moment about the axis a-a in Figure 2-91 due to the inertia force is  $F * H$ :

$$F * H = (3\pi p_0 / 8R_1) * (R_1^4 - R_2^4)$$

Solving for maximum bearing traction:

$$p_0 = 8F * H * R_1 / (3\pi (R_1^4 - R_2^4))$$

Vertical foam bearing traction due to  $W$  is:

$$p_1 = W / [\pi (R_1^2 - R_2^2)]$$

### 2.12.12.3 Base Foam Lateral Bearing Force

The foam bearing force at the shipping cradle wall due to inertia force,  $F$ , is illustrated in Figure 2-92. The traction distributions are assumed to be sinusoidal in the circumferential direction. For vertical bearing length  $B$ , the total wall bearing force is:

$$F = 2B \int_0^{\pi/2} q * R_1 * \cos\theta * d\theta$$

Integrating:

$$F = 2B * R_1 * q$$

$$q = F / 2B * R_1$$

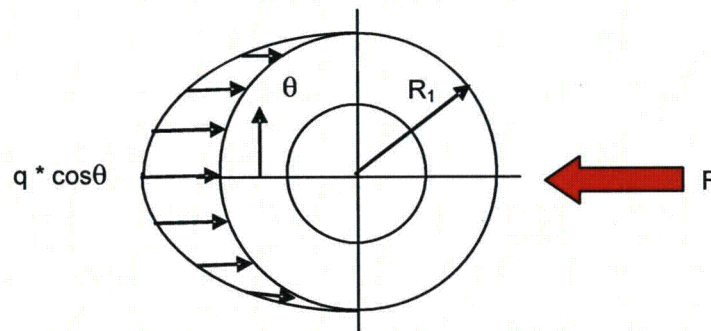


Figure 2-92. Schematic of Lateral Bearing Forces



#### 2.12.12.4 Summary of Stress Equations for Base Foam

B = Lateral shipping cradle wall bearing length

F = Lateral inertia force

H = Lateral inertia force moment arm

R<sub>1</sub> = Outside foam radius

R<sub>2</sub> = Inside foam radius

T = Cable tension force

W = Vertical inertia force

1. Foam vertical traction due to inertial overturning moment:

$$p_0 = 8F * H * R_1 / 3\pi (R_1^4 - R_2^4)$$

2. Foam vertical traction due to vertical inertia:

$$p_1 = W / \pi (R_1^2 - R_2^2)$$

3. Foam horizontal traction due to lateral inertia:

$$q = F / 2B * R_1$$

### 2.12.12.5 Cable Force

The cable forces react the overturning moment due to the inertia force,  $F$ , and height,  $H$ , in Figure 2-90. Moment equilibrium is taken about axis a-a in Figure 2-93, with cable forces assumed proportional to the distance from axis a-a.

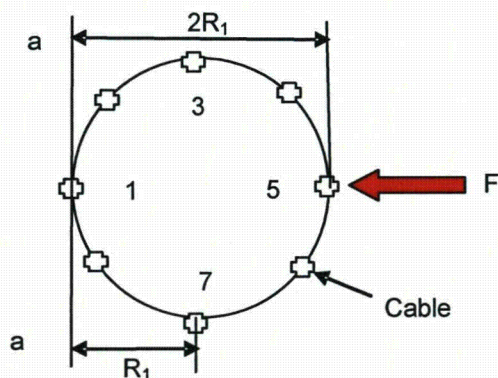


Figure 2-93. Tension Cables – Model AOS-100

Table 2-345. Model AOS-100 Cable Loads

Cable	d	P / T	d * P / T	P (k)
1	0.00000	0.00000	0.00000	0.0000
2	6.73654	0.14645	0.98656	3.0560
3	23.0000	0.50000	11.5000	10.435
4	39.2635	0.85355	33.5134	17.813
5	46.0000	1.00000	46.0000	20.870
6	39.2635	0.85355	33.5134	17.813
7	23.0000	0.50000	11.5000	10.435
8	6.73654	0.14645	0.98656	3.0560
$\Sigma$	-	4.00000	138.000	83.478

where:

- d = Distance to axis a-a
- T = Maximum cable tension force
- P = Cable tension force, in kips (k)

From Figure 2-90:

$$M = F * H$$

$$F = 120 \text{ k}$$

$$H = 24 \text{ in.}$$

$$M = 120 * 24 = 2,880 \text{ in-k}$$

From Table 2-345, the maximum and total cable forces are:

$$M = \sum d * P / T$$

$$T = M / 138 = 2,880 / 138 = 20.870 \text{ k}$$

$$\sum P = 4.00 * 20.870 = 83.480 \text{ k}$$

### 2.12.12.6 Tie-Down Ring Foam Bearing Pressure

The tie-down ring is in equilibrium under the cable forces and foam bearing pressures, as illustrated in Figure 2-94. The bearing pressure due to the cable resultant forces is:

$$\begin{aligned} p &= P / A \\ P &= 83.478 \\ A &= \pi * (R_1^2 - R_2^2) = 857.7 \text{ in}^2 \\ p &= 0.0973 \text{ lb/in}^2 \end{aligned}$$

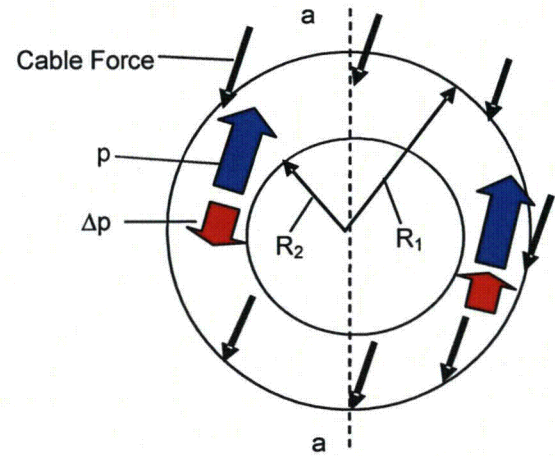


Figure 2-94. Bearing Pressure and Cable Forces

### 2.12.12.7 Tie-Down Ring Foam Differential Bearing Pressure

The moment about axis a-a in Figure 2-94 due to differential bearing pressure is:

$$\begin{aligned}M' &= 4 * \Delta p \int_0^{\pi/2} \int_{R_2}^{R_1} \cos\theta * r^2 * dr * d\theta \\ &= 4 / 3 * (R_1^3 - R_2^3) * \Delta p \\ \Delta p &= M' / [4 / 3 * (R_1^3 - R_2^3)]\end{aligned}$$

From Table 2-345, the moment about axis a-a in Figure 2-95 is:

$$\begin{aligned}M' &= M - (\Sigma P * R_1) \\ &= 2,880 - (83.480 * 23.0) \\ &= 961.34 \text{ in-k} \\ \Delta p &= 961.34 / 10,761 = 0.0893 \text{ lb/in}^2 \\ p + \Delta p &= 187.0 \text{ lb/in}^2 \\ p - \Delta p &= 8.000 \text{ lb/in}^2\end{aligned}$$

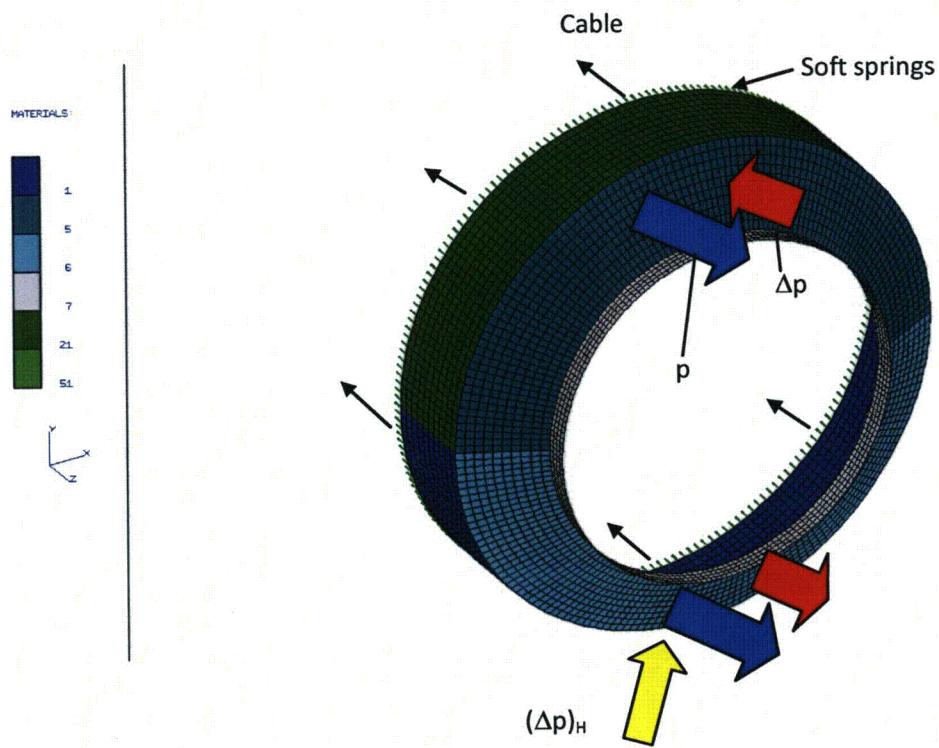


Figure 2-95. FEA Model of Tie-Down Ring

### 2.12.12.8 Horizontal Component of Differential Pressure

The  $\Delta p$  pressure acting on the conical shell produces a horizontal force resultant:

$$\begin{aligned} P_H &= 4 * \Delta p * \sin\alpha \int_0^{\pi/2} \int_{R_2}^{R_1} \cos\theta * r * dr * d\theta \\ &= 2 * \Delta p * \sin\alpha * (R_1^2 - R_2^2) \end{aligned}$$

where:

$$\alpha = \text{Conical shell base angle}$$

For radius,  $R_1$ , and cylinder height,  $h$ :

$$P_H = P_H / 2R_1 * h$$

$$P_H = 2 * 89.3 * \sin 27.2^\circ = 2.23 \times 10^4 \text{ lbs.}$$

$$p_H = 2.23 \times 10^4 / 46.0 * 9.0 = 53.8 \text{ psi}$$

### 2.12.12.9 Analysis of Tie-Down Ring

The tie-down ring is analyzed for a 10g lateral inertia force by finite elements, using the FEA model illustrated in Figure 2-95. The ring is analyzed as a shell structure, and the FEA model contains 26,400 DOF, with 4,400 nodes and 4,300 quad shell elements. The model is composed of two primary sections – a cylindrical shell and a conical shell. A ring of soft springs is modeled about the base of the cylindrical section to react out-of equilibrium forces.

The loads applied to the model are illustrated in Figure 2-95. These loads are in equilibrium, and consist of the cable loads developed in Table 2-345, and bearing tractions on the conical and cylindrical shells. In Figure 2-95, the resultants of the bearing pressure,  $p$ , and differential bearing pressure,  $\Delta p$ , balance the cable force and cable moment resultants. The differential pressure,  $\Delta p$ , acting on the conical shell produces a horizontal force resultant, and this resultant is balanced by the pressure  $(\Delta p)_H$  applied to the cylindrical shell.

Results of the tie-down ring stress analysis are presented in Figure 2-96 and Figure 2-97. Figure 2-96 illustrates lateral displacement of the conical shell, and Figure 2-97 illustrates the outer fiber maximum principal stress in the conical shell.

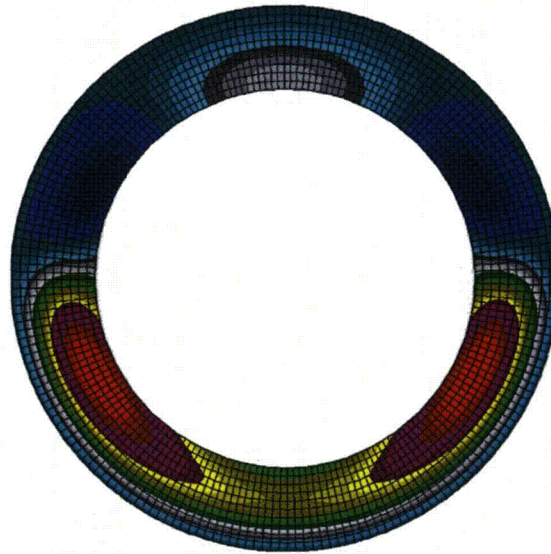


Figure 2-96. Lateral (Z) Displacement in Conical Shell – Model AOS-100

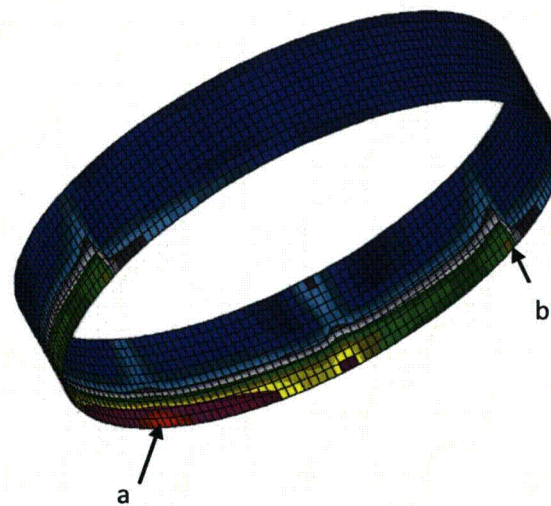


Figure 2-97. Maximum Principal Membrane Stress – Model AOS-100



### 2.12.12.10 Stress in Foam – Model AOS-100

The foam stress is limited to 10% strain to avoid excessive deformation. From the *Design Guide for Use of LAST-A-FOAM FR-3700 for Crash & Fire Protection of Radioactive Material Shipping Containers* (Reference [2.13]):

$$\begin{aligned}\sigma &= Y_{\text{int}} (\rho)^S \\ Y_{\text{int}} &= 4.3422 \\ \rho &= 12 \\ S &= 1.8809 \\ \sigma &= 4.3422 * 107.1 = 465.1 \text{ psi}\end{aligned}$$

Applying equations in Appendix 2.12.12.4:

$$\begin{aligned}B &= \text{Shipping cradle wall length} && 8.0 \text{ in.} \\ F &= \text{Lateral force} && 120,000.0 \text{ lbs.} \\ H &= \text{Cask center of gravity to shipping cradle} && 24.0 \text{ in.} \\ R_1 &= \text{Outside foam radius} && 23.0 \text{ in.} \\ R_2 &= \text{Inside foam radius} && 14.0 \text{ in.} \\ W &= \text{Vertical force} && 24,000.0 \text{ lbs.}\end{aligned}$$

Base foam vertical bearing stress (psi):

$$p = 8F * H * R_1 / 3\pi (R_1^4 - R_2^4) + W / \pi (R_1^2 - R_2^2) = 234 \text{ psi} (< 465.1)$$

Base foam lateral bearing stress (psi):

$$q = F / 2B * R_1 = 310 \text{ psi} (< 465.1)$$

From Appendix 2.12.12.7, the maximum foam bearing stress at the conical shell:

$$p + \Delta p = 187.0 \text{ psi} (< 465.1)$$

From Appendix 2.12.12.8, the maximum foam bearing stress at the cylindrical shell:

$$p_H = 107.7 \text{ psi} (< 465.1)$$

### 2.12.12.11 Stress in Tie-Down Ring – Model AOS-100

Figure 2-97 shows the maximum principal membrane stress for bending about the x-axis. The maximum stress occurs at location 'a', and is 31.7 ksi. For bending about the y-axis, the stress at location 'b' corresponds to the stress at location 'a'. The stress at location 'b' is 18.5 ksi for 10g loading. The combined stress due to 10g about the x-axis, and 5g about the y-axis, is then:

$$f = 32.2 + (1 / 2) * 18.5 = 41.5 \text{ ksi}$$

For AMS 4144F, aluminum alloy 2219T851, yield stress  $F_y = 46.0$  ksi:

$$MS = 46.0 / 41.5 - 1.0 = 0.11$$

### 2.12.12.12 Stress in Cables – Model AOS-100

$$P_1 = \text{Maximum cable load (Table 2-345, cable 5) due to 10g forward inertia}$$

$$P_2 = \text{Maximum cable load due to 5g lateral inertia}$$

$$P_3 = \text{Cable load due to 1g vertical inertia}$$

$$P_1 = 20.9 \text{ k}$$

$$P_2 = (1 / 2) * 20.9 = 10.5 \text{ k}$$

$$P_3 = 12 / 8 = 1.5 \text{ k}$$

$$P = P_1 + P_2 + P_3 = 32.9 \text{ k}$$

From *ASTM F1145 - 05(2011)*, Table 3 (Reference [2.27]), Jaw-Jaw,  $P_u = 60$  k:

$$MS = 60 / 32.9 - 1.0 = 0.82$$

### 2.12.12.13 Forces – Model AOS-050

**Note:** Refer to Appendix 2.12.12.7 and Appendix 2.12.12.8 for further details.

Maximum cable tension, moment about axis a-a:

$$M = F * H = 2R_1 * (T / 2) + R_1 * 2T = 3R_1 * T$$

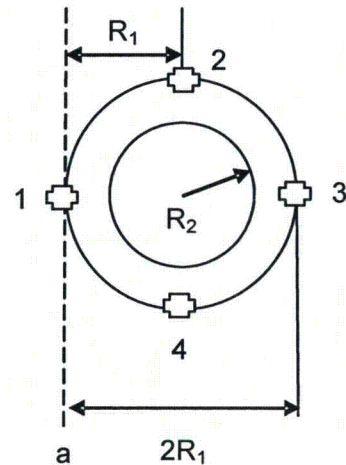
$$T = F * H / 3R_1$$

$$F = 11,810 \text{ lbs.}$$

$$H = 16 \text{ in.}$$

$$R_1 = 12 \text{ in.}$$

$$T = 5,248.9 \text{ lbs.}$$



Total force in cables:

$$P = T + 2 * T / 2 = 2T = 10,500 \text{ lbs.}$$

Conical shell bearing pressure:

$$p = P / A$$

$$P = 10,500$$

$$R_2 = 8.0$$

$$A = \pi * (R_1^2 - R_2^2) = 251.3 \text{ in}^2$$

$$p = 41.8 \text{ lb/in}^2$$

Differential conical shell bearing pressure:

$$\begin{aligned} M' &= 4/3 * (R_1^3 - R_2^3) * \Delta p \\ &= M - P * R_1 = 3R_1 * T - 2R_1 * T = R_1 * T \\ &= 12 * 10,500 = 1.26 \times 10^5 \text{ in-lb} \end{aligned}$$

$$\begin{aligned} \Delta p &= M' / [4/3 * (R_1^3 - R_2^3)] \\ &= 1.26 \times 10^5 / 1.621 \times 10^3 = 77.8 \text{ lb/in}^2 \end{aligned}$$

$$p + \Delta p = 119.6$$

$$p - \Delta p = -36.0$$

Pressure < 0, increase cable loads:

$$P' = A * (p - \Delta p) = 251.3 * 36.0 = 9,046.7 \text{ lbs.}$$

$$\Delta T = 9,046.7 / 4 = 2,261.7$$

$$T(1) = 0.0 + 2,261.7 = 2,261.7$$

$$T(2) = T(4) = 5,248.9 / 2 + 2,261.7 = 4,886.2 \text{ lbs.}$$

$$T(3) = 5,248.9 + 2,261.7 = 7,510.6 \text{ lbs.}$$

$$p + \Delta p = 119.6 + 36.0 = 155.6 \text{ psi}$$

$$p - \Delta p = -36.0 + 36.0 = 0.0$$

Horizontal component of differential pressure (refer to Appendix 2.12.12.8):

$$P_H = 2 * \Delta p * \sin \alpha * (R_1^2 - R_2^2)$$

$$\alpha = 27.2^\circ$$

$$P_H = 2 * 77.8 * 0.4571 * (12^2 - 8^2) = 5,690.0 \text{ lbs.}$$

$$p_H = P_H / 2R_1 * h = 5,690.0 / 24.0 * 4.5 = 52.6 \text{ psi}$$

#### 2.12.12.14 Stress in Cable – Model AOS-050

Maximum cable load from Appendix 2.12.12.13:

$$T = 7,510.6 \text{ lbs.}$$

From *ASTM F1145 - 05(2011)*, Table 3 (Reference [2.27]), Jaw-Jaw,  $P_u = 60 \text{ k}$ :

$$MS = 60 / 7.510 - 1 = 7.0$$

### 2.12.12.15 Stress in Foam – Model AOS-050

Allowable foam stress ( $\epsilon = 0.1$ ):

$$\begin{aligned}\sigma &= Y_{\text{int}} (\rho)^S \\ Y_{\text{int}} &= 4.3422 \\ \rho &= 10 \\ S &= 1.8809 \\ \sigma &= 4.3422 * 76.0 = 330.1 \text{ psi}\end{aligned}$$

Applying equations in Appendix 2.12.12.4:

B	=	Shipping cradle wall length	4.0 in.
F	=	Lateral force	11,810.0 lbs.
H	=	Cask center of gravity to shipping cradle	16.0 in.
R <sub>1</sub>	=	Outside foam radius	12.0 in.
R <sub>2</sub>	=	Inside foam radius	7.0 in.
W	=	Vertical force	2,362.0 lbs.

Base foam vertical bearing stress (psi):

$$p = 8F * H * R_1 / 3\pi (R_1^4 - R_2^4) + W / \pi (R_1^2 - R_2^2) = 112.9 \text{ psi} (< 330.1)$$

Base foam lateral bearing stress (psi):

$$q = F / 2B * R_1 = 123.0 \text{ psi} (< 330.1)$$

From Appendix 2.12.12.12, the maximum foam bearing stress at the conical shell:

$$p + \Delta p = 155.6 \text{ psi} (< 330.1)$$

$$p_H = 52.6 \text{ psi} (< 330.1)$$

### 2.12.12.16 Stress in Tie-Down Ring – Model AOS-050

Figure 2-98 illustrates the maximum principal membrane stress for bending about the x-axis. The maximum stress occurs at location 'a', and is 13.5 ksi. For bending about the y-axis, the stress at location 'b' corresponds to the stress at location 'a'. The stress at location 'b' is 5.3 ksi for 10g loading. The combined stress due to 10g about the x-axis, and 5g about the y-axis, is then:

$$f = 13.5 + (1/2) * 5.3 = 16.2 \text{ ksi}$$

For ASME SB-209 Alloy 6061 T6, Yield Strength  $F_y = 35.0$  ksi:

$$MS = 35.0 / 16.2 - 1.0 = 1.16$$

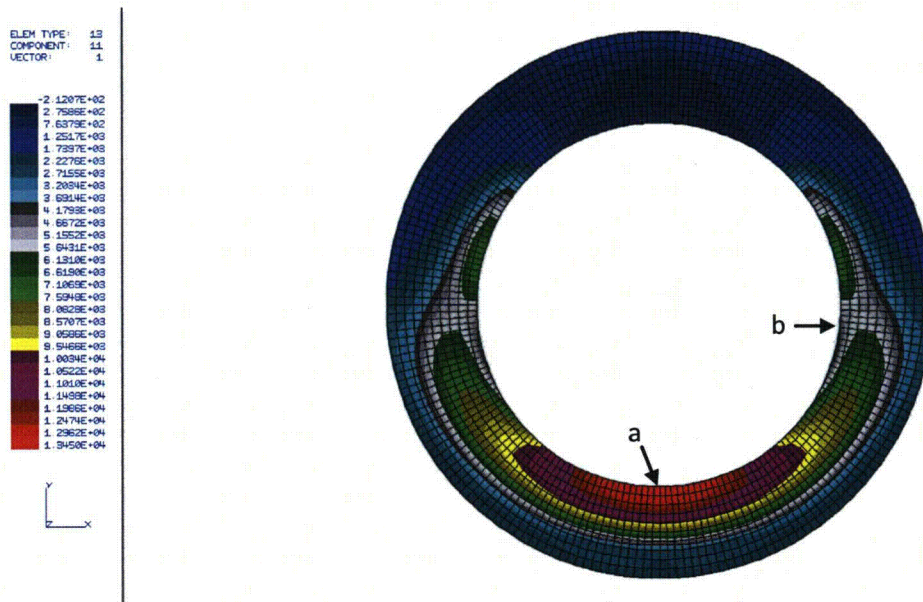


Figure 2-98. Maximum Principal Membrane Stress – Model AOS-050

### 2.12.12.17 Tie-Down Straps – Model AOS-025

Strap load:

$$\Sigma M_A = 0$$

$$11.8 * T_1 + 2T_1 / 2 * 5.9 = 1,680 * (16.25 - 2.30) / 2$$

$$T_1 = 1.172 \times 10^4 / 17.7 = 662.0 \text{ lbs.}$$

$$T_2 = T_1 / 2 = 331.0 \text{ lbs.}$$

$$T_3 = W / 4 = 42.0 \text{ lbs.}$$

$$T = T_1 + T_2 + T_3 = 1,035.0 \text{ lbs.}$$

For a 1.0-inch strap,  $P_u = 3,000$  lbs.:

$$MS = 3,000 / 1,035.0 - 1.0 = 1.90$$

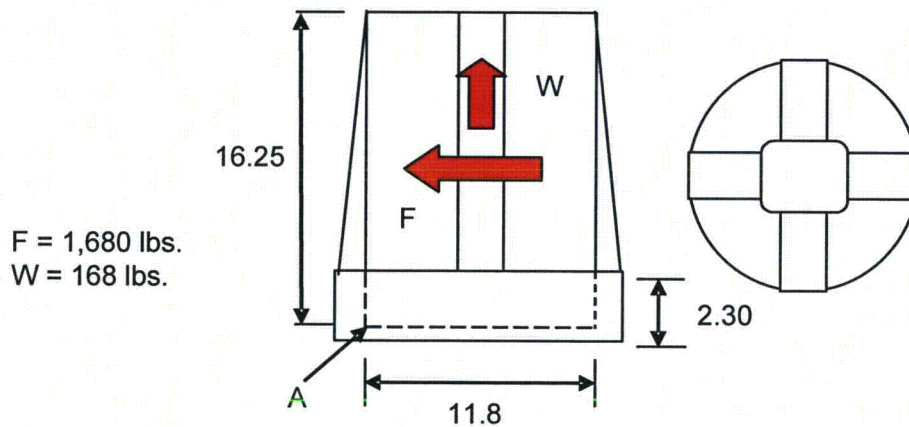


Figure 2-99. Tie-Down Strap Load – Model AOS-025

VECTOR: 1  
 DOF: 3  
 MIN: -2.0112E-03  
 MAX: 1.4486E-02

-2.0112E-03
-1.4220E-03
-9.3298E-04
-5.4385E-04
3.4546E-04
9.3465E-04
1.5236E-03
2.1130E-03
2.7922E-03
3.2913E-03
3.6905E-03
4.4037E-03
5.0586E-03
5.6480E-03
6.2372E-03
6.6265E-03
7.4155E-03
8.0047E-03
9.1896E-03
9.7722E-03
1.0361E-02
1.0951E-02
1.1540E-02
1.2129E-02
1.2718E-02
1.3307E-02
1.3896E-02
1.4486E-02

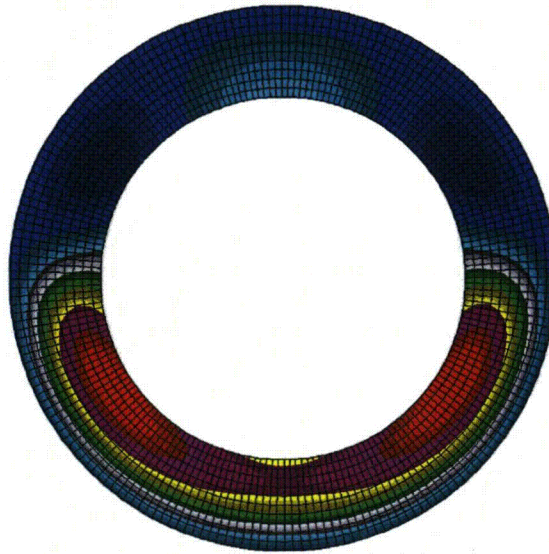



Figure 2-100. Lateral (Z) Displacement in Conical Shell – Model AOS-050



**2.12.13 Certificate of Conformance, General Plastics FR-3700 Series Foam –  
AOS-165A Prototype**

THIS PAGE INTENTIONALLY LEFT BLANK



4910 Burlington Way, Tacoma, Washington 98409  
T (253) 473.5000 F (253) 473.5104 TF (800) 806.6051 www.generalplastics.com

April 25, 2011

Alpha-Omega Services, Inc.  
General Electric Nuclear Energy  
6705 Vallecitos Road  
Sunol, CA 95486

CORRECTED COPY

Attention: Receiving Quality Inspection

Subject: **CERTIFICATE OF CONFORMANCE**

Purchase Order #: **AOS-3835 Rev 2**  
SJO Number: **5099-1**  
Gentlemen:

This letter certifies that the **AOS-165** Impact Limiter filled with **LAST-A-FOAM® FR-3720** has been manufactured, tested and inspected in accordance with purchase order requirements. These products are classified "Safety Class A." Applicable drawings, specifications and standards called for by the purchase order:

Material Specs, Drawings and Process Standards:

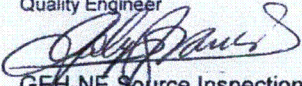
105E9694 Rev. 3  
22A9420 Rev. 1

Production control records and test reports covering subject material indicate conformance with applicable requirements and are attached.


Material: General Plastics Mfg. Co.'s  
**LAST-A-FOAM® FR-3720**  
Quantity: 5 each **AOS-165 Units 01-05**

Respectfully submitted,  
GENERAL PLASTICS MANUFACTURING COMPANY

  
Gerald Langston  
Quality Engineer

  
GEH-NE Source Inspection

5/17/2011

  
6-5-2011  
ALPHA-OMEGA SERVICES INC. QA

- Enclosures:
- 5 each Production Control Records, Units 01-05.
  - 1 each Formulation Test report, LAST-A-FOAM® FR-3720 Batch # 243-CR04489 (Density, c/s, flame, intumescence, leachable chlorides, thermal conductivity, specific heat, water absorption, chemical composition), 19 pages total.
  - 1 each Batch Test Report, LAST-A-FOAM® FR-3720 Batch # 243-CR04489 (Density, c/s, flame, Intumescence, leachable chlorides) 4 pages total.
  - General Plastics Reject Tag #'s 3095, 3099, 3109 & 3110.

THIS PAGE INTENTIONALLY LEFT BLANK

## 2.13 REFERENCES

- [2.1] U.S. Nuclear Regulatory Commission (NRC), *Title 10, Code of Federal Regulations, Part 71 (10 CFR 71)*, "Packaging and Transportation of Radioactive Material."
- [2.2] *International Atomic Energy Agency (IAEA) Safety Standards Series No. TS-R-1 (IAEA TS-R-1)*, "Regulations for the Safe Transport of Radioactive Material," 1996 Ed. (as amended 2003).
- [2.3] U.S. Nuclear Regulatory Commission (NRC), *Regulatory Guide 7.6*, "Design Criteria for the Structural Analysis of Shipping Cask Containment Vessels," Rev. 1, 1978.
- [2.4] U.S. Nuclear Regulatory Commission (NRC), *Regulatory Guide 7.8*, "Load Combinations for the Structural Analysis of Shipping Casks," Table 10, Rev. 1, 1989.
- [2.5] American Society of Mechanical Engineers, *ASME Boiler and Pressure Vessel Code*, Section II, Part D, 2004 Ed., No Addendum.
- [2.6] Gerard, George, *Introduction to Structural Stability Theory*, McGraw-Hill, New York, 1962, Equation 8-14, p. 142, and pp 143-146.
- [2.7] Kaminski, D. A., Ed., *Heat Transfer Data Book*, General Electric Company, New York, 1981, Section G515/29, p. 5.
- [2.8] American Society of Mechanical Engineers, *ASME Boiler and Pressure Vessel Code*, Section II, Part D, Table 3, p. 406, 2004 Ed., No Addendum.
- [2.9] D. Perry, *Aircraft Structures*, McGraw-Hill, 1950, pp. 398-400.
- [2.10] Metech Welded Mesh, Inc., Online Catalog, accessed June, 2010, <http://www.weldedwiremesh.net/>.
- [2.11] American National Standards Institute, *ANSI N14.5-1997*, "Radioactive Materials – Leakage Tests on Packages for Shipment," February 5, 1998.
- [2.12] MIL-STD-883B(3) NOT 2, "Dissimilar Metals," May, 1993.
- [2.13] General Plastics Manufacturing Company, *Design Guide for Use of LAST-A-FOAM FR-3700 for Crash & Fire Protection of Radioactive Material Shipping Containers*, Tacoma, WA, Issue 005.
- [2.14] ASME, Section III, Division 1, Appendices, Figure I-9.4, "Design Fatigue Curves for High Strength Steel Bolting for Temperatures Not Exceeding 700°F," 2004 Ed., No Addendum.
- [2.15] Caldwell, S.G., Ph.D., *Tungsten Heavy Alloy Engineering Manual*, ATI Firth Sterling, AL, v4.0.
- [2.16] Gibson, Lorna, J. and Michael F. Ashby, *Cellular Solids*, p. 193, Cambridge University Press, New York, NY, 2001.
- [2.17] Torrey Hills Technology, LLC, *High Density Tungsten Technical Data*, accessed September 19, 2010, <http://www.torreyhillstech.com/hddata.html>.
- [2.18] Lassner, Erik and Wolf-Dieter Schubert, *Tungsten – Properties, Chemistry, Technology of the Element, Alloys, and Chemical Compounds*, Kluwer Academic/Plenum Publishers, New York, NY, 1999.
- [2.19] General Plastics Manufacturing Company, *Design Guide for Use of LAST-A-FOAM FR-3700 for Crash & Fire Protection of Radioactive Material Shipping Containers*, Tacoma, WA, March, 1998 (revised October, 2003).

- [2.20] Communication from ATI Firth Sterling to Alpha-Omega Services, Inc., and GE Energy.
- [2.21] Parker O-Ring Division, *Evaluation of Parker Compound S1224-70 to ASTM D2000 7GE705 A19 B37 EA14 EO16 E036 F19 G11 Compound Data Sheet*, Kentucky, June 19, 1996.
- [2.22] Fitzroy, Nancy D., Ed., *Heat Transfer Data Book*, General Electric Company, New York, November, 1970 Edition, Section G502.5, p. 7.
- [2.23] Touloukian, Y. S., *Thermophysical Properties of Matter, Metallic Elements and Alloys*, 1971.
- [2.24] Fischer, L. E. and W. Lai, *NUREG/CR-3854, Fabrication Criteria for Shipping Containers*, Lawrence Livermore Laboratory, Prepared for U.S. Nuclear Regulatory Commission (NRC), Livermore, California, March, 1985.
- [2.25] Monroe, R. E, H. H. Woo, and R. G. Sears, *NUREG/CR-3019, Recommended Welding Criteria For Use in the Fabrication of Shipping Containers for Radioactive Materials*, Lawrence Livermore Laboratory, Prepared for U.S. Nuclear Regulatory Commission (NRC), Livermore, California, March, 1984.
- [2.26] American Society of Mechanical Engineers, *ASME Boiler and Pressure Vessel Code, Section III, Division 1, Subsection NB*, 2004 Ed., No Addendum.
- [2.27] ASTM International, *ASTM F1145 - 05(2011), Standard Specification for Turnbuckles, Swaged, Welded, Forged*, Table 3, West Conshohocken, PA, 2011.
- [2.28] Shigley, Joseph E., *Mechanical Engineering Design*, Chapter 6, "The Design of Screws, Fasteners, and Connections," McGraw Hill, Inc., 3<sup>rd</sup> Edition, 1977.

# 3 THERMAL EVALUATION

This chapter identifies, describes, discusses, and evaluates the principal thermal engineering design of the packaging, components, and systems important to safety, and describes how the package complies with the performance requirements specified by *10 CFR 71 [3.1]* and *IAEA TS-R-1 [3.2]*.

The evaluation accomplishes this objective by determining the temperature distributions within the transport package during Normal Accident conditions of transport (NCT) and Hypothetical Accident conditions (HAC) of transport. Additionally, the thermal results are compared against the performance requirements and temperature limits of the materials used. The approach taken assures the safe operation of the package.

## 3.1 DESCRIPTION OF THERMAL DESIGN

The AOS Transport Packaging System is designed with a thermally passive system to provide adequate thermal performance under Normal and Hypothetical Accident conditions of transport relying solely upon the design capacity to transmit and dissipate heat to the outside environment. The cask component is enclosed at both ends by an impact limiter structure, which functions as a thermal shield and mitigates regulatory impact loads, per regulatory requirements. In the case of the Model AOS-025, the impact limiter component of the AOS Transport Packaging System completely encloses the cask.

### 3.1.1 Design Features

The AOS Transport Packaging System consists of three (3) main components: (a) cask; (b) impact limiters; and (c) cask lid seal. Materials of construction are 300 series stainless steel (SS300) for structural members of the packaging; tungsten alloy or carbon steel for shielding material inserts; polyurethane foam for thermal shielding and impact load mitigation; and selected silicone/SS300 series for the cask lid elastomeric seal and silver/nickel-chromium alloy/SS304L combination for the Helicoflex<sup>®</sup> cask lid metallic seal. Refer to Section 1.2, "Package Description," for further details regarding these main and other minor components. Principal packaging dimensions are presented in Table 1-1, "AOS Transport Packaging System Dimensions and Maximum Authorized Package Weight – All Models."

Due to fabrication dimension tolerances, there is a series of gaps throughout the cask body. To minimize their impact upon the heat transfer characteristics of this component, the largest gaps are either packed with stainless steel wool or shim stock. The conservative approaches taken for the treatment of these gaps within the analytical model are discussed further in this chapter.

The temperature distributions for the AOS Transport Packaging System models are determined for the thermal environments listed in Table 3-1.

All thermal conditions were analyzed using the LIBRA Finite Element program, with the exception of Thermal Conditions 5 and 7, where uniform temperature fields of -40°C and -29°C (-40°F and -20°F, respectively) were assigned. A description of the LIBRA Finite Element program heat transfer module is provided in Appendix 3.5.3, which also includes the qualifications and verification program conducted by GE to support the modeling techniques and assumptions taken throughout the thermal evaluation. To further verify the thermal model, a heat test was conducted, using a 165%-scaled geometry of the Model AOS-100A transport package. In this test, a 7-kW electrical heat source was placed inside the cask cavity. The cask was then closed and placed within a pit. Placing the cask inside the pit helped to maintain the environment temperature constant. Temperatures inside and outside of the cask, and the ambient temperature inside the pit, were recorded during the cask heating and cooling cycles. Refer to Appendix 3.5.7 for a detailed account of the heat test and its results.

The maximum decay heat for each AOS Transport Packaging System model is distributed across the cask cavity surface. Condition 3 (fire transient) analysis is initiated at the steady-state Condition 1, in which the maximum solar load is applied.

**Table 3-1. Transport Package Thermal Environment Conditions – All Models**

Condition	Conditions of Transport	Thermal Environment
1	Normal	38°C (100°F) ambient with maximum decay heat and maximum solar load.
2	Normal	38°C (100°F) ambient with maximum decay heat.
3	Hypothetical Accident (Fire)	Fire transient, t = 0 to 8.0 hours.
4	Normal	-40°C (-40°F) ambient with maximum decay heat.
5	Normal	-40°C (-40°F) ambient.
6	Normal	-29°C (-20°F) ambient with maximum decay heat.
7	Normal	-29°C (-20°F) ambient.

### 3.1.2 Contents' Decay Heat

Table 1-2, "Activity Limits – All Models," provides the maximum decay heat and radioactivity for the contents of the AOS Transport Packaging System. This includes Decay Heat (Ci/W) values for each radioisotope listed, showing that the decay heat is consistent with the maximum quantity of radioactivity contents. A summary of the Decay Heat values is shown in Table 3-2.

**Table 3-2. Contents' Decay Heat – All Models**

Model	Contents' Decay Heat (W)
AOS-025A	10
AOS-050A	100
AOS-100A	400
AOS-100B	400
AOS-100A-S	400



### 3.1.3 Summary Tables of Temperatures

Table 3-3. Maximum Temperature Summary, Normal Conditions of Transport – All Models

Model	Component <sup>a</sup>	Thermal Temperatures, by Condition <sup>b</sup>												Regulatory/ Component Criteria (Temperature Range)
		1		2		4		5		6		7		°C °F
		°C	°F	°C	°F	°C	°F	°C	°F	°C	°F	°C	°F	
AOS-025A	Cask Outer Shell	124	256	77	170	3	37	-40	-40	13	56	-29	-20	-40 to 538 -40 to 1,000
	Cask Cavity	125	257	78	172	4	39	-40	-40	14	58	-29	-20	
	Cask Lid	124	255	77	170	2	36	-40	-40	13	55	-29	-20	
	Cask Lid Plug	126	258	78	173	4	40	-40	-40	15	59	-29	-20	
	Bottom Plate	124	255	76	169	2	36	-40	-40	13	55	-29	-20	
	Shielding	124	256	77	171	3	37	-40	-40	13	56	-29	-20	
	Cask Lid Seal Area	124	255	77	170	2	36	-40	-40	13	56	-29	-20	Elastomeric: -40 to 232 -40 to 450  Metallic: -40 to 300 -40 to 572 <sup>c</sup>
	Cask Vent Port	124	255	77	170	2	36	-40	-40	13	55	-29	-20	-40 to 232 -40 to 450
	Cask Drain Port	124	255	76	170	2	36	-40	-40	13	55	-29	-20	
	Test Port	124	255	76	170	2	36	-40	-40	13	55	-29	-20	
	Cask Vent Port Pipe Plug	124	255	77	170	2	36	-40	-40	13	55	-29	-20	-40 to 360 -40 to 680
	Cask Drain Port Pipe Plug	124	255	76	170	2	36	-40	-40	13	55	-29	-20	
	Cask Vent Port Conical Seal	124	255	77	170	2	36	-40	-40	13	56	-29	-20	Thread Sealant: -54 to 277 -65 to 530
	Cask Drain Port Conical Seal	124	255	77	170	3	37	-40	-40	13	56	-29	-20	
	Cavity Bottom	125	257	78	172	4	39	-40	-40	14	58	-29	-20	-40 to 538 -40 to 1,000
Cavity Side	125	257	77	171	3	38	-40	-40	14	57	-29	-20		
Cavity Top	126	258	78	173	4	40	-40	-40	15	59	-29	-20		
Impact Limiter, Foam	94 <sup>d</sup>	202 <sup>d</sup>	73	163	-2	29	-40	-40	9	48	-29	-20	-40 to 127 -40 to 260	
Accessible Outside Surface <sup>e</sup>	-	-	48	119	-	-	-	-	-	-	-	-	50°C (122°F) Non-Exclusive Use 85°C (185°F) Exclusive Use	

**Table 3-3. Maximum Temperature Summary,  
Normal Conditions of Transport – All Models (Continued)**

Model	Component <sup>a</sup>	Thermal Temperatures, by Condition <sup>b</sup>											Regulatory/ Component Criteria (Temperature Range)	
		1		2		4		5		6		7		°C °F
		°C	°F	°C	°F	°C	°F	°C	°F	°C	°F	°C	°F	
AOS-050A	Cask Outer Shell	142	287	102	216	30	86	-40	-40	40	105	-29	-20	-40 to 538 -40 to 1,000
	Cask Cavity	147	296	107	225	35	96	-40	-40	46	114	-29	-20	
	Cask Lid	141	286	102	216	30	85	-40	-40	40	104	-29	-20	
	Cask Lid Plug	148	298	109	229	38	100	-40	-40	48	119	-29	-20	
	Bottom Plate	141	286	102	215	29	85	-40	-40	40	104	-29	-20	
	Shielding	142	288	103	218	31	88	-40	-40	41	107	-29	-20	
	Cask Lid Seal Area	141	286	102	215	30	85	-40	-40	40	104	-29	-20	Elastomeric: -40 to 232 -40 to 450  Metallic: -40 to 300 -40 to 572 <sup>c</sup>
	Cask Vent Port	140	284	101	214	29	84	-40	-40	39	103	-29	-20	-40 to 232 -40 to 450
	Cask Drain Port	141	286	101	214	29	84	-40	-40	39	103	-29	-20	
	Test Port	141	286	102	215	29	85	-40	-40	40	104	-29	-20	
	Cask Vent Port Pipe Plug	140	285	101	214	29	84	-40	-40	39	103	-29	-20	-40 to 360 -40 to 680
	Cask Drain Port Pipe Plug	141	286	101	214	29	84	-40	-40	39	103	-29	-20	
	Cask Vent Port Conical Seal	141	286	102	216	30	85	-40	-40	40	104	-29	-20	Thread Sealant: -54 to 277 -65 to 530
	Cask Drain Port Conical Seal	142	288	103	217	30	87	-40	-40	41	106	-29	-20	
	Cavity Bottom	147	296	107	225	35	96	-40	-40	46	114	-29	-20	-40 to 538 -40 to 1,000
	Cavity Side	144	292	105	221	33	91	-40	-40	43	110	-29	-20	
	Cavity Top	148	298	109	229	38	100	-40	-40	48	119	-29	-20	
	Impact Limiter, Foam	117 <sup>d</sup>	242 <sup>d</sup>	94	201	21	71	-40	-40	32	90	-29	-20	-40 to 127 -40 to 260
	Accessible Outside Surface <sup>e</sup>	-	-	45	113	-	-	-	-	-	-	-	-	50°C (122°F) Non-Exclusive Use 85°C (185°F) Exclusive Use

**Table 3-3. Maximum Temperature Summary,  
Normal Conditions of Transport – All Models (Continued)**

Model	Component <sup>a</sup>	Thermal Temperatures, by Condition <sup>b</sup>												Regulatory/ Component Criteria (Temperature Range)
		1		2		4		5		6		7		°C °F
		°C	°F	°C	°F	°C	°F	°C	°F	°C	°F	°C	°F	
AOS-100A, AOS-100A-S	Cask Outer Shell	146	295	101	214	30	86	-40	-40	41	105	-29	-20	-40 to 538 -40 to 1,000
	Cask Cavity	155	312	111	232	41	105	-40	-40	51	124	-29	-20	
	Cask Lid	145	294	101	214	30	86	-40	-40	41	105	-29	-20	
	Cask Lid Plug	158	317	115	239	45	113	-40	-40	55	132	-29	-20	
	Bottom Plate	146	294	101	213	29	85	-40	-40	40	104	-29	-20	
	Shielding	148	298	103	218	33	91	-40	-40	43	110	-29	-20	
	Cask Lid Seal Area	145	293	101	214	30	86	-40	-40	40	104	-29	-20	Elastomeric: -40 to 232 -40 to 450  Metallic: -40 to 300 -40 to 572 <sup>c</sup>
	Cask Vent Port	143	290	99	210	28	82	-40	-40	38	101	-29	-20	-40 to 232 -40 to 450
	Cask Drain Port	144	291	99	210	28	82	-40	-40	38	101	-29	-20	
	Test Port	145	293	101	213	30	85	-40	-40	40	104	-29	-20	
	Cask Vent Port Pipe Plug	143	290	99	211	28	83	-40	-40	39	101	-29	-20	-40 to 360 -40 to 680
	Cask Drain Port Pipe Plug	144	292	99	210	28	82	-40	-40	38	101	-29	-20	
	Cask Vent Port Conical Seal	145	293	101	214	30	86	-40	-40	41	105	-29	-20	Thread Sealant: -54 to 277 -65 to 530
	Cask Drain Port Conical Seal	147	296	102	216	31	88	-40	-40	41	107	-29	-20	
	Cavity Bottom	155	312	111	232	41	105	-40	-40	51	124	-29	-20	-40 to 538 -40 to 1,000
	Cavity Side	151	305	107	225	36	98	-40	-40	47	116	-29	-20	
	Cavity Top	158	317	115	239	45	113	-40	-40	55	132	-29	-20	
	Impact Limiter, Foam	111 <sup>d</sup>	231 <sup>d</sup>	93	199	21	70	-40	-40	32	89	-29	-20	-40 to 127 -40 to 260
Accessible Outside Surface <sup>e</sup>	-	-	41	106	-	-	-	-	-	-	-	-	50°C (122°F) Non-Exclusive Use 85°C (185°F) Exclusive Use	

**Table 3-3. Maximum Temperature Summary,  
Normal Conditions of Transport – All Models (Continued)**

Model	Component <sup>a</sup>	Thermal Temperatures, by Condition <sup>b</sup>												Regulatory/ Component Criteria (Temperature Range)
		1		2		4		5		6		7		°C °F
		°C	°F	°C	°F	°C	°F	°C	°F	°C	°F	°C	°F	
AOS-100B	Cask Outer Shell	146	295	101	214	30	86	-40	-40	41	105	-29	-20	-40 to 538 -40 to 1,000
	Cask Cavity	156	312	111	232	41	106	-40	-40	51	124	-29	-20	
	Cask Lid	145	294	101	214	30	86	-40	-40	41	105	-29	-20	
	Cask Lid Plug	158	317	115	239	45	114	-40	-40	56	132	-29	-20	
	Bottom Plate	146	294	101	213	29	85	-40	-40	40	104	-29	-20	
	Shielding	148	298	103	218	33	91	-40	-40	43	110	-29	-20	
	Cask Lid Seal Area	145	293	101	214	30	86	-40	-40	40	105	-29	-20	Elastomeric: -40 to 232 -40 to 450  Metallic: -40 to 300 -40 to 572 <sup>c</sup>
	Cask Vent Port	143	290	99	210	28	82	-40	-40	38	101	-29	-20	-40 to 232 -40 to 450
	Cask Drain Port	144	291	99	210	28	82	-40	-40	38	101	-29	-20	
	Test Port	145	293	101	213	30	85	-40	-40	40	104	-29	-20	
	Cask Vent Port Pipe Plug	143	290	99	211	28	83	-40	-40	39	101	-29	-20	-40 to 360 -40 to 680
	Cask Drain Port Pipe Plug	144	292	99	210	28	82	-40	-40	38	101	-29	-20	
	Cask Vent Port Conical Seal	145	293	101	214	30	86	-40	-40	41	105	-29	-20	Thread Sealant: -54 to 277 -65 to 530
	Cask Drain Port Conical Seal	147	297	102	216	31	88	-40	-40	41	107	-29	-20	
	Cavity Bottom	156	312	111	232	41	106	-40	-40	51	124	-29	-20	-40 to 538 -40 to 1,000
	Cavity Side	151	305	107	225	37	98	-40	-40	47	117	-29	-20	
Cavity Top	158	317	115	239	45	114	-40	-40	56	132	-29	-20		
Impact Limiter, Foam	111 <sup>d</sup>	231 <sup>d</sup>	93	199	21	70	-40	-40	32	89	-29	-20	-40 to 127 -40 to 260	
Accessible Outside Surface <sup>e</sup>	-	-	41	106	-	-	-	-	-	-	-	-	50°C (122°F) Non-Exclusive Use 85°C (185°F) Exclusive Use	

- a. Refer to Appendix 3.5.9 for locations of nodes representing copper seal locations within the analytical model.  
b. Refer to Table 3-1 for Condition descriptions.  
c. Refer to Appendix 3.5.10.

d. Refer to Appendix 3.5.4.7.

e. Maximum temperature on the impact limiter surfaces, "Insolation Heat Load Analysis for FR-3700 Series Foam Under Condition 1 for Table 3-3".

**Table 3-4. Maximum Temperature Summary,  
Hypothetical Accident Conditions of Transport (Condition 3) – All Models**

Model	Component <sup>a</sup>	Thermal Temperatures and Time						Regulatory/Component Criteria (Temperature Range)
		During Fire			Post Fire			
		Temperature		Time	Temperature		Time <sup>b</sup>	°C °F
		°C	°F	hr	°C	°F	hr	
AOS-025A	Cask Outer Shell	145	294	0.5	145	294	0.5	-40 to 538 -40 to 1,000
	Cask Cavity	134	273	0.5	136	277	1.0	
	Cask Lid	128	263	0.5	134	274	3.0	
	Cask Lid Plug	130	267	0.5	136	277	2.8	
	Bottom Plate	132	269	0.5	137	279	0.8	
	Shielding	133	272	0.5	135	276	1.0	
	Cask Lid Seal Area	128	263	0.5	134	274	3.0	Elastomeric: -40 to 232 -40 to 450  Metallic: -40 to 300 -40 to 572 <sup>c</sup>
	Cask Vent Port	129	264	0.5	134	274	2.8	-40 to 232 -40 to 450
	Cask Drain Port	133	272	0.5	135	276	0.6	
	Test Port	128	262	0.5	134	274	2.8	
	Cask Vent Port Pipe Plug	129	264	0.5	134	274	2.8	-40 to 360 -40 to 680
	Cask Drain Port Pipe Plug	133	272	0.5	135	276	0.6	
	Cask Vent Port Conical Seal	129	265	0.5	134	274	2.8	Thread Sealant: -54 to 277 -65 to 530
	Cask Drain Port Conical Seal	132	270	0.5	135	276	1.0	
	Cavity Bottom	133	272	0.5	136	277	1.0	-40 to 538 -40 to 1,000
	Cavity Side	134	273	0.5	135	275	1.0	
Cavity Top	130	267	0.0	136	277	2.9		

**Table 3-4. Maximum Temperature Summary,  
Hypothetical Accident Conditions of Transport (Condition 3) – All Models (Continued)**

Model	Component <sup>a</sup>	Thermal Temperatures and Time						Regulatory/Component Criteria (Temperature Range)
		During Fire			Post Fire			
		Temperature		Time	Temperature		Time <sup>b</sup>	°C °F
		°C	°F	hr	°C	°F	hr	
AOS-050A	Cask Outer Shell	414	777	0.5	414	777	0.5	-40 to 538 -40 to 1,000
	Cask Cavity	241	465	0.5	259	499	0.7	
	Cask Lid	170	338	0.5	223	433	2.3	
	Cask Lid Plug	196	385	0.5	230	446	2.0	
	Bottom Plate	175	347	0.5	224	435	2.4	
	Shielding	250	483	0.5	262	504	0.6	
	Cask Lid Seal Area	170	337	0.5	223	434	1.9	Elastomeric: -40 to 232 -40 to 450  Metallic: -40 to 300 -40 to 572 <sup>c</sup>
	Cask Vent Port	197	386	0.5	225	437	1.2	-40 to 232 -40 to 450
	Cask Drain Port	195	384	0.5	227	440	1.2	
	Test Port	166	330	0.5	223	433	2.2	
	Cask Vent Port Pipe Plug	196	386	0.5	225	437	1.2	-40 to 360 -40 to 680  Thread Sealant: -54 to 277 -65 to 530
	Cask Drain Port Pipe Plug	195	384	0.5	227	441	1.2	
	Cask Vent Port Conical Seal	194	382	0.5	224	435	1.8	
	Cask Drain Port Conical Seal	195	384	0.5	224	436	2.2	
	Cavity Bottom	201	395	0.5	231	447	0.8	-40 to 538 -40 to 1,000
	Cavity Side	240	465	0.5	259	499	0.7	
	Cavity Top	196	385	0.0	230	446	2.0	

**Table 3-4. Maximum Temperature Summary,  
Hypothetical Accident Conditions of Transport (Condition 3) – All Models (Continued)**

Model	Component <sup>a</sup>	Thermal Temperatures and Time						Regulatory/Component Criteria (Temperature Range)
		During Fire			Post Fire			
		Temperature		Time	Temperature		Time <sup>b</sup>	°C °F
		°C	°F	hr	°C	°F	hr	
AOS-100A, AOS-100A-S	Cask Outer Shell	463	866	0.5	463	866	0.5	-40 to 538 -40 to 1,000
	Cask Cavity	179	354	0.5	246	476	1.4	
	Cask Lid	147	297	0.5	206	403	6.8	
	Cask Lid Plug	159	318	0.5	219	426	5.4	
	Bottom Plate	149	300	0.5	207	405	7.1	
	Shielding	191	375	0.5	246	475	1.2	
	Cask Lid Seal Area	147	297	0.5	207	404	5.4	Elastomeric: -40 to 232 -40 to 450  Metallic: -40 to 300 -40 to 572 <sup>c</sup>
	Cask Vent Port	195	383	0.5	208	407	2.6	-40 to 232 -40 to 450
	Cask Drain Port	193	379	0.5	210	410	2.6	
	Test Port	146	295	0.5	206	402	6.4	
	Cask Vent Port Pipe Plug	192	378	0.5	209	407	2.6	-40 to 360 -40 to 680  Thread Sealant: -54 to 277 -65 to 530
	Cask Drain Port Pipe Plug	190	374	0.5	211	411	2.6	
	Cask Vent Port Conical Seal	160	321	0.5	207	405	4.8	
	Cask Drain Port Conical Seal	162	323	0.5	208	407	6.1	
	Cavity Bottom	160	321	0.5	218	424	4.0	-40 to 538 -40 to 1,000
Cavity Side	178	352	0.5	246	476	1.4		
Cavity Top	159	318	0.0	219	426	5.4		

**Table 3-4. Maximum Temperature Summary, Hypothetical Accident Conditions of Transport (Condition 3) – All Models (Continued)**

Model	Component <sup>a</sup>	Thermal Temperatures and Time						Regulatory/Component Criteria (Temperature Range)
		During Fire			Post Fire			
		Temperature		Time	Temperature		Time <sup>b</sup>	°C °F
		°C	°F	hr	°C	°F	hr	
AOS-100B	Cask Outer Shell	463	866	0.5	463	866	0.5	-40 to 538 -40 to 1,000
	Cask Cavity	173	343	0.5	241	467	1.5	
	Cask Lid	147	297	0.5	203	398	7.2	
	Cask Lid Plug	158	317	0.5	216	421	5.8	
	Bottom Plate	148	298	0.5	205	401	7.4	
	Shielding	189	372	0.5	242	467	1.2	
	Cask Lid Seal Area	147	296	0.5	204	399	5.7	Elastomeric: -40 to 232 -40 to 450  Metallic: -40 to 300 -40 to 572 <sup>c</sup>
	Cask Vent Port	195	383	0.5	206	403	0.8	-40 to 232 -40 to 450
	Cask Drain Port	193	379	0.5	207	405	2.8	
	Test Port	146	295	0.5	203	397	6.8	
	Cask Vent Port Pipe Plug	192	378	0.5	206	402	2.8	-40 to 360 -40 to 680
	Cask Drain Port Pipe Plug	190	374	0.5	208	406	2.6	
	Cask Vent Port Conical Seal	159	317	0.5	205	400	5.0	Thread Sealant: -54 to 277 -65 to 530
	Cask Drain Port Conical Seal	160	320	0.5	206	402	6.5	
	Cavity Bottom	157	315	0.5	215	420	4.6	-40 to 538 -40 to 1,000
Cavity Side	172	342	0.5	241	467	1.5		
Cavity Top	158	317	0.0	216	421	5.8		

- a. Refer to Appendix 3.5.9 for locations of nodes representing copper seal locations within the analytical model.
- b. Temperatures are computed every 0.001 hours. Time is the time at which the maximum temperature occurs, to the nearest 0.1 hour.
- c. Refer to Appendix 3.5.10.

### 3.1.4 Summary Tables of Maximum Pressures

The maximum cask cavity pressures due to Normal and Hypothetical Accident conditions of transport are provided in Table 4-6, "Maximum Cask Cavity Pressure Due to Normal Conditions of Transport – All Models," and Table 4-7, "Maximum Cask Cavity Pressure Due to Fire Condition – All Models," respectively, by model.



## **3.2 MATERIAL PROPERTIES AND COMPONENT SPECIFICATIONS**

The thermal properties of each material are provided in the following subsections. The curve fit functions, which provide the property variations with temperature, are also provided. These property functions are used in all analyses, to update the material properties as the temperature changes.

Selected material properties are also provided in Appendix 2.12.5, "Selected Material Properties References."

### **3.2.1 Material Properties**

The transport packages consist of four (4) materials:

- Stainless Steel, 300 Series (SS300)
- Tungsten Alloy or SA-105 Carbon Steel
- Air
- LAST-A-FOAM FR-3700 Series Foams

Each is described in the paragraphs that follow.

### 3.2.1.1 Stainless Steel, 300 Series (SS300)

Table 3-5 lists the thermophysical properties of Type 304 Stainless Steel (SS304), as they apply to the transport packages. Refer to Appendix 3.5.4.1.1 for English units and values of the properties that are used in the analyses, and plots of the equations that represent them. Appendix 3.5.5 shows how these properties are entered into the LIBRA input files.

**Table 3-5. Type 304 Stainless Steel (SS304) Thermophysical Properties (Reference [3.16])<sup>a</sup>**

Temperature (°C)	Diffusivity $\alpha$ (m <sup>2</sup> /hr.)	Specific Heat $C_p$ (KJ/kg-°C)	Conductivity K (W/m-°C)
21.1	0.0140	0.477	14.88
37.8	0.0141	0.479	15.06
93.3	0.0145	0.498	16.10
148.9	0.0149	0.510	16.96
204.4	0.0153	0.528	18.00
260.0	0.0158	0.535	18.86
315.6	0.0162	0.542	19.56
371.1	0.0166	0.552	20.42
426.7	0.0171	0.554	21.11
482.2	0.0176	0.560	21.98
537.8	0.0180	0.569	22.85
593.3	0.0184	0.574	23.54
648.9	0.0189	0.575	24.23
704.4	0.0193	0.583	25.10
760.0	0.0197	0.587	25.79
815.6	0.0201	0.591	26.48

a. "Table TCD," Material Group J, page 663 (Reference [3.16]).

Specific Heat,  $C_p$  (Btu/lb-°F)

$$C_p(T) = K(T) / \alpha(T) (\rho)$$

$$= 1.120 \times 10^{-1} + 3.504 \times 10^{-5}T - 1.080 \times 10^{-8}T^2$$

Conductivity, K (Btu/hr-in-°F)

$$K(T) = 6.851 \times 10^{-1} + 4.544 \times 10^{-4}T - 4.126 \times 10^{-8}T^2$$

Density,  $\rho$ (lb/in<sup>3</sup>)

$$\rho = 0.29$$

### 3.2.1.2 Tungsten Alloy

Table 3-6 lists the thermophysical properties of the tungsten alloy used for shielding, as they apply to the transport packages that include suffix A in their model numbers. Refer to Appendix 3.5.4.1.2 for English units and values of the properties that are used in the analyses, and plots of the equations that represent them. Refer also to Appendix 2.12.5, "Selected Material Properties References," for further details.

**Table 3-6. Tungsten Alloy Thermophysical Properties (Reference [3.3])<sup>a</sup> – Models AOS-025A, AOS-050A, AOS-100A, and AOS-100A-S**

Temperature (°C)	Density $\rho$ (g/cc)	Diffusivity $\alpha$ (cm <sup>2</sup> /sec.)	Specific Heat $C_p$ (J/kg-°K)	Conductivity K (W/m-°K)
25	18.11	0.2742	154.7	76.8
97		0.2700	159.2	77.8
206		0.2624	163.4	77.6
316		0.2553	170.3	78.8
427		0.2451	173.9	77.2

a. All table values were obtained by testing.

Density,  $\rho$  (lb/in<sup>3</sup>)

$$\rho = 0.654$$

Specific Heat,  $C_p$  (Btu/lb-°F)

$$C_p(T) = 3.631 \times 10^{-2} + 8.017 \times 10^{-6}T - 1.807 \times 10^{-9}T^2$$

Conductivity, K (Btu/hr-in-°F)

$$K(T) = 3.673 + 4.028 \times 10^{-4}T - 4.167 \times 10^{-7}T^2$$

### 3.2.1.3 SA-105 Carbon Steel

Table 3-7 lists the thermophysical properties of SA-105 carbon steel (used for shielding), as they apply to the Model AOS-100B transport package. Refer to Appendix 3.5.4.1.3 for English units and values of the properties that are used in the analyses, and plots of the equations that represent them.

**Table 3-7. Carbon Steel Properties – Model AOS-100B (Reference [3.16])<sup>a</sup>**

Temperature (°C)	Conductivity (W/m-°C)	Thermal Diffusivity (m <sup>2</sup> /hr)	Specific Heat (KJ/kg-°C)
<b>Material: SA-105, Carbon Steel Forging</b>			
21.1	60.75	0.06457	0.4324
37.8	60.06	0.06262	0.4408
65.6	59.02	0.05992	0.4527
93.3	58.15	0.05695	0.4693
121.1	56.94	0.05435	0.4815
148.9	55.90	0.05212	0.4930
204.4	53.48	0.04757	0.5167
260.0	51.06	0.04385	0.5351
315.6	48.46	0.04023	0.5537
343.3	47.25	0.03846	0.5646
371.1	46.04	0.03660	0.5780
398.9	44.83	0.03475	0.5929
426.7	43.61	0.03298	0.6078
454.4	42.40	0.03112	0.6262
482.2	41.19	0.02945	0.6483

a. "Table TCD," Material Group A, page 662 (Reference [3.16]).

$$\text{Density} = 7,832.8 \text{ kg/m}^3 (0.283 \text{ lb/in}^3)$$

The conductivity property as a function of temperature is defined as:

$$K = 3.002 - 1.027 \times 10^{-3}T - 1.249 \times 10^{-7}T^2$$

where:

$$K = \text{Conductivity, Btu/hr-in-}^\circ\text{F}$$

$$T = \text{Temperature, }^\circ\text{F}$$

The specific heat property as a function of temperature is defined as:

$$C_p = 0.1009 + 4.847 \times 10^{-5}T + 9.493 \times 10^{-9}T^2$$

where:

$$C_p = \text{Specific heat, Btu/lb-}^\circ\text{F}$$

$$T = \text{Temperature, }^\circ\text{F}$$

### 3.2.1.4 Air

Table 3-8 lists the thermophysical properties of air, as they apply to the transport packages. Refer to Appendix 3.5.4.1.4 for English units and values of the properties that are used in the analyses, and plots of the equations that represent them.

**Table 3-8. Air Thermophysical Properties (Reference [3.4])<sup>a</sup>**

Temperature		Density $\rho$ (kg/m <sup>3</sup> )	Dynamic Viscosity $\mu \times 10^{-7}$ (N-sec/m <sup>2</sup> )	Specific Heat $C_p$ (KJ/kg-°K)	Conductivity $K \times 10^{-3}$ (W/m-°K)	Prandtl Number (Pr)
°C	°F					
27	80.6	1.1614	184.6	1.007	26.3	0.707
77	170.6	0.9950	208.2	1.009	30.0	0.700
127	260.6	0.8711	230.1	1.014	33.8	0.690
177	350.6	0.7740	250.7	1.021	37.3	0.686
227	440.6	0.6964	270.1	1.030	40.7	0.684
277	530.6	0.6329	288.4	1.040	43.9	0.683
327	620.6	0.5804	305.8	1.051	46.9	0.685
377	710.6	0.5356	322.5	1.063	49.7	0.690
427	800.6	0.4975	338.8	1.075	52.4	0.695
477	890.6	0.4643	354.6	1.087	54.9	0.702
527	980.6	0.4354	369.8	1.099	57.3	0.709
577	1,070.6	0.4097	384.3	1.110	59.6	0.716
627	1,160.6	0.3868	398.1	1.121	62.0	0.720
677	1,250.6	0.3666	411.3	1.131	64.3	0.723
727	1,340.6	0.3482	424.4	1.141	66.7	0.726

a. Table A.4, page 839.

**Note:** The temperature unit used in the following equations is °F.

Density,  $\rho$  (lb/in<sup>3</sup>)

$$\rho(T) = 4.684 \times 10^{-5} - 7.150 \times 10^{-8}T + 5.869 \times 10^{-11}T^2 - 1.834 \times 10^{-14}T^3$$

Specific Heat,  $C_p$  (Btu/lb-°F)

$$C_p(T) = 0.2402 - 1.401 \times 10^{-6}T + 3.995 \times 10^{-8}T^2 - 1.570 \times 10^{-11}T^3$$

Conductivity,  $K$  (Btu/hr-in-°F)

$$K(T) = 1.110 \times 10^{-3} + 2.083 \times 10^{-6}T - 3.956 \times 10^{-10}T^2$$

### 3.2.1.5 LAST-A-FOAM FR-3700 Series Foams

Table 3-9 lists the thermophysical properties of the General Plastics LAST-A-FOAM FR-3700 series foam used by each transport package model. Refer also to Appendix 2.12.5, "Selected Material Properties References," for further details.

**Table 3-9. LAST-A-FOAM FR-3700 Series Foam Thermophysical Properties – All Models (Reference [3.19])<sup>a, b</sup>**

Model	Load Conditions of Transport	Density (lb/ft <sup>3</sup> )	Conductivity		Specific Heat	
			Btu/hr-in-°F	W/m-°C	Btu/lb-°F	KJ/kg-°C
AOS-025	Normal	20	0.00242	0.0503	0.353	1.477
	Fire Condition, Upper Impact Limiter	25	0.00288	0.0597		
	Fire Condition, Lower Impact Limiter	20	0.00242	0.0503		
AOS-050	Normal	10	0.00148	0.0307	0.353	1.477
	Fire Condition, Upper Impact Limiter	12.5	0.00172	0.0357		
	Fire Condition, Lower Impact Limiter	10	0.00148	0.0307		
AOS-100	Normal	12	0.00167	0.0347	0.353	1.477
	Fire Condition, Upper Impact Limiter	14.6	0.00192	0.0399		
	Fire Condition, Lower Impact Limiter	12	0.00167	0.0347		

- a. Reference [3.19] applies only to Normal conditions of transport. For Hypothetical Accident conditions of transport, the property values provided in Table 3-9 were arrived at using the same procedures as shown in Appendix 3.5.4.2.5.
- b. The foam properties presented are those used for the analyses within this chapter, for both Normal and Hypothetical Accident conditions of transport. Newer foam values are now in use (18, 8, and 11 pcf, for the Model AOS-025, AOS-050, and AOS-100, respectively). There is no significant variation of the property values listed above, and the new foam values.

### 3.2.2 Component Specifications

The component material within the transport package that is considered to be temperature-sensitive is the elastomeric material used in the cask lid elastomeric seal and port plug O-Rings. The elastomeric material is a silicone-based compound (Parker O-Ring Division, S1224-70 compound), with a recommended temperature limit of 232°C (450°F) (Reference [3.20]). The following containment boundary components are not explicitly modeled within the analysis; only the temperature at their locations is monitored:

- Cask lid metallic seal (Jacket: Silver, ASTM B742; Spring: Nickel-chromium alloy 90 UNS N07090; Lining: SS304L UNS S30403)
- Conical copper alloy seal (C10100, C10200, or C11000 copper, foil or strip, chemical composition per ASTM B152 or ASTM F68 and mechanical properties per AMS 4500)



### 3.3 THERMAL EVALUATION UNDER NORMAL CONDITIONS OF TRANSPORT

The thermal evaluation of the AOS Transport Packaging System is conducted by analysis, using finite element methods. The computer program applied in the analysis, LIBRA, is a multi-purpose finite element program applicable to static and dynamic analyses of linear and non-linear structural systems, as well as thermal analysis. A thermal test is also conducted to verify that the cask's temperature distribution is similar to the one predicted by the analytical model. The analytical model developed represents the standard configuration of the cask component (only the "A" version of the cask). Therefore, the Model AOS-100A-S was not analyzed. This approach is justified, based on the cask component symmetry, in geometry and material selection. The cask lid/cask lid plug combination is similar to the bottom area of the "A" version of the cask. Furthermore, when the cask vent port pipe plug (top of cask) and cask drain port pipe plug (bottom of cask) area temperature results on the A versions of the casks are compared, it can be concluded that these areas have similar temperature results in Normal and Hypothetical Accident conditions of transport environments.

#### 3.3.1 Heat and Cold

In the thermal evaluation, the following conditions and assumptions were applied to all transport package models:

- For Normal conditions of transport, existing gaps were increased over nominal values by drawing tolerance, 0.01 in. In addition, for surface interfaces with null gap, heat transfer was assumed by contact resistance, and contact resistance values increased by a factor of 10 over nominal values. The contact resistance was set to 0.30 hr-ft<sup>2</sup>-°F/Btu, where nominal contact resistance is 0.03 hr-ft<sup>2</sup>-°F/Btu [3.10].
- For Hypothetical Accident conditions of transport, all gaps were assumed closed. Interface heat transfer was by contact resistance, and nominal contact resistance values were decreased by a factor of 10, to 0.003 hr-ft<sup>2</sup>-°F/Btu. For the Fire event's Cool-Down cycle, the analysis proceeded with gaps open to expanded values, and the contact resistance was increased to 0.30 hr-ft<sup>2</sup>-°F/Btu. This procedure was found to be the most conservative.
- All cask component conduction and convection properties were modeled with temperature-dependent properties, except for the impact limiter foam. During the Fire event's Cool-Down cycle, foam properties were replaced with air properties.
- For Fire events, impact limiter geometries were modified to reflect deformations due to 30-ft. Head-On Drop events.
- Ribs inside the impact limiter are not included in the analysis models. A study has been performed that shows for Normal conditions of transport, temperatures are slightly higher without the ribs modeled. Under Normal conditions of transport, neglecting the ribs is conservative. Under Hypothetical Accident conditions of transport, temperatures at some areas are slightly higher with the ribs included, and do not significantly impact the final temperatures. Details are provided in Appendix 3.5.4.8.
- Foam thermal property values used in the analyses were the nominal values provided in the manufacturer's (General Plastics) literature. The property values variation listed in Table 8-5, "LAST-A-FOAM FR-3700 Series Foams – Testing Program," provides the acceptance criteria for the foam. Using the ranges from the table, sensitivity analyses were performed. The analyses used a ±15% variation in density, and a ±20% variation in specific heat. The analyses results demonstrated a temperature change of less than 1°F. Further details are provided in Appendix 3.5.4.9.

### 3.3.2 Maximum Normal Operating Pressure

The maximum operating pressure, based upon steady state temperatures for Normal conditions of transport are 20 psia, 21 psia, and 21 psia for Models AOS-025, AOS-050, and AOS-100, respectively. The calculation is applied by using the Ideal Gas Law, a relationship of temperature and pressure. The volume parameter does not enter into the calculation, because it is constant. Refer to Table 4-6, "Maximum Cask Cavity Pressure Due to Normal Conditions of Transport – All Models," for pressure calculation details.

The AOS Transport Packaging System can be loaded dry or wet; however, if loaded wet, the cask cavity must be vacuum-dried to remove all water or other moisture. Subsequently, only the relative humidity in the loading environment is trapped within the cavity. None of the contents undergo alpha decay in any appreciable amount, neither neutron emitters nor boron systems, that could generate helium gas.

### 3.3.3 Thermal Finite Element Model

The thermal evaluation of the AOS Transport Packaging System is conducted using the thermal analysis modulus of the LIBRA computer program, **MAIN12**. This heat conduction solution determines both steady-state and transient temperature fields. For transient thermal problems, the user can control the integration scheme by specifying the integration parameter. A zero (0) value for this parameter provides an explicit integration scheme; while between zero (0) and one (1) provide implicit schemes. A value of one (1) is used in the evaluation, corresponding to a backward difference integration technique. Temperature-dependent properties are either incorporated into an algorithm or implemented by a user-written subroutine. In this evaluation, the temperature-dependent properties are provided by an algorithm, and are shown in Subsection 3.2.1, "Material Properties."

The thick stainless steel cask outer shell, which comprises the bulk of the cask, defines the outside dimensions of the cask. The cask cavity is defined by the cask cavity shell, which is secured to the cask outer shell. The cask lid plug shell is secured by the cask lid and cask cavity shell. Four-node quadrilateral conduction elements are used to model the cask outer shell, cask cavity shell, and cask lid plug shell. Also, the bottom plate and cask lid are modeled with four-node quadrilateral conduction elements. Figure 3-1 shows the analytical model used in the evaluation of Normal conditions of transport. Refer to Appendix 3.5.4.2 and Appendix 3.5.4.3 for descriptions of the analytical model used in this evaluation.

The side tungsten alloy or carbon steel shielding is encapsulated by the cask outer shell and cask cavity shell. The vertical wall between the shielding and cask outer shell is packed with stainless steel wool on one side, and between the shielding and cask cavity shell, an air gap exists on the other. At the top and bottom horizontal surfaces, existing gaps within the cask cavity shell are filled with stainless steel shim plates. Two-node conduction elements are used in the model for the surface contact resistance and conduction through the stainless steel wool. Other surface interfaces, between cask components, are assembled with zero (0) gap, and are modeled with two-node conduction elements that have pressure surface-contact resistance properties.

The analytical FEA methodology and model are validated by a thermal test, the details of which are provided in Appendix 3.5.7.

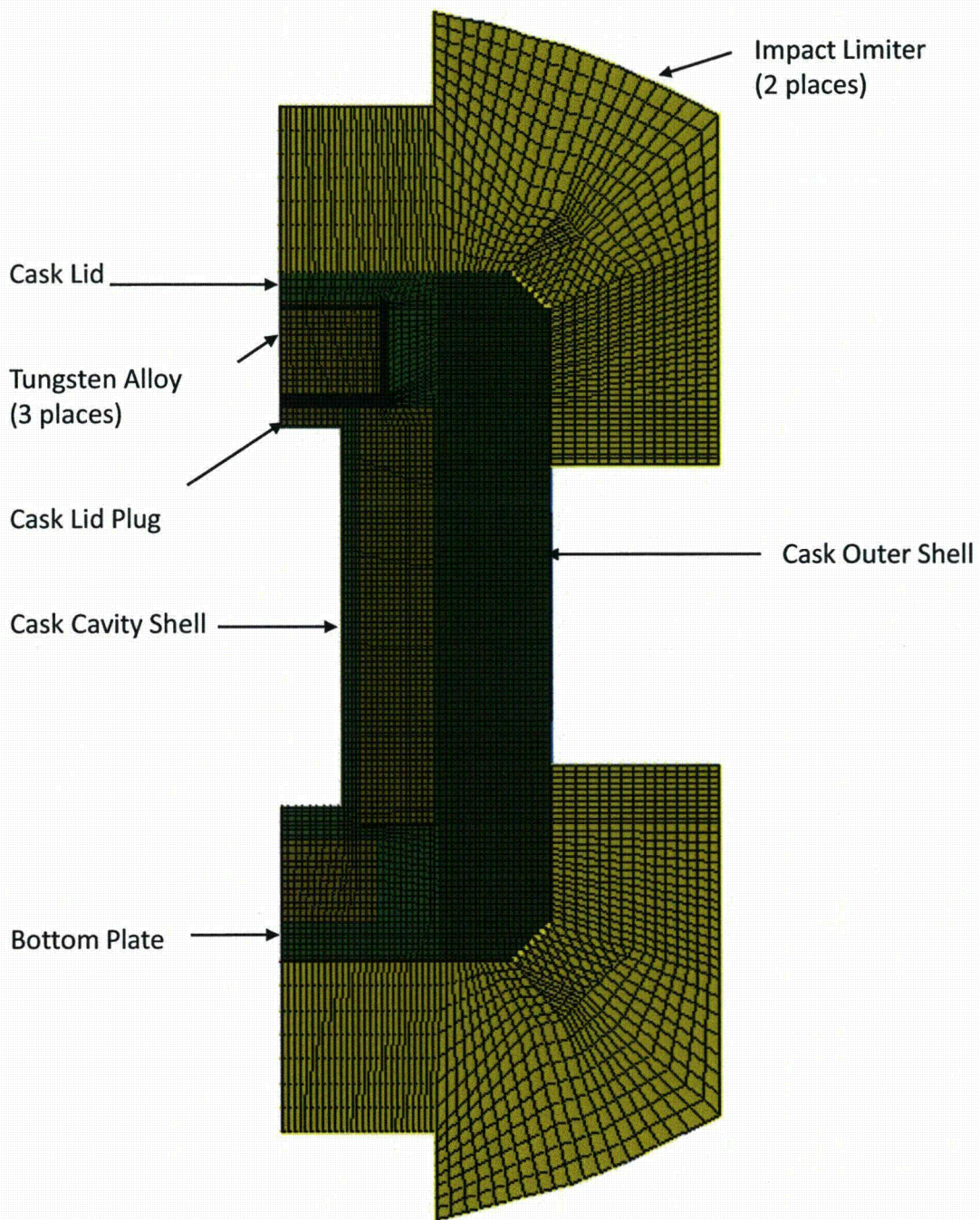


Figure 3-1. Analytical FEA Model – Normal Conditions of Transport

The bottom tungsten alloy or carbon steel shielding is encapsulated by the cask cavity shell and bottom plate. The top and bottom horizontal surfaces have zero (0) gaps, and heat transfer across these interfaces by a low-pressure, surface-contact resistance. The gap between the shielding vertical side wall and cask cavity shell is packed with stainless steel wool.

The top shielding is completely encapsulated by the cask lid plug shell. In a manner similar to the bottom shielding, the shielding top and bottom horizontal surfaces have zero (0) gaps, and heat transfers through these interfaces by a low-pressure, surface-contact resistance. A gap between the vertical side wall and cask lid plug shell is packed with stainless steel wool. Two-node conduction elements are used in the model for the surface contact resistance and conduction through the stainless steel wool.

A zero-gap surface thermal contact resistance,  $1/h_c$ , a value of  $0.03 \text{ hr-ft}^2\text{-}^\circ\text{F/Btu}$  (refer to Appendix 2.12.5, "Selected Material Properties References," and Reference [3.10]) represents a low-contact pressure of less than 50 psi. In thermal situations, where lower resistance would provide higher temperatures, a resistance value of  $0.003 \text{ hr-ft}^2\text{-}^\circ\text{F/Btu}$  is used at all pressure contact interfaces. This situation occurs during Thermal Condition 3, the 30-minute Fire event. The other six (6) thermal events use a higher resistance of  $0.30 \text{ hr-ft}^2\text{-}^\circ\text{F/Btu}$ , at all contact interfaces, which provides for higher temperatures within the cask.

Packed steel wool conductive and density thermal properties are assumed to be approximately 10% that of the SS304 material, and its specific heat is approximated to that of air.

$$K = 0.068 \text{ Btu/hr-in-}^\circ\text{F}$$

$$C_p = 0.24 \text{ Btu/lb-}^\circ\text{F}$$

$$\text{Density} = 0.029 \text{ lb/in}^3$$

Several interface surfaces have air gaps. Air gaps are modeled with two-node conduction elements, with conduction and radiation properties. The six (6) air gaps are located between the:

1. Cask outer shell and upper section of the cask cavity shell and cask lid.
2. Cask cavity shell and cask lid plug shell lower section.
3. Cask cavity shell and cask lid plug shell upper section.
4. Cask lid plug shell top horizontal surface and cask lid.
5. Cask outer shell corner and side, impact limiter.
6. Cask cavity shell and shielding (tungsten alloy or carbon steel).

In thermal situations, where a smaller gap would provide higher temperatures, all gaps are closed, and at the interface, a low-contact resistance value of  $0.003 \text{ hr-ft}^2\text{-}^\circ\text{F/Btu}$  is used. This situation occurs during Thermal Condition 3, the 30-minute Fire event. The other six (6) thermal conditions use gaps that are increased by 0.01 inches over their nominal values, which allows dimensional tolerance to be considered. Table 3-11 lists the analyses values for the six (6) gaps used in all models.

The impact limiter structure is a spherical head, axisymmetric (2D) structure. The impact limiter's stainless steel outer shell is modeled by two-node conduction/convection elements. The interior is filled with General Plastics LAST-A-FOAM FR-3700 series foam, and modeled by four-node quadrilateral elements.

The decay heat of the cask contents is introduced in the model by two-node convective boundary elements, along the cask cavity surface. In the model, it is assumed that the load is uniformly distributed across the entire surface.

Boundary elements define the convective and radiative properties at the interface located between the impact limiter outside surface and regulatory-required environments. A second convective surface is located on the exposed cask outer shell, between the impact limiters. In addition to convective and radiative properties, these boundary two-node elements have the capability to include required solar heat flux loads.

Figure 3-4 illustrates all thermal model components and interfaces. The dimensions of all AOS Transport Packaging System models are provided in Appendix 3.5.4.

### 3.3.3.1 Heat Flux Property Set

Convective boundary elements, located within the model's cask cavity, define the prescribed heat flux due to decay heat. The Model AOS-100 transport package's maximum heat load is 400W. This load is applied as a uniform surface heat flux to the entire cavity surface area. Its value is calculated, as follows:

$$q = \frac{Q}{A} = \frac{(400)}{(2\pi)[(0.08255)^2 + (0.08255)(0.508)]}$$

$$= 1,305.9 \text{ W/m}^2$$

The justification for this approach is presented in Appendix 3.5.6.

Uniform decay heat flux values for all models are provided in Table 3-10.

**Table 3-10. Heat Flux Values – All Models**

Model	Decay Heat (W)	Cavity Area (in <sup>2</sup> )	Heat Flux (Btu/hr-in <sup>2</sup> )
AOS-025	10	29.65	1.15
AOS-050	100	118.63	2.88
AOS-100	400	474.77	2.88

### 3.3.3.2 Enclosed Air Space Property Sets

Six element property sets represent the previously described enclosed air spaces.

For convective heat transfer in an enclosed vertical air space, Gebhart [3.5] provides the following:

$$\text{Nu} = 0.18 \sqrt[4]{Gr} (H/S)^{(-1/9)} \quad \text{For } 2 \times 10^4 < Gr < 2 \times 10^5$$

$$\text{Nu} = 0.065 \sqrt[3]{Gr} (H/S)^{(-1/9)} \quad \text{For } 2 \times 10^5 < Gr < 11 \times 10^6$$

where:

Nu = Nusselt Number

Gr = Grashof Number, based upon S

S = Distance across enclosed space

H = Height of enclosed space

For Gr less than 2,000, the process is simple conduction,  $Nu = 1.0$ . The Grashof Number is defined, as follows:

$$Gr = \frac{\rho^2 g \beta S^3 \Delta T}{\mu^2} = \frac{g S^3 \Delta T}{T \nu^2}$$

where:

$$\rho = \text{Density, kg/m}^3$$

$$g = \text{Acceleration of gravity (9.8 m/s}^2\text{)}$$

$$\beta = \text{Coefficient of the thermal expansion (}^\circ\text{C)} = \frac{1}{T} \text{ for ideal gases}$$

$$\Delta T = \text{Temperature difference across enclosure (}^\circ\text{C)}$$

$$\mu = \text{Dynamic viscosity (kg/m-s)}$$

$$\nu = \text{Kinematic viscosity (m}^2\text{/s)} = \mu/\rho$$

$$T = \text{Absolute temperature (}^\circ\text{K)}$$

The convective heat transfer in an enclosed horizontal air space depends upon the temperatures of the upper and lower plates. From Gebhart [3.7], when the upper plate's temperature is higher than the lower plate's temperature, the process is simple conduction:

$$Nu = 1.0$$

From Gebhart [3.7], when the lower plate's temperature is higher than the upper plate's temperature, then:

$$Nu = 0.195 \sqrt[4]{Gr} \quad 10^4 < Gr < 4 \times 10^5$$

$$Nu = 0.068 \sqrt[3]{Gr} \quad 4 \times 10^5 < Gr$$

For values of Gr below 1,700, pure conduction is observed and  $Nu = 1.0$ . Therefore, the heat transfer process is simple conduction.

The Grashof Number, Gr, is evaluated at each gap, for the Model AOS-025, AOS-050, and AOS-100 transport packages. Enclosed gaps are small and in all cases, Gr is less than 1,700. It is concluded that convection is not a mode of heat transfer across all gaps. Details for this evaluation are provided in Appendix 3.5.4.4.3.



After Nu is known, the convective heat transfer coefficient,  $h_c$ , can be determined by the following expression in both cases, vertical and horizontal air spaces:

$$h_c = \frac{Nu * k}{S}$$

where:

$k$  = Thermal conductivity (W/m-°C)

$S$  = Distance across the space (m)

For radiative heat transfer:

$$h_r = \sigma F (T_1^2 + T_2^2)(T_1 + T_2)$$

where:

$T_1, T_2$  = Temperatures on either side of air space (°K)

$\sigma$  =  $5.669 \times 10^{-8}$  (W/m<sup>2</sup>-°K<sup>4</sup>)

$F$  = Gray body shape factor

The gray body shape factor,  $F$ , is defined as follows:

$$F = \frac{1}{\left(\frac{1}{\epsilon_1} - 1\right) + \frac{A_1}{A_2} \left(\frac{1}{\epsilon_2} - 1\right) + \frac{1}{F_{12}}}$$

where:

$A_1$  = Area of smaller surface

$A_2$  = Area of larger surface

$\epsilon_1, \epsilon_2$  = Emissivities

$F_{12}$  = Shape factor

The gray body shape factor,  $F$ , is a geometric function of the system. When body A is completely enclosed by body  $A_2$  and  $A_1$ , it cannot see itself, as is the case here,  $F_{12} = 1.0$  (Reference [3.8]).

From Reference [3.9], for oxidized SS304,  $\epsilon_1 = \epsilon_2 = 0.52$  and assuming  $A_1 = A_2$ , then:

$$F = 0.351$$

for all material sets that have SS304 matching interface surface materials.

For Model AOS-100A, at Gap 6, the interface materials are SS304 to tungsten alloy. The emissivity for tungsten is 0.27 (Reference [3.17]), resulting in a gray body shape factor of:

$$F = 0.216$$

For the Model AOS-100B transport package, at Gap 6, the interface materials are SS304 to carbon steel. The emissivity for carbon steel is 0.58 (Reference [3.18]), resulting in a gray body shape factor of:

$$F = 0.378$$

The finite element model represents these air spaces with conductive elements. The conversions from  $h$  to  $k$  are as follows:

$$k = h * S$$

where:

$$k = \text{Conduction}$$

$$h = \text{Convection}$$

$$S = \text{Distance across the air space}$$

In general, the effective conductivity across the air gap,  $k_a$ , is due to conduction plus radiation, because it was previously proven that convection does not influence the heat transfer across the gaps ( $Gr \leq 1,700$ ). Therefore,  $k_a$  can be as follows:

$$k_a = k + h_r * S$$

Table 3-11 lists the thermal properties used in the analysis as a function of temperature, for the six (6) air gaps located within each AOS Transport Packaging System model. Appendix 3.5.4.4 provides information regarding curve-fitting data for all air gaps.

**Table 3-11. Thermal Properties Used in Analysis as Function of Temperature, with Respect to the Air Gaps – All Models**

Model	Air Gap	Effective Conductivity (Btu/hr-in-°F), Including Radiation	
		S <sup>a</sup> (in.)	k <sub>a</sub> (T) <sup>b</sup>
AOS-025	1	0.0118	1.122E-3 + 2.085E-6T + 2.527E-10T <sup>2</sup>
	2	0.0124	1.122E-3 + 2.085E-6T + 2.527E-10T <sup>2</sup>
	3	0.0176	1.132E-3 + 2.070E-6T + 5.343E-10T <sup>2</sup>
	4	0.0147	1.122E-3 + 2.085E-6T + 2.527E-10T <sup>2</sup>
	5	0.0403	1.178E-3 + 2.005E-6T + 1.763E-9T <sup>2</sup>
	6	0.0108	1.111E-3 + 2.101E-6T - 5.217E-11T <sup>2</sup>
AOS-050	1	0.0140	1.127E-3 + 2.077E-6T + 3.935E-10T <sup>2</sup>
	2	0.0150	1.127E-3 + 2.077E-6T + 3.935E-10T <sup>2</sup>
	3	0.0250	1.147E-3 + 2.049E-6T + 9.350E-10T <sup>2</sup>
	4	0.0190	1.127E-3 + 2.077E-6T + 3.935E-10T <sup>2</sup>
	5	0.0710	1.239E-3 + 1.916E-6T + 3.426E-9T <sup>2</sup>
	6	0.0120	1.112E-3 + 2.099E-6T - 1.885E-11T <sup>2</sup>
AOS-100A	1	0.0170	1.131E-3 + 2.072E-6T + 5.018E-10T <sup>2</sup>
	2	0.0200	1.137E-3 + 2.063E-6T + 6.642E-10T <sup>2</sup>
	3	0.0400	1.177E-3 + 2.005E-6T + 1.747E-9T <sup>2</sup>
	4	0.0290	1.155E-3 + 2.037E-6T + 1.152E-9T <sup>2</sup>
	5	0.1310	1.359E-3 + 1.743E-6T + 6.675E-9T <sup>2</sup>
	6	0.0130	1.113E-3 + 2.097E-6T + 1.447E-11T <sup>2</sup>
AOS-100B	1	0.0170	1.131E-3 + 2.072E-6T + 5.018E-10T <sup>2</sup>
	2	0.0200	1.137E-3 + 2.063E-6T + 6.642E-10T <sup>2</sup>
	3	0.0400	1.177E-3 + 2.005E-6T + 1.747E-9T <sup>2</sup>
	4	0.0290	1.155E-3 + 2.037E-6T + 1.152E-9T <sup>2</sup>
	5	0.1310	1.359E-3 + 1.743E-6T + 6.675E-9T <sup>2</sup>
	6	0.0130	1.125E-3 + 2.080E-6T + 3.393E-10T <sup>2</sup>

a. S = Distance across the air space.

b. Temperature unit is °F.

### 3.3.3.3 Boundary Property Sets

The transport packages are transported in a vertical position. Eleven (11) material property sets define the outside cask surface and link the transport package with the external environment. These sets also define the film coefficient, ambient temperature, and solar heat flux values. All models are evaluated with Surfaces 1, 2, and 3 having no convection nor solar loads. However, during the Fire event, all surfaces are exposed to the fire environment.

In addition, each property set specifies the free convective coefficient, ambient temperature, and solar heat flux value for a portion of the cask boundary. Free convective coefficients are determined in accordance with empirical equations provided in Reference [3.4]. In general, convection coefficients are determined by finding the Nusselt Number, and then using the following equation to solve for h:

$$\text{Nu} = h * L / k$$

where:

h = Convective film coefficient

L = Characteristic length

k = Air conductive coefficient

The empirical formulations used to determine the Nusselt Numbers used in the vertical and horizontal surface cask analyses are presented in Paragraph 3.3.3.4 and Paragraph 3.3.3.5, respectively.

Convective film coefficient values are dependent upon the plate shape, size, and orientation. The film temperature is assumed to be the average between the transport package surface and required regulatory ambient temperatures. The film coefficient is then evaluated with air properties defined at the film temperature. Detailed information regarding the surface convective coefficient is provided in Appendix 3.5.4.5.

For all models, Table 3-12 (Normal conditions of transport) and Table 3-13 (Fire condition) list the orientation, shape, and size of the cask assembly's external surfaces. (Refer also to Table 3-14 and Table 3-15.) Appendix 3.5.4.5 provides additional information regarding the dimensional values used in all models. Figure 3-2 and Figure 3-3 illustrate the external surface locations for Normal and Hypothetical Accident conditions of transport, respectively.

All transport packages have several curved vertical surfaces that are considered flat vertical plates, in their evaluations for surface convection. In the analyses, a vertical cylinder is treated as a flat vertical plate when it meets the criterion,  $D/L \geq 35 / Gr^{1/4}$ . It is shown in Appendix 3.5.4.6 that this criterion is met for all curved vertical surfaces.

**Table 3-12. Cask Assembly External Surface Orientation and Size, Normal Conditions of Transport – All Models**

Model	Surface	Orientation	Length (m)	Width (m)
AOS-025 (Transported Vertically)	1	Bottom Horizontal	0.091	0.091
	2	Vertical	0.030	0.030
	3	Bottom Horizontal	0.290	0.290
	4	Vertical	0.343	0.343
	9	Top Horizontal	0.290	0.290
	10	Vertical	0.030	0.030
	11	Top Horizontal	0.091	0.091
AOS-050 (Transported Vertically)	1	Bottom Horizontal	0.183	0.183
	2	Vertical	0.061	0.061
	3	Bottom Horizontal	0.579	0.579
	4	Vertical	0.282	0.282
	5	Top Horizontal	0.579	0.579
	6	Vertical	0.099	0.099
	7	Bottom Horizontal	0.579	0.579
	8	Vertical	0.282	0.282
	9	Top Horizontal	0.579	0.579
	10	Vertical	0.061	0.061
	11	Top Horizontal	0.183	0.183
AOS-100 (Transported Vertically)	1	Bottom Horizontal	0.364	0.364
	2	Vertical	0.190	0.190
	3	Bottom Horizontal	1.159	1.159
	4	Vertical	0.464	0.464
	5	Top Horizontal	1.159	1.159
	6	Vertical	0.400	0.400
	7	Bottom Horizontal	1.159	1.159
	8	Vertical	0.464	0.464
	9	Top Horizontal	1.159	1.159
	10	Vertical	0.190	0.190
	11	Top Horizontal	0.364	0.364

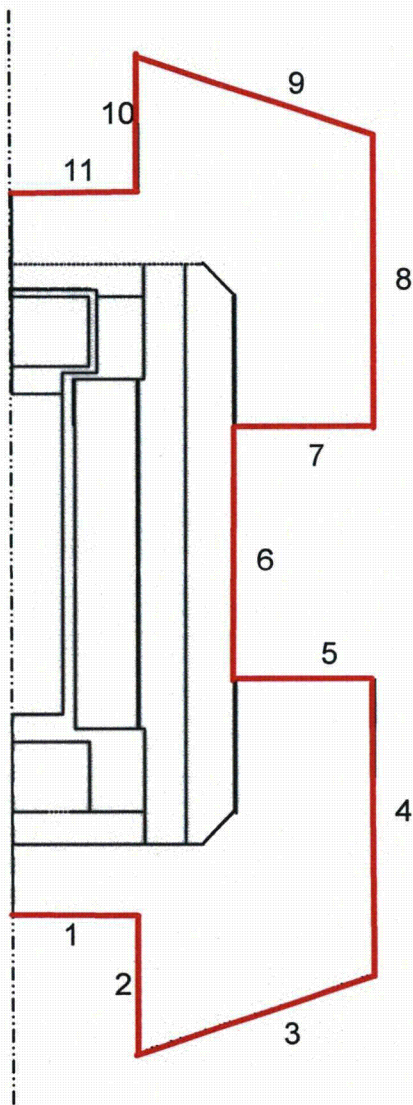


**Figure 3-2. Cask Assembly External Surface Identification, Normal Conditions of Transport – All Models (Typical; Surfaces 5, 6, 7, and 8 are not used on Model AOS-025)**

*Note: The figure depicts the package orientation during transport.*

**Table 3-13. Cask Assembly External Surface Orientation and Size, Fire Condition – All Models**

Model	Surface	Orientation	Length (m)	Width (m)
AOS-025 Fire Model (Transported Vertically)	1	Bottom Horizontal	0.091	0.091
	2	Vertical	0.030	0.030
	3	Bottom Horizontal	0.290	0.290
	4	Vertical	0.343	0.343
	11	Top Horizontal	0.257	0.257
AOS-050 Fire Model (Transported Vertically)	1	Bottom Horizontal	0.183	0.183
	2	Vertical	0.061	0.061
	3	Bottom Horizontal	0.579	0.579
	4	Vertical	0.282	0.282
	5	Top Horizontal	0.503	0.503
	6	Vertical	0.099	0.099
	7	Bottom Horizontal	0.579	0.579
	8	Vertical	0.264	0.264
	11	Top Horizontal	0.513	0.513
AOS-100 Fire Model (Transported Vertically)	1	Bottom Horizontal	0.364	0.364
	2	Vertical	0.190	0.190
	3	Bottom Horizontal	1.159	1.159
	4	Vertical	0.464	0.464
	5	Top Horizontal	1.159	1.159
	6	Vertical	0.400	0.400
	7	Bottom Horizontal	1.159	1.159
	8	Vertical	0.452	0.452
	11	Top Horizontal	1.027	1.027

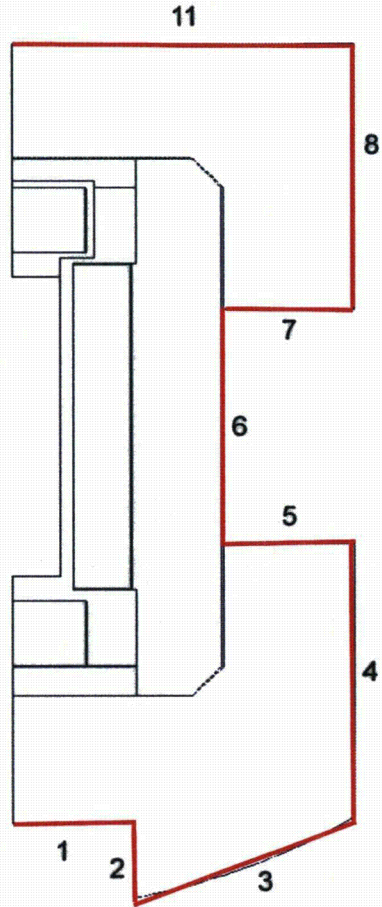


**Figure 3-3. Cask Assembly External Surface Identification, Fire Condition – All Models (Typical; Surfaces 5, 6, 7, and 8 are not used on Model AOS-025)**

**Note:** *The figure depicts the package orientation during transport.*



In addition to convection, the cask surface interacts radiatively with its surroundings. The radiative heat transfer coefficient,  $h_r$ , is calculated, using the equations provided in Paragraph 3.3.3.2. Regulatory environments place the transport package in an outside environment. Therefore, in evaluating the equation for the gray body shape factor, it is assumed that  $A_1$  is negligible, when compared with  $A_2$ , and  $F_{12} = 1.0$ . The impact limiter outside surface is oxidized SS304, and the surface emissivity is 0.52. The cask outside surface is polished, and an emissivity of 0.20. Both of these values can be found in Reference [3.9].

The effective film coefficient,  $h$  (Btu/hr-in<sup>2</sup>-°F), is as follows:

$$h = h_c + h_r$$

The three (3) regulatory required ambient temperatures are 38°C, -29°C, and -40°C (100°F, -20°F, and -40°F, respectively). Convective properties, including radiation, used in the analysis as a function of temperature have a form:

$$h(T) = a_0 + a_1T + a_2T^2 + a_3T^3$$

where:

$$h(T) = \text{Btu/hr-in}^2\text{-}^\circ\text{F}$$

$$T = \text{Surface temperature, } ^\circ\text{F}$$

Table 3-14 (Normal conditions of transport) defines the polynomial coefficients used in the equivalent convective property of each ambient temperature and external surface, for each AOS Transport Packaging System model.

Two sets of convective properties are used due to the change in geometry for the Hypothetical Accident conditions of transport:

- One set of properties (defined in Table 3-15) is used for the steady-state analysis that leads into the fire transient. This set of properties is also used for the cool-down transient analysis. A sample calculation is included in Appendix 3.5.4.5.3, which provides the computation for the effective film coefficient of a vertical plate within the Model AOS-100. Appendix 3.5.4 also includes curve-fitting data for all models and environments.
- The second set of properties is used only for the Fire event, which is defined in Paragraph 3.3.3.8.

**Table 3-14. Polynomial Coefficients Used in Equivalent Convective Property of Ambient Temperature and External Surface, Normal Conditions of Transport – All Models**

Model	Ambient Temperature		Surface	Polynomial Coefficient			
	°C	°F		a <sub>0</sub>	a <sub>1</sub>	a <sub>2</sub>	a <sub>3</sub>
AOS-025	37.78	100	4	2.149E-03	4.387E-05	-2.977E-08	2.231E-11
			9	1.405E-03	6.306E-05	-5.279E-08	3.117E-11
			10	7.659E-04	8.122E-05	-7.456E-08	3.957E-11
			11	7.659E-04	8.122E-05	-7.456E-08	3.957E-11
	-28.89	-20	4	4.988E-03	3.463E-05	-2.796E-08	2.399E-11
			9	6.394E-03	4.944E-05	-4.937E-08	3.367E-11
			10	7.787E-03	6.350E-05	-6.974E-08	4.291E-11
			11	7.787E-03	6.350E-05	-6.974E-08	4.291E-11
	-40	-40	4	5.452E-03	3.314E-05	-2.772E-08	2.439E-11
			9	7.193E-03	4.723E-05	-4.890E-08	3.425E-11
			10	8.902E-03	6.062E-05	-6.907E-08	4.369E-11
			11	8.902E-03	6.062E-05	-6.907E-08	4.369E-11

**Table 3-14. Polynomial Coefficients Used in Equivalent Convective Property of Ambient Temperature and External Surface, Normal Conditions of Transport – All Models (Continued)**

Model	Ambient Temperature		Surface	Polynomial Coefficient			
	°C	°F		a <sub>0</sub>	a <sub>1</sub>	a <sub>2</sub>	a <sub>3</sub>
AOS-050	37.78	100	4	2.101E-03	4.562E-05	-3.187E-08	2.312E-11
			5	2.101E-03	4.562E-05	-3.187E-08	2.312E-11
			6	-1.782E-04	5.110E-05	-5.237E-08	2.439E-11
			7	2.506E-03	3.176E-05	-1.526E-08	1.669E-11
			8	2.101E-03	4.562E-05	-3.187E-08	2.312E-11
			9	2.101E-03	4.562E-05	-3.187E-08	2.312E-11
			10	1.774E-03	6.288E-05	-5.234E-08	3.101E-11
			11	1.774E-03	6.288E-05	-5.234E-08	3.101E-11
	-28.89	-20	4	5.034E-03	3.803E-05	-3.569E-08	2.885E-11
			5	6.114E-03	5.269E-05	-6.023E-08	4.052E-11
			6	4.585E-03	4.254E-05	-5.666E-08	3.182E-11
			7	3.993E-03	2.521E-05	-1.425E-08	1.774E-11
			8	5.034E-03	3.803E-05	-3.569E-08	2.885E-11
			9	6.114E-03	5.269E-05	-6.023E-08	4.052E-11
			10	6.688E-03	4.944E-05	-4.915E-08	3.360E-11
			11	6.688E-03	4.944E-05	-4.915E-08	3.360E-11
	-40	-40	4	5.628E-03	3.444E-05	-2.967E-08	2.529E-11
			5	7.165E-03	4.791E-05	-5.230E-08	3.581E-11
			6	5.487E-03	3.808E-05	-4.872E-08	2.720E-11
			7	4.246E-03	2.415E-05	-1.412E-08	1.799E-11
			8	5.628E-03	3.444E-05	-2.967E-08	2.529E-11
			9	7.165E-03	4.791E-05	-5.230E-08	3.581E-11
			10	7.477E-03	4.725E-05	-4.871E-08	3.420E-11
			11	7.477E-03	4.725E-05	-4.871E-08	3.420E-11

**Table 3-14. Polynomial Coefficients Used in Equivalent Convective Property of Ambient Temperature and External Surface, Normal Conditions of Transport – All Models (Continued)**

Model	Ambient Temperature		Surface	Polynomial Coefficient			
	°C	°F		a <sub>0</sub>	a <sub>1</sub>	a <sub>2</sub>	a <sub>3</sub>
AOS-100	37.78	100	4	2.222E-03	4.132E-05	-2.673E-08	2.113E-11
			5	1.265E-03	5.985E-05	-4.941E-08	2.965E-11
			6	1.521E-04	3.699E-05	-3.557E-08	1.790E-11
			7	2.634E-03	2.814E-05	-1.092E-08	1.502E-11
			8	2.222E-03	4.132E-05	-2.673E-08	2.113E-11
			9	1.265E-03	5.985E-05	-4.941E-08	2.965E-11
			10	1.265E-03	5.985E-05	-4.941E-08	2.965E-11
			11	1.265E-03	5.985E-05	-4.941E-08	2.965E-11
	-28.89	-20	4	5.405E-03	3.722E-05	-3.825E-08	3.034E-11
			5	6.261E-03	4.969E-05	-5.170E-08	3.465E-11
			6	3.493E-03	2.892E-05	-3.340E-08	1.951E-11
			7	3.715E-03	2.240E-05	-1.019E-08	1.590E-11
			8	5.405E-03	3.722E-05	-3.825E-08	3.034E-11
			9	6.261E-03	4.969E-05	-5.170E-08	3.465E-11
			10	5.458E-03	3.897E-05	-3.420E-08	2.682E-11
			11	6.261E-03	4.969E-05	-5.170E-08	3.465E-11
	-40	-40	4	6.442E-03	3.974E-05	-4.914E-08	3.711E-11
			5	6.912E-03	4.503E-05	-4.558E-08	3.270E-11
			6	4.024E-03	2.761E-05	-3.310E-08	1.988E-11
			7	3.848E-03	2.316E-05	-1.524E-08	1.980E-11
			8	6.442E-03	3.974E-05	-4.914E-08	3.711E-11
			9	6.912E-03	4.503E-05	-4.558E-08	3.270E-11
			10	6.019E-03	3.727E-05	-3.390E-08	2.727E-11
			11	6.912E-03	4.503E-05	-4.558E-08	3.270E-11

**Table 3-15. Polynomial Coefficients Used in Equivalent Convective Property of Ambient Temperature and External Surface, Steady-State Leading to the Fire and Cool-Down Conditions – All Models**

Model	Ambient Temperature		Surface	Polynomial Coefficient			
	°C	°F		a <sub>0</sub>	a <sub>1</sub>	a <sub>2</sub>	a <sub>3</sub>
AOS-025	37.78	100	4	2.149E-03	4.387E-05	-2.977E-08	2.231E-11
			11	1.346E-03	6.472E-05	-5.477E-08	3.193E-11
AOS-050	37.78	100	4	2.150E-03	4.597E-05	-3.272E-08	2.364E-11
			5	1.657E-03	5.588E-05	-4.418E-08	2.785E-11
			6	-1.782E-04	5.110E-05	-5.237E-08	2.438E-11
			7	2.506E-03	3.176E-05	-1.526E-08	1.669E-11
			8	2.150E-03	4.597E-05	-3.272E-08	2.364E-11
			11	1.657E-03	5.588E-05	-4.418E-08	2.785E-11
AOS-100	37.78	100	4	2.216E-03	4.153E-05	-2.698E-08	2.123E-11
			5	1.265E-03	5.985E-05	-4.941E-08	2.965E-11
			6	1.521E-04	3.699E-05	-3.557E-08	1.790E-11
			7	2.606E-03	2.837E-05	-1.138E-08	1.527E-11
			8	2.216E-03	4.153E-05	-2.698E-08	2.123E-11
			11	1.265E-03	5.985E-05	-4.941E-08	2.965E-11

### 3.3.3.4 Vertical Surface

The Nusselt Number used for convection from a vertical surface under laminar flow,  $Ra \leq 10^9$ , is determined from Reference [3.4], Equation 9.27:

$$Nu = 0.68 + A / B$$

$$A = 0.670 * Ra^{1/4}$$

$$B = [1 + (0.492 / Pr)^{9/16}]^{4/9}$$

where:

$$Pr = \text{Prandtl Number}$$

The Nusselt Number for turbulent flow,  $Ra \geq 10^9$ , is determined from Reference [3.4], Equation 9.26:

$$Nu = \{0.825 + A / B\}^2$$

$$A = 0.387 * Ra^{1/6}$$

$$B = [1 + (0.492 / Pr)^{9/16}]^{8/27}$$

where:

$$Ra = Pr * Gr, \text{ Rayleigh Number}$$

### 3.3.3.5 Horizontal Surface

The Nusselt Number used for convection from a horizontal, upper surface under laminar flow,  $10^4 \leq Ra \leq 10^7$ , is determined from Reference [3.4], Equation 9.30:

$$Nu = 0.54 * Ra^{1/4}$$

The Nusselt Number for turbulent flow,  $10^7 \leq Ra \leq 10^{11}$ , is determined from Reference [3.4], Equation 9.31:

$$Nu = 0.15 * Ra^{1/3}$$

The Nusselt Number used for convection from a horizontal, lower surface,  $10^5 \leq Ra \leq 10^{10}$ , is determined from Reference [3.4], Equation 9.32:

$$Nu = 0.27 * Ra^{1/4}$$

### 3.3.3.6 Horizontal Cylinder

The Nusselt Number used for convection from a horizontal cylinder with  $Ra \leq 10^{12}$  is determined from Reference [3.4], Equation 9.34:

$$Nu = \{0.60 + A / B\}^2$$

$$A = 0.387 * Ra^{1/6}$$

$$B = [1 + (0.559 / Pr)^{9/16}]^{8/27}$$

where:

$$Pr = \text{Prandtl Number}$$

### 3.3.3.7 Solar Heat Load

The total heat load per unit area is defined by the surface type and orientation, over a 12-hour period. For steady-state and fire-transient solutions, the heat load is divided by 12 hours, to determine the heat flow rate. (Refer also to Appendix 3.5.4.7 for FR-3700 Series foam materials, under Thermal Condition 1 of Table 3-3.)

Table 3-16 defines the solar heat applied to the cask's outside surfaces for Thermal Conditions 1 and 3.

**Table 3-16. Solar Heat Application to Cask Outside Surfaces – All Models**

Model	Surface	Total Insolation		Heat Rate
		Cal/cm <sup>2</sup>	Btu/in <sup>2</sup>	Btu/hr-in <sup>2</sup>
AOS-025	1, 2, 3	0	0	0
	4	400	10.24	0.8533
	5, 6, 7, 8	–	–	–
	9	800	20.48	1.7070
	10	400	10.24	0.8533
	11	800	20.48	1.7070
AOS-050	1, 2, 3	0	0	0
	4, 8	400	10.24	0.8533
	5	800	20.48	1.7070
	6	400	10.24	0.8533
	7	200	5.12	0.4267
	9	800	20.48	1.7070
	10	400	10.24	0.8533
	11	800	20.48	1.7070
AOS-100	1, 2, 3	0	0	0
	4	400	10.24	0.8533
	5	800	20.48	1.7070
	6	400	10.24	0.8533
	7	200	5.12	0.4267
	8	400	10.24	0.8533
	9	800	20.48	1.7070
	10	400	10.24	0.8533
	11	800	20.48	1.7070



### 3.3.3.8 Cask Boundary Surfaces at 1,475°F Environment

During the 30-minute Fire condition, the ambient air is 1,475°F. Using the relationship provided in Paragraph 3.3.3.2 for convection due to radiation,  $h_r$ , the surface convective coefficient is:

$$h_r = S * F * (T_1^2 + 1,935^2) * (T_1 + 1,935)$$

where:

$$S = \text{Stefan-Boltzmann constant} = 1.1944\text{E-}11 \text{ Btu/hr-in}^2\text{-}^\circ\text{R}^4$$

$$F = \text{Gray body shape factor}$$

$$= 0.8$$

$$T_1 = \text{Surface temperature, } ^\circ\text{R}$$

Then:

$$h_r = 9.5552\text{E-}12 * (T_1^3 + 1,935 * T_1^2 + 1,935^2 * T_1 + 1,935^3)$$

A convective heat transfer,  $h_c$  is also present during the Fire condition:

$$h_c = 10 \text{ w/m}^2\text{-}^\circ\text{C} (0.01223 \text{ Btu/hr-in}^2\text{-}^\circ\text{F})$$

Combining the effects of both radiation and convection, total surface convection during the Fire condition, defined as a function of temperature, is:

$$h_t = h_c + h_r$$

$$h_t = 1.051\text{E-}1 + 4.370\text{E-}5 * T + 5.461\text{E-}8 * T^2$$

where:

$$T = \text{Surface temperature, } ^\circ\text{F}$$

Additional information is provided in Appendix 3.5.4.5.2.4.

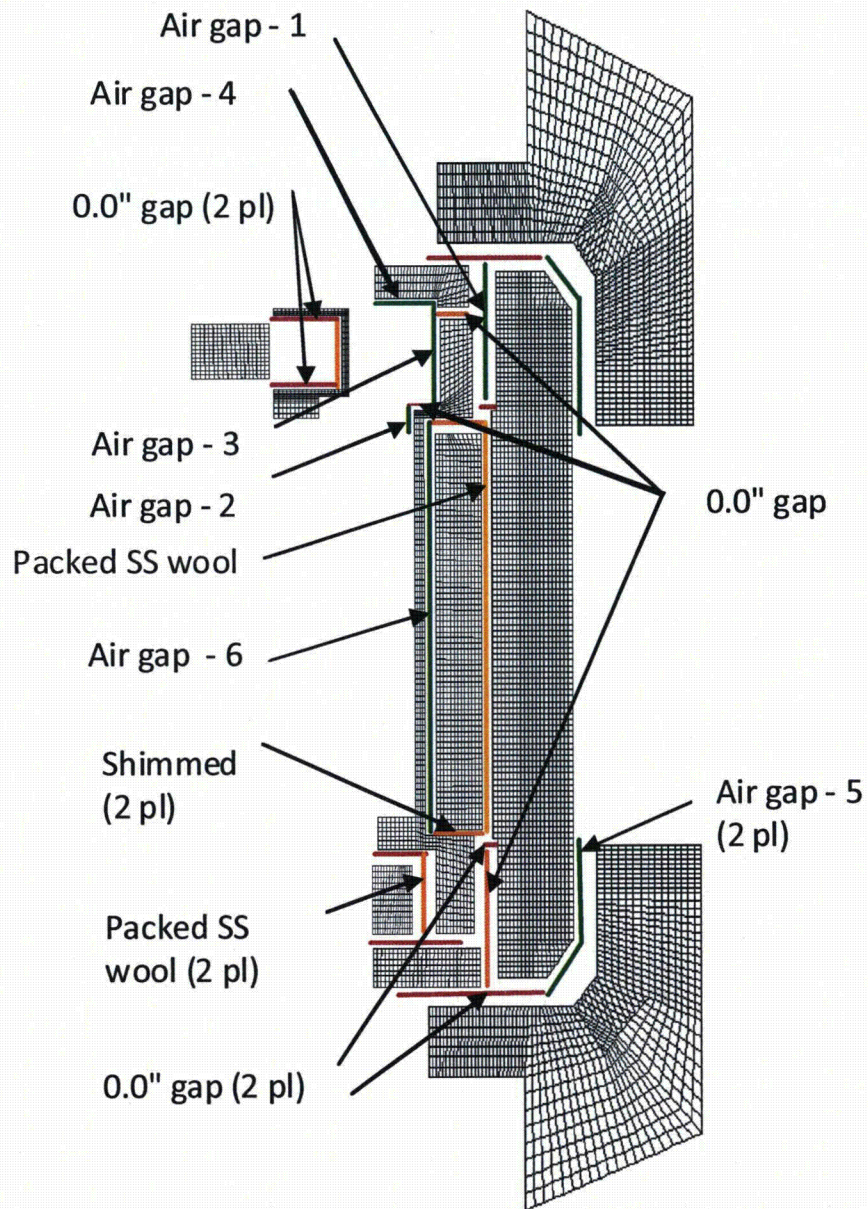


Figure 3-4. Expanded View of Thermal Model Defining Component Interfaces

### **3.3.4 Normal Conditions of Transport Thermal Results**

The tables and figures provided in Appendix 3.5.2, "Thermal Evaluation Results – Models AOS-025, AOS-050, and AOS-100," contain the nodal temperatures determined for all Normal conditions of transport thermal conditions specified in *Regulatory Guide 7.8* (Reference [3.21]). The maximum component temperatures summarized in Table 3-3 show that all component temperatures meet their regulatory/ component criteria.

### 3.4 THERMAL EVALUATION UNDER HYPOTHETICAL ACCIDENT CONDITIONS

The AOS Transport Packaging System models are analyzed for the Hypothetical Accident conditions of transport Fire event – a 1/2-hour fire engulfing the entire cask, after a 30-ft. free drop, followed by a natural cool-down. The transport package's impact limiters are assumed to be deformed as a result of the free drop. Thermal analysis of the Fire event is conducted using the LIBRA Finite Element program, using an axisymmetric model. In the LIBRA analyses, model element thermal properties are updated every tenth time step, to account for the changes in material properties during the Fire event.

AOS considered the Head-On Drop condition the more damaging condition under the Fire event. This is supported by the analysis provided in [Appendix 3.5.4.2.5](#). In this analysis, the model includes the combined deformation of all three (3) drop orientations – Head-On, Side and Slap Down. The results show little change in the maximum cask component temperature when compared with the uncrushed configuration results. Furthermore, the maximum cask component temperatures usually occur during the cool-down period of the Hypothetical Accident conditions of transport. During this period, the impact limiter foam is assumed to be gone (destroyed) and replaced with air. Therefore, the geometry due to a puncture deformation is not a significant factor in the resulting temperatures.

Figure 3-5 illustrates the LIBRA Finite Element thermal model used in this analysis. The analytical model shown in Figure 3-5 is that of the Model AOS-100A transport package. Similar models are developed to represent the Model AOS-025 and AOS-050 transport packages. In this LIBRA model, the impact limiter is conservatively modeled to reflect deformations due to a hypothetical 30-ft. Head-On Drop. The impact limiter model height is reduced by 5.9 in. for the Head-On Drop, reflecting 100% of the computed deformation. In the analytical model, this deformation is applied to the axisymmetric model. Further details on this approach are provided in [Appendix 3.5.4.2](#).

The impact limiter foam thermal properties are adjusted to account for the change in volume resulting from the free drop. The value adjustment is proportional to the volume reduction.

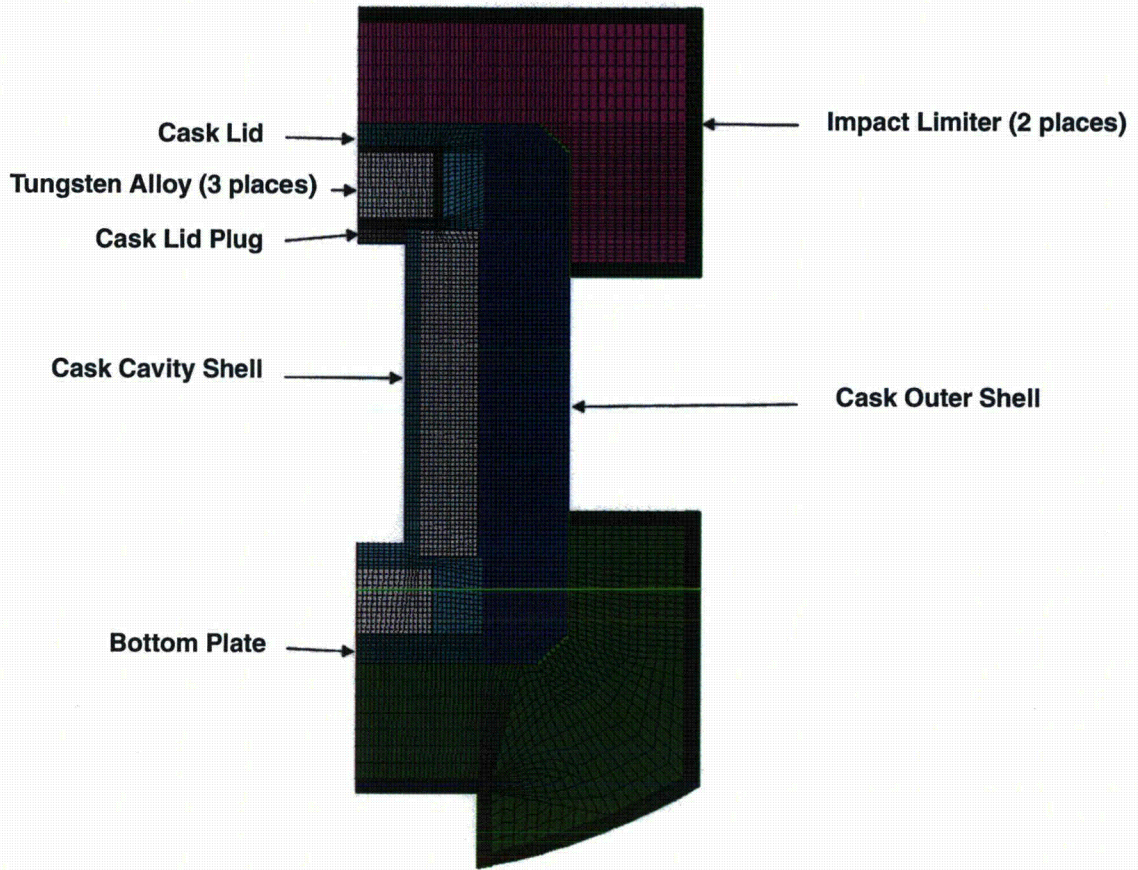


Figure 3-5. Thermal Finite Element Model – Fire Conditions

### **3.4.1 Initial Conditions**

The package is subjected to two (2) free drops – one from a height of 914.4 cm (30 ft.), and another from a height of 121.92 cm (4 ft.) onto a cylindrical punch. The orientation of the package during the drops is selected to provide the greatest damage potential by aiming for the weakest point along the containment boundary. However, because the impact limiter encloses all of these areas, the critical factor becomes how much energy the impact limiter can absorb. The initial condition for the Fire event is the Normal condition of transport – 38°C (100°F) ambient temperature – with maximum decay heat and solar load. The analytical model used in the evaluation is the same as the one used to evaluate the Normal condition, with the section representing the impact limiter modified to represent the deformed geometry of this structure because of the free-drop condition.

### **3.4.2 Fire Test Conditions**

As discussed in Subsection 3.4.1, the Fire condition analysis begins at the 38°C (100°F) ambient temperature, with maximum decay heat and solar load solution. At time zero, an ambient temperature of 800°C (1,475°F) is applied to the model. Also, all gaps are closed, and conduction across all interfacing surfaces are assumed to be by contact resistance. Contact resistance is reduced for the fire's duration. This ambient temperature is maintained for 0.5 hours. At this time, the ambient condition is reversed to the initial condition and all gaps are reopened and contact resistance is increased by a factor of 100. The post fire phase of this analysis assumes the foam is gone and in its place air properties are used. The analysis continues until eight (8) hours elapse.

### **3.4.3 Maximum Temperatures and Pressures**

The maximum temperatures are reported in Table 3-4. Temperature tables and contour plots of the Fire condition follows. The maximum pressures are reported in Table 4-7, "Maximum Cask Cavity Pressure Due to Fire Condition – All Models."

### **3.4.4 Maximum Thermal Stresses**

Thermal stresses resulting from temperature gradients and differential thermal expansion for all transport package models are provided in Appendix 2.12.2, "Structural Evaluation Results – Models AOS-025, AOS-050, and AOS-100."

### **3.4.5 Accident Conditions for Fissile Material Packages for Air Transport**

Not applicable. Fissile material is not an authorized content for the AOS Transport Packaging System.

### **3.4.6 Hypothetical Accident Conditions of Transport Thermal Results**

The tables and figures provided in [Appendix 3.5.2](#) contain the nodal temperatures determined for the Fire event, as specified in References [\[3.1\]](#) and [\[3.2\]](#). The maximum component temperatures summarized in [Table 3-4](#) show that all component temperatures meet their regulatory/component criteria.

During the 30-minute Fire condition, conductivity is increased across all gaps and contact surfaces. During the initial start of this event, temperatures briefly decrease within the interior region of the cask. This phenomenon is caused by increased conductivity due to gap closures for this fire condition. The closed gap is a conservative assumption during the fire period, to increase heat flow. There is a brief period following gap closure when conductivity is increased and the fire heat has not yet reached the plug.

THIS PAGE INTENTIONALLY LEFT BLANK.



### 3.5 APPENDIX

This appendix presents the following information:

- Data CDs
- Thermal Evaluation Results – Models AOS-025, AOS-050, and AOS-100
  - Thermal Evaluation Results – Model AOS-025A
  - Thermal Evaluation Results – Model AOS-050A
  - Thermal Evaluation Results – Models AOS-100A and AOS-100A-S
  - Thermal Evaluation Results – Model AOS-100B
- LIBRA Finite Element Program Heat Transfer Module
- Analysis Modeling Data
  - Material Properties
  - Model Dimensions
  - Analysis FEA Models
  - Enclosed Gaps, Equivalent Conductivity
  - Surface Convective Coefficients
  - Curved Vertical Plates Used as Flat Vertical Plates, Criteria Check
  - Insulation Heat Load Analysis for FR-3700 Series Foam under Condition 1 of Table 3-3
  - Impact Limiter Rib Study
- LIBRA File Input Showing Material Property Assignment
- Justification for Use of Uniformly Distributed Decay Heat throughout Cask Cavity
- Thermal Tests
  - Heat Test Report – AOS-165A Prototype
  - Copper Seal Locations with Analytical Model (with Cask Lid Metallic Seal)
  - Garlock Helicoflex Report, Helicoflex Seal Temperature Limit – Cask Lid Metallic Seal

### **3.5.1 Data CDs**

All thermal input/output files, as well as all Autodesk Inventor files, are attached on the Compact Discs (CDs), as listed below:

- **CDs 1, 2, and 3** – All analytical files, including the LIBRA FEA program
- **CD 4** – Autodesk Inventor files